'Bad' Oil, 'Worse' Oil and Carbon Misallocation

Renaud Coulomb, Fanny Henriet, Léo Reitzmann

PARIS SCHOOL OF ECONOMICS
ECOLE D'ECONOMIE DE PARIS

WORKING PAPER N° 2021 – 38

'Bad' Oil, 'Worse' Oil and Carbon Misallocation

Renaud Coulomb
Fanny Henriet
Léo Reitzmann

JEL Codes: Q35, Q54, Q58, L71.
Keywords: climate change, oil, carbon mitigation, misallocation, stranded assets.

Funded by a French government subsidy managed by the ANR under the framework of the Investissements d'avenir programme reference ANR-17-EURE-001

'Bad' Oil, 'Worse' Oil and Carbon Misallocation*

Renaud Coulomb[a], Fanny Henriet[b], Léo Reitzmann[c]

May 2021

Abstract

Not all barrels of oil are created equal: their extraction varies in both private cost and carbon intensity. Using a rich micro-dataset on World oil fields and estimates of their carbon intensities and private extraction costs, this paper quantifies the additional emissions and costs from having extracted the 'wrong' deposits. We do so by comparing historic deposit-level supplies to counterfactuals that factor in pollution costs, while keeping annual global consumption unchanged. Between 1992 and 2018, carbon misallocation amounted to at least 10.02 $GtCO_2$ with an environmental cost evaluated at US$ 2 trillion (US$ 2018). This translates into a significant supply-side ecological debt for major producers of dirty oil. Looking towards the future, we estimate the gains from making deposit-level extraction socially-optimal, and document the very unequal distribution of the subsequent stranded oil reserves across countries.

KEYWORDS: Climate change, oil, carbon mitigation, misallocation, stranded assets.
JEL CODES: Q35, Q54, Q58, L71.

*We thank seminar participants at the Paris School of Economics, the Toulouse School of Economics, the University of Amsterdam, the Graduate Institute Geneva, the Banque de France, and participants at the 11th FAERE Thematic Workshop "Energy transition" in Paris. We are grateful to Jeff Borland, Julien Daubanes, Antoine Dechezlepretre, John Freebairn, Geoffrey Heal, Leslie Martin, Rick van der Ploeg, and Yanos Zylberberg for their helpful comments, and Léo Jean for outstanding research assistance. We also thank Mohammad S. Masnadi for sharing part of the data used in our robustness checks. Financial support from the Agence Nationale de la Recherche (ANR-16-CE03-0011 and EUR ANR-17-EURE-0001) is gratefully acknowledged.

[a]University of Melbourne, 111 Barry Street, VIC 3010, Australia. E-mail: renaud.coulomb@unimelb.edu.au.

[b]Paris School of Economics-CNRS: 48 Bd Jourdan, 75014 Paris, France. E-mail: fanny.henriet@psemail.eu.

[c]Paris School of Economics: 48 Bd Jourdan, 75014 Paris, France. E-mail: leo.reitzmann@gmail.com.

1 Introduction

Oil deposits vary in their private and social marginal extraction costs. These two costs differ markedly as oil extraction generates substantial Greenhouse gas (GhG) emissions that are not internalized by oil producers. These emissions vary across deposits, and depend on oil and reservoir characteristics and the associated extractive technologies (Masnadi et al., 2018). For instance, producing a barrel of crude from bitumen in Canada emits twice as much Greenhouse gas as a barrel of light crude from Saudi Arabia. As keeping the rise in global temperature below 2°C requires leaving large oil reserves forever untapped (Meinshausen et al., 2009), choosing the right deposits to exploit can be a key lever for emission abatement in a sector that is otherwise difficult to decarbonize (Creutzig et al., 2015). However, despite the global recognition of the climate-change risk, since at least the 1992 Earth Summit, production-related GhG emissions from oil have mostly been ignored (World Bank, 2020). Poor or absent regulations are a major source of carbon misallocation in this industry, with dirty oil (e.g., heavy oils) being extracted instead of lower carbon-intensity oil.

This paper is the first to quantify the environmental cost of misallocation in oil supply. We leverage a rich micro-dataset of World oil fields and estimates of their carbon intensities and private extraction costs to measure the additional emissions and costs of historic oil supply since the 1992 Earth Summit as compared to the socially-efficient allocation. We then assess the social gains of optimal future supply, compared to a competitive extraction that matches the same aggregate supply path. Overall, we show that supply recomposition, through the choice of the cumulative amount to be extracted from each deposit and the sequencing of deposits use, can produce large emission reductions at zero or low cost, while leaving the demand-side unchanged.

Our estimation of past carbon misallocation relies on the difference in cumulative pollution between the historic oil-supply curve and the socially-optimal counterfactual that minimizes environmental and private extraction costs, while leaving annual global aggregate extraction unchanged. As any barrel used before 2018 is no longer available in the future, our measure of past misallocation accounts for the opportunity costs attached to the extraction of barrels in the past. More precisely, our counterfactual takes oil to be optimally extracted from 1992 up to 2050, the date at which carbon neutrality is reached (IPCC, 2018; European Council, 2019). This counterfactual is compared to the extraction path from the historic 1992-2018 supply and a future supply (with the same annual global production up to 2050) that we take to be either competitive and ignoring pollution heterogeneity, or optimal.[1]

[1]We also consider alternative dates for carbon neutrality (2066 and 2080), with similar results. As our supply recomposition does not come with a change in aggregate supply, the 'optimal counterfactual' is actually the optimal structure of the aggregate supply, and thus represents a second-best.

Our central findings indicate that inefficient emissions from oil misallocation over the 1992-2018 period amount at least to 10.02 gigatons of CO_2 ($GtCO_2$). These emissions are substantial, representing two years of life-cycle emissions of the global transportation sector, and their cost is estimated at 2 trillion US$.[2] We also find that the optimal allocation of extraction across deposits results not only in less carbon-intensive extraction but also lower private extraction costs, as our optimal counterfactual solves both carbon mispricing and other market imperfections. Though the historic deposit-level supplies reveal that deposits' carbon heterogeneity was ignored *and* extraction was not competitive, we document that inefficient emissions can be attributed to carbon mispricing, rather than imperfect competition. Solving only private cost misallocation in oil supply, that is expensive oil was extracted in lieu of cheaper oil, while ignoring pollution reduces cumulative emissions by 1.87 $GtCO_2$ only. Thus, carbon misallocation is distinct from private cost misallocation.

In a next step, we use our deposit-level data to map countries' supply-side 'ecological debts', i.e., their over-extraction from the comparison of their aggregate historical supply to their optimal supply. This allows us to determine the winners and losers from carbon misallocation. We in particular show that Annex B countries, which committed to mitigation targets in the 1997 Kyoto Protocol, over-extracted oil by 66% in the 1992-2018 period, whereas the Rest of the World under-extracted by 30%.

We then evaluate the gains from the optimal extraction of resources in the future, as compared to a perfectly-competitive future supply with identical annual demands in which pollution heterogeneity is ignored. Extracting oil optimally starting in 2019 yields future emission savings of 7.64 $GtCO_2$. We then estimate the stranded reserves of oil-producing countries, i.e., the share of their 2019 oil reserves that should optimally remain underground. These vary widely across countries, from a figure of 15.3% in Kuwait to 97.4% in Canada.

Finally, we consider alternative dates to start the recomposition of past supply, as the 1992 Earth Summit was not the only missed window of opportunity. We show that starting to extract optimally one year earlier always yields large additional environmental benefits, even for periods that are as far in the past as the 1970s. We also show that the post-2010 rise in US Shale Oil production and Canada's Oil Sands production, which are expensive to extract, and the 'Oil Counter-Shock' (1980-1986) are behind substantial misallocation.

Our findings inform the debate on climate-change mitigation costs, and produce three key policy recommendations. First, as the variation in crude-oil carbon intensity originates in the upstream and midstream sectors, any regulation of downstream emissions (combustion)

[2]These results are derived for a social cost of carbon (SCC) of US$ 200 per ton of CO_2 in 2018, in line with Lemoine (2021) and the DICE2016R scenario of keeping the temperature rise below 2.5°C over the next 100 years (Nordhaus, 2017). The inefficient emissions in the past are of the same magnitude for a large range of SCC, varying from 7 to 12.5 $GtCO_2$ as the SCC rises from $50 to $400 per tCO_2.

that treats all crudes similarly misses out on important mitigation opportunities.[3] A second policy recommendation concerns what can still be changed in the future. We document that, as the opportunity costs of using good resources are only small, delaying mitigation is costly. The post-2018 gains from optimal extraction would be almost the same were oil to have been extracted optimally since 1992. A third important message is that the misallocation attributable to poor carbon regulation has little in common with production inefficiencies arising from OPEC's market power. The need for environmental regulations should not be confused with pro-competition policy and should receive the same attention from policymakers.

Optimal extraction entails a large reallocation of aggregate production between countries, as compared to observed extraction pre-2019. This reallocation may be difficult to implement politically, due to country preferences for domestic productions, e.g. job-related, public-finance or energy-security concerns, or difficulties in setting up international compensation. Recomposing supply without changing countries' observed annual production still yields large emission reductions of about 9.57 $GtCO_2$ over the 1992-2018 period, which is due to significant within-country heterogeneity in carbon intensities. Overall, limiting *country-level* production changes still leaves large potential gains from (past or future) supply recomposition, which alleviates feasibility concerns. Which policy instruments should be used to attain the recommended deposit-level supplies? Carbon pricing on the supply-side is obviously an interesting instrument but may face obstacles such as lobbying activities of firms, non-cooperative countries that refuse to implement the tax domestically, or tax-incidence issues that arise from the finite nature of oil deposits (Heal and Schlenker, 2019). An alternative would be to prevent any country from consuming dirty oil, in a supply-side policy *à la* Harstad (2012). Precluding extraction from dirty-oil deposits and then extracting other deposits in a competitive way without further pollution considerations so as to obtain the same emission reduction as under optimal supply, would raise private extraction costs by 1.6 trillion US$ compared to optimal extraction.

This paper is the first to empirically assess inefficiencies in global oil production, factoring in pollution. Environmental concerns are largely absent from the literature on misalloca-

[3]Upstream regulation is usually out of scope for most consumer countries, although attempts have been made to reduce the life-cycle emissions of fuels. An example is the EU's Fuel Quality Directive (FQD), the purpose of which is to reduce automotive-fuels carbon footprints in 2020 by 6% compared to 2010 (Malins et al., 2014a). Each fuel supplier has to achieve the 6% reduction target but all suppliers report annually the same EU-wide carbon intensity value for fossil petrol and diesel, whether their products originate from high-carbon sources or not. Mitigation assessments in the transport sector tend to ignore oil-supply recomposition (Replogle et al., 2013; Vimmerstedt et al., 2015) but focus on fuel switching, e.g., from oil to natural gas, bio-methane or bio-fuels, (Sims et al., 2014), despite potentially large adjustment costs (due to fuel-specific existing installations, for example) and industry lobbying efforts against the transition (Knaus, 2019; Lipton, 2020).

tion, with the exception of some recent contributions: Sexton et al. (2018) and Lamp and Samano (2020) examine environmental misallocations in residential solar installations and Correa et al. (2020) in the copper industry. Our methodology is close to Borenstein et al. (2002) and Asker et al. (2019), who relate misallocation in production factors to the under-utilization of *observed* lower-cost production units in a given sector.[4] Our paper builds upon the analysis of production misallocation due to market power in the oil industry in Asker et al. (2019). In contrast to their work, we consider an additional source of social inefficiency: heterogeneity in the carbon externality associated with extraction and refining. The only source of inefficiency in observed production in their paper comes from resource-extraction sequencing that does not correspond to Herfindahl 1967's "least-cost first" rule, i.e. extracting the cheapest resource first, as all deposits are eventually exhausted. By way of contrast, many deposits in a carbon-constrained world should be left untapped forever or be only partially exploited, and optimal deposit-selection depends on the trade-off between the economic and environmental costs.[5] This trade-off is empirically significant. At the fine level of disaggregation of our data, carbon intensities and private extraction costs are not strongly correlated, so the inefficiencies from omitted pollution costs do not mirror extraction-cost inefficiencies. We compute the total cost of misallocation attributable to OPEC market power as the cost of moving from the optimal supply to the second best supply obtained under the constraint that each OPEC's country keeps the same annual production as observed in the data. We show that this cost is of the same order of magnitude as the misallocation cost attributable to carbon mispricing, i.e. the cost of moving from the optimal supply to a competitive supply in which pollution is ignored.

Our findings contrast with recent theoretical literature (Benchekroun et al., 2020) that has used a two-resource model to show how cartels like OPEC can actually speed up pollution by enabling producers of expensive and dirtier resources to enter the market earlier than they would have under perfect competition. We show that this mechanism is indeed at work here, but accounts for only a small part of carbon misallocation: switching to the competitive supply brings about an emission reduction that is about one tenth of that of the optimal supply structure over the 1992-2050 period. There is significant pollution heterogeneity in the

[4] A large body of literature analyzes the impact of misallocation on economic objects such as TFP (see e.g., Hsieh and Klenow 2009) or focuses on the possible sources of misallocation (e.g., Hopenhayn and Rogerson, 1993; Guner et al., 2008; Restuccia and Rogerson, 2008); see Hopenhayn (2014) for a review.

[5] Furthermore, 'oil abundance' and the presence of capacity constraints have considerable implications for the order of extraction: resources extracted along the optimal path are not necessarily extracted "least-cost first". Theoretical work has analyzed the extraction of multiple polluting resources (Chakravorty et al., 2008; Van der Ploeg and Withagen, 2012; Michielsen, 2014; Fischer and Salant, 2017; Coulomb and Henriet, 2018). However, the literature is almost silent on the properties of the optimal extraction of multiple exhaustible resources that differ in both their private extraction costs and pollution content.

oil available within (or outside) OPEC, and there are cheap but polluting resources within (or outside) OPEC. This explains why a cost-effective supply brings little environmental gain, so that OPEC market power contributes little to carbon misallocation.[6]

Both Asker et al. (2019) and Benchekroun et al. (2020) relate supply inefficiencies to the wrong sequencing of deposits only: as all deposits are exhausted, there is no selection as to which to use and which to leave. On the contrary, we highlight that, in a carbon-constrained world, the selection of the deposits to use is key for lower social-extraction costs. In our setting, while 88% of extraction-cost misallocation can be attributed to the wrong order of resource extraction, all of the environmental gains come from the selection of deposits.

Last, we contribute to the literature on stranded assets. The scientific literature has raised awareness of the issue of unburnable fuels (Meinshausen et al., 2009; McCollum et al., 2014) and their unequal distribution (McGlade and Ekins, 2015). Recent research (McGlade and Ekins, 2014; Brandt et al., 2018) has acknowledged that oil carbon-intensity heterogeneity should be accounted for to mitigate future emissions, but does not provide any measure of carbon misallocation. As such, McGlade and Ekins (2014) and Brandt et al. (2018) do not explore the trade-off between production costs and emission reductions. In contrast, we look at the social cost of extracting from the wrong deposits in the past and the future, and quantify carbon misallocation.

The remainder of this paper is organized as follows. Section 2 describes the oil-deposit microdata and the estimation of deposit-level carbon intensities. Section 3 sketches the method used to quantify carbon misallocation in oil supply, and how we disentangle this from inefficiencies in private extraction costs. Section 4 then presents our results and their sensitivity to changes in the main assumptions. Last, Section 5 concludes and elaborates on ways to implement field-level supply changes.

2 Oil data, extraction costs and carbon intensities

Quantifying the carbon misallocation from the use of 'wrong' deposits (from a climate-wise perspective) first requires us to estimate field-level carbon intensities and private production costs. In particular, we need to have data on the carbon intensities and costs of those sections of the oil-supply chain in which these vary significantly across barrels. Our analysis

[6]Market power has been considered rather positively through the lenses of resource conservation (Hotelling, 1931; Solow, 1974), and thus pollution mitigation. We do not analyze the impact of market power on aggregate supply, as we want to keep the global oil consumption stream unchanged in order to quantify supply-side misallocation: the aggregate supply is thus considered exogenous. Furthermore, analyzing the nature of OPEC market power (Hansen and Lindholt, 2008) and its interaction with carbon policies (Andrade de Sá and Daubanes, 2016; Van der Meijden et al., 2018) is beyond the scope of this paper.

thus focuses on upstream (oil extraction) and midstream (refining) carbon intensities[7] and extraction costs.[8]

This section briefly presents the oilfield data (see Appendix A for a more-detailed description). We then explain how we calculate field-level private extraction costs. Finally, we describe how we estimate carbon intensities.

2.1 Oil-deposit data

The Rystad Upstream dataset. Our empirical analysis is based on one of the most-comprehensive datasets of oil fields, the Rystad UCube Database (Rystad, afterwards). This covers most of World oil production, with 12,463 active deposits between 1970 and 2018. It includes precise field-level data on oil production, exploitable reserves, discoveries, capital and operational expenditures from exploration to field decommission, current governance (e.g., ownership and operators), field-development dates (discovery, license, start-up, and production end), and oil characteristics (e.g., oil type, density and sulfur content) and reservoir information (e.g., water depth, basin and location).

The Rystad dataset does not contain information on fields' upstream carbon intensities. However, it does record the key variables that influence emissions from extraction or refining, such as oil type (e.g., bitumen or light), API gravity, gas-to-oil ratio, sulfur content, use of steam injection, and the location of the field offshore or onshore.

Additional data. Two extraction techniques that affect emissions from extraction—methane flaring and steam injection— are not recorded precisely in Rystad. Flaring consists in the burning on-site of the methane that comes with oil. This mitigates the risk of explosion from methane accumulation near an installation. As only a minority of countries and companies collect and publish data on flared gas, this information is missing for nearly 95% of the fields in Rystad. We complement these data using the geocoded flaring volumes calculated by the Visible Infrared Imaging Radiometer Suite (VIIRS) algorithm from National Oceanic and Atmospheric Administration (NOAA) satellite observations. Steam injection is a thermal Oil Enhanced Recovery (EOR) technique employed in some fields—mostly those producing heavy oil— to facilitate extraction. Rystad data identify the use of steam injection

[7] See Appendix B.3 for a discussion of downstream emissions. In a nutshell, downstream emissions include mostly combustion-related emissions and transport to the end consumer. Combustion-related emissions are large (an average of 75.82 gCO_2eq/MJ, weighted by 2018 production) but do not vary much by crude origin for a given end-use. Transport emissions to consumers will be affected by the recomposition of supply. However, these emissions are small and do not vary much. We therefore restrict our main analysis to upstream and midstream sectors, where carbon-intensity heterogeneity is found.

[8] Midstream and downstream costs vary by oil, but are small relative to the standard deviation of crude extraction costs (see Appendix C.3.3 for a discussion of the transportation and refining costs).

only for bitumen fields. We add steam-injection data from the International Energy Agency (IEA, 2018b).

2.2 Deposit extraction costs

The annual field expenditures reported in Rystad database are "well" and "facility" capital expenditures, and "selling, general and administrative", "transportation" and "production" operational expenditures.

For each deposit, we assume that the total present cost of extracting any stream of production (x_{dt}), from exploration to shutdown $[t_1; t_2]$, can be written as $\sum_{t_1}^{t_2} c_d x_{dt} e^{-rt}$, so that c_d can be estimated as the levelized cost of extraction (LCOE) of the field. Denoting by x_{dt} the annual deposit production, c_{dt} total opex and capex expenditures of deposit d in year t as reported in Rystad, and r the annual discount rate (set at 3%), the levelized cost of extracting a barrel from deposit d over its life from exploration to shutdown $[t_1; t_2]$ is $c_d = (\sum_{t_1}^{t_2} c_{dt} e^{-rt})/(\sum_{t_1}^{t_2} x_{dt} e^{-rt})$. This represents the field break-even price or the equivalent constant cost of a barrel for a field over its lifetime. In this approach, extraction costs are exogenous to the policies implemented, as in Asker et al. (2019). This echoes that extraction methods, field installations and energy needs are largely determined by exogenous factors such as the physical properties of the hydrocarbons (e.g., viscosity and density) and the reservoir geophysical characteristics (e.g., rock porosity and permeability, and reservoir complexity and depth). For instance, oil located in ultra-deep or complex reservoirs is more expensive to extract (IEA, 2008).

We consider other definitions of field-level private extraction costs in our robustness checks. We first use average cost instead of LCOE. Second, we deduct expenditures and production that occurred before the starting date of optimization from the LCOE calculation, in order to account for potential sunk start-up costs. Third, we allow private extraction cost to vary over time, assuming the existence of two exogenous Martingale processes governing input costs (one common to all onshore fields and the other common to all offshore fields), to account for potential annual shocks on input prices, in line with Asker et al. (2019).

Appendix C.3 describes the data, our main approach to calculate field-level private extraction costs, and the alternative cost measures.

2.3 The carbon intensity of deposits

Upstream carbon intensity. Before oil extraction starts, GhG emissions are generated from field exploration and the setting up of injecting and extracting wells.[9] After production begins, activities such as well maintenance, oil extraction and surface processing, as well as transport to the refinery inlet, emit GhG emissions.

Field-level carbon intensities are assumed to be exogenous to carbon policies and time-invariant in our main approach: this reflects the role of exogenous factors, such as oil viscosity and density in emissions from extraction and refining. Emissions are also linked to extraction techniques, which are largely tied to oil type. For example, lifting heavy oils requires a more intensive use of Enhanced Oil Recovery (EOR) techniques, such as thermal EOR or Gas-EOR. Another example is flaring: when crude oil is extracted from oil wells, the natural gas associated with the oil is brought to the surface at the same time, and vast amounts of this gas is commonly flared as waste. Flaring is typically associated with high carbon intensity, and is largely determined by exogenous factors such as the reservoir's gas-to-oil ratio and the distance to a significant consumer market for gas. Less flaring could, however, in theory be implemented by operators. We abstract from this possibility in our main specification for two reasons. First, abatement-cost estimates vary significantly across studies, and no field-level estimates are available for global oil production (Malins et al., 2014b). Second, flaring regulation seems to be ineffective globally (Farina, 2011; Calel and Mahdavi, 2020), and even counterproductive if as little as 7% of the non-flared methane is instead vented directly into the atmosphere, due to the much greater warming potential of methane as compared to carbon dioxide. As Calel and Mahdavi (2020) note, whereas flares are visible to remote-sensing instruments, vented gas is on the other hand invisible: this casts doubt on whether flaring reductions genuinely correspond to lower GhG emissions. Due to data limitations on the field-level costs of abating flaring emissions, and the difficulty in relating less flaring to true GhG-emission reductions, our main specification will assume fixed field flaring-to-oil ratios (FORs). Overall, our approach (fixed technologies) is conservative, as allowing for endogenous technology changes would bring larger environmental gains. In a robustness check, we update upstream carbon intensities with a 10% lower field-level flaring-to-oil ratio (FOR) at no cost.

We use the *Oil Production Greenhouse Gas Emissions Estimator* (OPGEE) of the Oil-Climate Index (OCI, Carnegie Endowment for International Peace) to estimate upstream emissions. We proceed as follows: we first run the OPGEE using data on 958 deposits, formatted to be used as model inputs and publicly available from Masnadi et al. (2018).

[9] We will use the terms carbon emissions, pollution and CO_2 to refer to GhG emissions. All CO_2 quantities are CO_2-equivalent (CO_2eq). Local (air/water/soil) pollution from oil extraction and refining is ignored.

These represent 54% of 2015 World production. We then match these deposits to those in the Rystad dataset, and select the estimation model that best explains OPGEE carbon intensities using the variables in the Rystad dataset and supplementary sources (IEA and NOAA-VIIRS). The explanatory variables are selected based on the scientific literature (Brandt et al., 2015; Gordon et al., 2015; Masnadi et al., 2018). We find that field upstream carbon intensity varies by oil type (e.g., regular or heavy), the gas-to-oil and flaring-to-oil ratios, and the use of steam injection. Offshore location and operator size also play a role, but to a lesser extent. The chosen reduced-form model with these explanatory variables yields an Adjusted R-squared of 0.95 (Appendix Table B1). Finally, we predict the carbon intensities of the remaining fields in the Rystad dataset using this model. These predicted values are robust to changes in the sample of fields used to estimate the model.[10] Our estimates are consistent with those in the scientific literature (Appendix Figure B3). Appendix B.1 describes OPGEE, the matching procedure and results, the estimation model and the robustness checks in more detail.

Midstream carbon intensity. After reaching a refinery, crude oil from different fields is combined and refined into petroleum products, such as gasoline and other fuels. Refining processes emit mostly CO_2, CH_4 and N_2O that are the main GhG sources of this sector. We employ the OCI *Petroleum Refinery Life-Cycle Inventory Model* (PRELIM)[11] to assess midstream carbon intensities (see Appendix B.2). This engineering-based model requires very detailed information on the physical and chemical properties of oils ("crude assays"). As detailed oil properties are only partially available in Rystad, we proceed as follows. We first run PRELIM with the 149 assays of major oil crudes (from companies, specialized websites and past research) that are publicly available with PRELIM. We associate these crudes to their extraction site using operator and crude names, and location information in Rystad data. We then estimate PRELIM carbon intensities using the Rystad variables related to oil characteristics and known to impact refining carbon intensity: the API gravity index and the sulfur content. These determine the main refining configuration (deep/medium conversion or hydroskimming), that is the level of processing intensity.[12] Our approach

[10] Appendix B includes a series of robustness checks regarding CI estimation. We first investigate its potential sensitivity to some observations. The bottom panel of Appendix Figure B1 presents the correlation coefficients of OPGEE carbon intensities and the predicted values obtained when estimating (9) after having removed the OPGEE fields one-by-one, while Appendix Figure B2 depicts how the coefficients on the explanatory variables vary. We then consider model behavior when excluding a set of "influential" observations instead of each single observation (Appendix Table B2.) The definition of influential observations is based on Cook's distance. Overall, our model is robust to changes in the sample of deposits used to estimate (9).

[11] PRELIM and OPGEE use the same units of energy, and are designed so that their carbon intensities can be summed to track emissions from oil exploration through refining.

[12] A dummy for the largest private oil companies (the "Majors") is also added to capture unobservable oil characteristics that could affect refining and are tied to Majors' preferences regarding the chemical and

assumes that refineries are fixed,[13] so that heterogeneity in pollution due to installations or country particularities (from local air pollutant regulations, for example) can be ignored. We here focus on those midstream emissions that are tied to the nature of the extracted oil, i.e. that could be affected by a change in deposit extraction. Our parsimonious model explains more than half of the total variance in midstream carbon intensity. Last, we predict midstream CI for the rest of the crudes/fields in the Rystad dataset.

2.4 Descriptive evidence

This section provides descriptive evidence that: (i) the carbon intensity of oil extraction (and that of crude refining to a lesser extent) differs significantly across deposits; (ii) carbon intensities and private extraction costs are not strongly correlated; and (iii) proven oil reserves exceed climate-wise future demand.

Carbon intensity varies across oil deposits. From our estimation, the average upstream carbon intensity of oil in 2018 was 10.15 gCO_2eq/MJ, while average midstream carbon intensity was 5.15 gCO_2eq/MJ. Both upstream and midstream emissions vary across deposits. The distribution of upstream carbon intensities has considerable variance: 25% of the upstream CI distribution is under 6.65 gCO_2eq/MJ, 50% under 8.55, and 75% under 10.84. There is less variance in midstream carbon intensity: 25% of the midstream CI distribution is under 4.24 gCO_2eq/MJ, 50% under 4.87, and 75% under 5.19.

The combined upstream and midstream carbon intensities of oils extracted since 1992 vary by oil type (Figure 1(a)). Unconventional oils, such as heavy and extra-heavy oils, are about twice as polluting as conventional oils, such as light oils. Flaring and steam injection also play a role, and partly explain the large variation in carbon intensity within oil categories. As countries have different kinds of oils, the average carbon intensity of an oil barrel varies by country of extraction (Figure 1(b)): oil extracted in Indonesia, Algeria, Venezuela and Canada emits about twice as many emissions than the average barrel pumped in Saudi Arabia or Kuwait. There exists significant within-country heterogeneity: for instance, Canada is host to very different types of oils (oil sands, shale oil, conventional oil), whereas some other countries, such as Saudi Arabia or Kuwait, have more homogeneous oil located in only a few fields. OPEC members (the grey bars in the figure) are not a homogeneous group in terms

physical properties of their oils. This dummy has little influence on emissions.

[13] Assuming that refining technologies could change, or new refineries could be set up with the best-in-class climate-wise process, would add another lever of carbon mitigation and bring overall larger emission reductions (Jing et al., 2020). Our approach also assumes that refineries that treat heavy and extra heavy oil can be reconfigured at low cost to refine lighter oil. This assumption is consistent with heavy oil refining requiring complex configurations of refining units that include those used to refine lighter oils (see e.g., U.S. Energy Information Administration, 2020a).

of oil carbon intensity. As is apparent in Figures 1(a)-1(b), since 1992, polluting oil types have been extracted, refined and combusted instead of cleaner — and sometimes cheaper — alternatives.

Little correlation between carbon intensities and private extraction costs. Private extraction costs also differ across deposits. These vary with oil type (Appendix Figure C1, top panel), which translates into some countries, e.g. Kuwait, having average extraction costs around three to four times cheaper than those in countries with the most expensive oil, e.g. Canada and Brazil (Appendix Figure C1, bottom panel). These figures are consistent with the rankings based on country of extraction or/and oil types in IEA (2008) and Wood Mackenzie (2019).

At the fine level of disaggregation of our data, there is only little correlation between carbon intensity and private extraction costs (Appendix Figure F1).[14] Introducing production-based (the dashed best linear fit line) or reserve-based (the unbroken best linear fit line) weights does not change this conclusion: the low correlation applies to both barrels that have been extracted and barrels that are available for extraction. We then conjecture that cost-effective carbon mitigation in the oil industry implies a very different extraction path to that under a pro-competition policy that ignores pollution.

Too much oil. The scientific literature has highlighted that oil assets are too abundant, given the estimated carbon budgets, to keep the average-temperature increase under 1.5 or 2°C throughout the century (Meinshausen et al., 2009; McCollum et al., 2014; McGlade and Ekins, 2014). The back-of-the-envelope calculation in Covert et al. (2016) suggests that burning all fossil fuels in proven reserves would lead to a temperature rise of between 5.6 and 8.3°C. Using our carbon intensity estimates, extracting, refining and burning all proven reserves of oil (as recorded in Rystad) would generate about 692.5 $GtCO_2$, which is between 1.6 and over 3 times the average *total* remaining carbon budget (that encompasses emissions from oil, gas and coal, and land transformation) required to keep the temperature increase below 1.5°C (IPCC, 2014, 2018; Rogelj et al., 2019).[15] Figure 2(a) depicts the carbon intensity of remaining recoverable reserves in 1992—the year of the Rio Summit—together with the post-1992 demand to fulfill; these reserves vary significantly in carbon intensity, and more than half should be left untapped. These reserves also differ by private extraction cost (Figure 2(b)), and carbon intensity varies significantly within each bin of costs.

[14] The correlation coefficients between carbon intensity and private extraction costs are 0.07 and 0.05 when deposits are weighted by their 1992 reserves and total productions over the period 1992-2018, respectively.

[15] Extracting and refining all reserves would generate about 138.5 $GtCO_2$. The production and combustion of all reserves would generate 692.5 $GtCO_2$ life-cycle emissions assuming that downstream emissions account for 80% of life-cycle emissions for the average oil barrel, which is what we find when estimating historical downstream emissions using the *Oil Products Emissions Module* (OPEM) of the Oil-Climate Index.

Oil abundance in a carbon-constrained world, together with deposit heterogeneity in terms of private extraction costs and carbon intensity, emphasizes the importance of deposit selection and extraction order. Assuming no annual extraction limits and all of the resources available in 1992, a social planner interested only in reducing emissions would extract deposits to the left of the cumulative demand (vertical bar) in Figure 2(a); if only private extraction costs mattered, the preferred supply would chronologically follow extraction described by the cumulative cost-based supply in Figure 2(b), starting with the cheapest resource. With a mixed objective including both pollution costs and private economic costs, the selection of the deposits to exploit depends on the trade-off between private production and environmental costs. Section 3 clarifies this trade-off and the construction of the social planner's preferred counterfactual supply.

3 Measuring carbon misallocation

In this section, we present our method of estimating carbon misallocation in the oil industry, or equivalently the gains from supply recomposition. We first describe the construction of the counterfactual optimal supply. We then explain how we calculate the social gains of supply recomposition as the difference in discounted social costs between a baseline and a counterfactual supply, and how we account for the opportunity costs of barrel extraction that come from the finite nature of oil deposits. Last, we discuss the sources of social gains from supply recomposition: these relate to optimally selecting deposits in the counterfactual and correctly ordering their extraction over time.

3.1 Optimal extraction path

The optimal extraction path minimizes the discounted social cost (that factors in pollution), assuming that baseline annual demand is met. The current value of the marginal carbon cost, denoted by μ_t, increases at the rate of the social discount rate. The 2018 cost of a pollution unit, e.g., a ton of CO_2, is then constant over all emission years, and we call μ the discounted pollution cost in 2018: $\mu_t = \mu e^{r(t-2018)}$, with r being the social discount rate. Environmental costs are only a function of accumulated emissions, and the timing of pollution does not matter. This is consistent with regulation in the form of a global carbon budget constraint. As deposits have different carbon contents per barrel (θ_d), the carbon cost per barrel ($\theta_d \mu_t$) varies across deposits.

The construction of the (optimal) counterfactual is restricted by a number of feasibility constraints. First, a deposit's cumulative extraction is capped by its reserves. Second, annual

production from a deposit is limited by the capacities installed (that equal 10% of initial reserves, or the maximum observed production since 1970 if the latter is larger) to account for observed plateauing in field-level production (Höök et al., 2014).[16] Last, extraction from a deposit can only start after its (exogenous) historical discovery year.[17]

Let T_0 be the starting date of supply recomposition, T_f the end of the oil era, x_{dt} deposit d's annual production in barrels in year t, θ_d its carbon content per barrel,[18] c_d its extraction cost (current value), k_d its extractive capacities, t_d the discovery year ($t_d \leq T_f$), $R_{d,t}$ its reserves at the beginning of year t (with the convention that $R_{d,t} = R_{d,t_d}$ for all $t \leq t_d$), D_t World oil demand at date t, and r the social discount rate. Taking 2018 as the reference year, the social-cost minimization program is then:

$$\mathcal{P}_1(T_0, T_f, \mu): \quad \min_{x_{dt}} \quad \sum_{T_0}^{T_f} \sum_{d} (c_d + \theta_d \mu_t) x_{dt} e^{-r(t-2018)}$$

s.t.

$$\sum_{d} x_{dt} \geq D_t \text{ for all } t \tag{1}$$

$$\sum_{T_0}^{T_f} x_{dt} \leq R_{d,T_0} \text{ for all } d \tag{2}$$

$$0 \leq x_{dt} \leq k_d \text{ for all } t,\ d \tag{3}$$

$$x_{dt} = 0 \text{ for all } t < t_d \tag{4}$$

$$\mu_t = \mu e^{r(t-2018)} \text{ for all } t \tag{5}$$

where (1) ensures that annual demands are met, (2) that the cumulative production of a deposit does not exceed its reserves, (3) that the annual production of a deposit is below its extractive capacities, (4) that extraction cannot start before the deposit discovery year, and (5) is the time path of the social cost of carbon.

We refer to the vector of counterfactual annual deposit productions, $x^* \equiv (x^*_{dt})$, that satisfies $\mathcal{P}_1(T_0, T_f, \mu)$, as the *Optimum*. This extraction path is not trivial, and in particular we show that the following lemma holds:

[16] We allow extractive capacities to vary with depletion in a robustness check.

[17] Both reserves and deposit-discovery dates are assumed to be exogenous to carbon mitigation: this is a conservative assumption, as allowing for endogenous exploration would increase emission reductions from supply recomposition. In a robustness check, we consider a counterfactual in which all resources discovered post-1992 are available as early as 1992.

[18] Deposits' carbon intensities are assumed to be exogenous to carbon policy, as they are mostly driven by oil and reservoir characteristics, and technologies that are largely tied to these characteristics. However, allowing for endogenous technological change in response to carbon policy (thereby making carbon intensities endogenous) would produce greater gains from carbon pricing. In some robustness checks, we consider, for example, alternative carbon intensities that are updated to account for less flaring.

Lemma 1 *On the optimal extraction path:*

1. *As long as $\mu > 0$, the cheapest resource to extract might be left untapped forever.*

2. *The Herfindahl (1967) least-cost-first principle of extraction, generalized by Asker et al. (2019) with capacity constraints*[19] *when all oil resources end up being exhausted, does not hold. We can identify vectors of private extraction costs (c_i), annual demands (D_t), discovery dates (t_i), reserves (R_{i,T_0}), and extractive capacities (k_i) such that, with (x^*_{it}) being the solution of $\mathcal{P}_1(T_0, T_f, \mu)$:*

$$\exists (l, j, t, p > t) \text{ s.t. } \begin{array}{ll} c_l & < c_j \\ 0 < x^*_{lt} & < k_l \\ \sum\limits_{T_0 \leq s \leq t} x^*_{ls} & < R_{l,T_0} \\ x^*_{jt} & > 0 \\ t & \geq \max(t_l, t_j, T_0) \\ x^*_{lp} & > 0 \end{array}$$

3. *Even if (c_i) and (θ_i) are perfectly correlated, the extraction path that minimizes the discounted sum of private extraction costs (i.e. that solves $\mathcal{P}_1(T_0, T_f, 0)$) does not in general coincide with the optimal extraction path (that solves $\mathcal{P}_1(T_0, T_f, \mu)$ for $\mu > 0$).*

This lemma first notes that the pollution cost of some resources can prevent them from being exploited along the optimal path, even if they are cheaper than other extracted resources (part 1). It also indicates that a resource may be used in a given year, whereas a cheaper resource is available to be extracted more intensively that year (and will be in the future), which does not respect the least-cost first rule (part 2). This result — which holds even if pollution is ignored as long as all oil resources do not end up exhausted — is due to the potential opportunity cost of using a resource in a given year that is related to the cost of the different capacity constraints and reserve constraints over the entire extraction path. Deviating from "least-cost first" sometimes produces a lower overall discounted private extraction cost by the greater cumulative use of cheaper resources. For instance, an average-cost resource can be used to save a cheaper one in a certain year, so that this cheaper resource can be used later on to avoid using a worse resource in a year when the average-cost resource cannot be used more intensively as its capacity constraint binds. If the worse

[19] This principle amended to account for exogenous capacity constraints can be formulated as: For all years, using a resource in a given year implies that the capacity or reserve constraints bind for all cheaper resources that year.

resource is expensive enough, the gain from displacing this resource will be larger than the short-term cost of the deviation (due to the discounting). Finally, even if extraction costs and carbon intensities are perfectly correlated, the pollution-ignorant cost-effective supply may differ from the optimal supply (part 3). The proof of Lemma 1 appears in Appendix D.

As oil is abundant in a carbon-constrained world, extracting least-cost first is not necessarily a property of the optimal path, as shown in Lemma 1. In addition, the selection of the best pool of resources from which to extract, which depends on annual trade-offs between private extraction costs and pollution costs, is complex. As a consequence, we directly solve the cost-minimization program.

3.2 Carbon misallocation in a dynamic setting

Accounting for the dynamics. To measure carbon and private-cost misallocations, for instance since the 1992 Rio Summit, we compare the baseline supply structure to the cost-effective counterfactual that factors in deposit pollution costs described above, holding aggregate annual consumption constant. Were oil to no longer be used after 2018, this would boil down to comparing the social cost of the observed 1992-2018 production sequence to that of the counterfactual in which this cost is minimized over the same period, i.e the counterfactual that solves $\mathcal{P}_1(1992, 2018, \mu)$. This is what we do first. However, there is likely an opportunity cost of using barrels before 2018, as these would then be unavailable in the future. As such, any measure of carbon misallocation has to account for the value of the reserves left for later use.

We measure misallocation in this dynamic context by comparing the optimal counterfactual over the whole 1992-2050 period, i.e the counterfactual that solves $\mathcal{P}_1(1992, 2050, \mu)$, to a pollution-ignorant baseline composed of two sequences: (i) the observed 1992-2018 deposit-level extraction, and (ii) a future hypothetical private-cost-effective extraction over the 2019-2050 period. Total annual demand is the same in both the baseline and the counterfactual over 1992-2050. The pre-2019 annual oil demands are the observed ones. The post-2018 annual demands are consistent with the scenario in which demand falls linearly to reach carbon neutrality in 2050, in line with IPCC (2018) and European Council (2019) (see Appendix C).

Baseline extraction. Let $\tilde{x}_{dt}$ be the annual deposit production in the baseline. Baseline extraction is thus composed of two consecutive sequences: (i) observed production from T_0 to 2018 (inclusive), and (ii) a future hypothetical extraction path from 2019 to T_f, where T_f is the end of the oil era (with zero demand from that year onward). Historical deposit-level production up to 2018 comes from Rystad. The post-2018 sequence, when we assume that

oil will continue to be produced after 2018, is such that future private extraction costs are minimized while future annual demands are met. More precisely, the future baseline supply is the solution of the cost-minimization program $\mathcal{P}_1$ with 2019 as the starting date and 2050 as the end date ($T_0 = 2019$, $T_f = 2050$), while ignoring pollution ($\mu = 0$). This hypothetical future is consistent with current policies that aim to reduce emissions only via lower oil consumption, while ignoring heterogeneity in upstream and midstream carbon intensities.

Other parameters. In our main exercise, the social cost of carbon (SCC) in 2018 is set to $\mu = \$200$ per ton of CO_2eq. This is in line with the SCC in DICE2016R when the temperature increase is kept strictly below 2.5°C over the next 100 years (Nordhaus, 2017). We consider that oil-supply restructuring starts in $T_0 = 1992$. This is the year of the Rio Summit where participating countries acknowledged the necessity to abate World carbon emissions and promote cost-effective ways of doing so (see Appendix E). Deposit-level private extraction costs c_d, carbon intensities θ_d and reserves R_{dt} are described in Section 2 and Appendices B-C. The social discount rate is set to 3%.

3.3 Misallocation channels

The *Optimum* counterfactual supply reduces the social production cost (as compared to the baseline) via two channels. The first is the change in deposit-level cumulative extraction. As oil is abundant and deposits differ in their carbon intensities and private extraction costs, selecting the right cumulative quantities to extract from each deposit reduces social energy costs. These quantities depend on the trade-off between private extraction costs and environmental damage. The social gains are made up of environmental gains ($\sum_{1992}^{2050}\sum_d \theta_d\mu(\tilde{x}_{dt}-x^*_{dt})$) and private economic gains ($\sum_{1992}^{2050}\sum_d c_d(\tilde{x}_{dt} - x^*_{dt})e^{-r(t-2018)}$): environmental costs can only be reduced by changing deposits' cumulative extraction since the (discounted) carbon cost of a pollution unit is independent of the emission year. In contrast, economic gains can originate from both the selection of cheaper resources and the reordering of extraction to benefit from discounting. The second channel is the extraction order. Were the cumulative extractions from each deposit to be constrained to match those in the baseline, the social gains from supply restructuring would come only from the economic gains due to extraction reordering.

4 Results

The main measure of the cost from carbon and private extraction cost misallocations is the gap between the discounted total cost of the counterfactual production when supply

is restructured post-1991 and that from the baseline path. More precisely, let $\tilde{x}_{dt}$ be the baseline production of deposit d in year t. We define $\mathcal{MC}$ the misallocation cost saved by the counterfactual extraction path (x_{dt}), where d stands for the deposit d, between T_0 and T_f, when the social cost of carbon at date t is μ_t as :

$$\mathcal{MC} : ((\mu_t), (x_{dt}), T_0, T_f) \to \sum_{T_0}^{T_f} \sum_{d} (c_d + \theta_d \mu_t) \tilde{x}_{dt} e^{-r(t-2018)} - \sum_{T_0}^{T_f} \sum_{d} (c_d + \theta_d \mu_t) x_{dt} e^{-r(t-2018)}$$

This section presents the social gains from starting supply recomposition in 1992 or 2019. We then separate the gains from carbon pricing from those that relate to correcting pure private-cost misallocation. Third, we quantify countries' over- or under-extraction over the 1992-2018 period and their stranded assets, i.e. the part of their current reserves that should stay underground forever. Finally, we explore missed windows of mitigation opportunities, and quantify the gains from starting supply recomposition one year earlier when the start year varies between 1970 and 2018.

4.1 Gains from supply recomposition starting in 1992 or 2019

Upper bound of the gains. We first compare the counterfactual extraction path in which oil is extracted optimally from 1992 until 2018 to observed extraction over the same period. This counterfactual is constructed by minimizing social costs, comprised of environmental and private extraction costs, while leaving aggregate annual production unchanged and assuming oil is no longer used after 2018, i.e. it is the solution of $\mathcal{P}_1(T_0 = 1992, T_f = 2019, \mu = 200)$. This produces emissions that are 15.54 gigatons of CO_2 ($GtCO_2$) lower. This figure is an upper bound for the extra emissions due to misallocation over 1992-2018 as past supply recomposition limits our capacity to improve future supply as compared to the baseline future. 'Good' reserves are finite, and those resources that enter recomposed past supply are likely also to be those we would like to exploit to improve future extraction. To avoid overestimating misallocation, we consider also future extraction in our main exercise.[20]

Main exercise. In our main exercise, we compare the baseline to a counterfactual in which production is optimal over the whole 1992-2050 period (*Optimum*), i.e. that solves $\mathcal{P}_1(T_0 = 1992, T_f = 2050, \mu = 200)$. Let $x^*(1992, 2050, 200)$ be the counterfactual extraction vector. We denote by x^*_{dt} the corresponding production of deposit d in year t. The (full) Misallocation Cost ($\mathcal{MC}$) of the baseline over the 1992-2050 period with environmental

[20]The pre-2019 gains from the optimal supply computed over the 1992-2050 period are, in general, *strictly* smaller than the pre-2019 gains of the supply with no future. See Appendix D.

damage valued at $\mu_t = \mu e^{r(t-2018)}$, where $\mu = 200$, is:

$$\mathcal{MC}((\mu_t),(x^*_{dt}),1992,2050) \equiv \sum_{1992}^{2050}\sum_{d}(c_d + \theta_d\mu_t)\,(\tilde{x}_{dt} - x^*_{dt})\,e^{-r(t-2018)} \tag{6}$$

These misallocation costs are equal to the policy gains of suppressing the misallocation: throughout the paper, we will refer either to the misallocation costs of the baseline or the policy gains from supply restructuring. The corresponding fall in CO_2 emissions is:

$$\sum_{1992}^{2050}\sum_{d}\theta_d\tilde{x}_{dt} - \sum_{1992}^{2050}\sum_{d}\theta_d x^*_{dt} \tag{7}$$

The results appear in the first row of Table 1. The first column shows the total gains given in (6), from both reduced private extraction costs and lower emissions, while the second lists the corresponding drop in CO_2 emissions given in (7). These latter fall by 17.66 $GtCO_2$ over the whole 1992-2050 period, representing 60% of the maximum-possible emission reduction (29.3 $GtCO_2$ that we would obtain were μ infinite). These environmental gains are economically significant: they are valued at 3.53 trillion dollars when the social cost of carbon is \$200 (2018 present value). This represents a fall of 16% in total upstream and midstream oil emissions, while the aggregate quantity of oil supplied each year is unchanged. The IPCC estimates that the remaining carbon budget for *all* anthropic GhG emissions (as of the beginning of 2018) corresponding to a 66% chance of avoiding 1.5°C warming is between 120 and 420 $GtCO_2$ (IPCC, 2014, 2018). Carbon misallocation thus represents 15% (4%) of the lower (upper) bound of the remaining carbon budget. Of these 17.66 $GtCO_2$, 11.0 $GtCO_2$ come from reductions in emissions over the 1992-2018 period and 6.66 $GtCO_2$ over the 2019-2050 period. As actual 1992-2018 emissions were 69.8 $GtCO_2$, while 41 $GtCO_2$ are emitted post-2018 in the baseline, emissions dropped in the *Optimum* counterfactual by about 16% in both periods.

Missed opportunities and what can still be changed. We now look at the possible future gains from carbon pricing starting in 2019 (*Clean future*), compared to the baseline. Recall that the post-2019 baseline production minimizes the sum of discounted extraction costs. To determine the future supplies associated with the *Clean future* counterfactual and the baseline, we solve $\mathcal{P}_1(T_0 = 2019, T_f = 2050, \mu)$ with $\mu = \$200$ and $\mu = \$0$, respectively. We find emissions that are 7.64 $GtCO_2$ lower in the *Clean future* with associated social gains of 0.99 trillion US\$: see the first two columns and the second row in Table 1. These results call for three comments. First, despite the lower future demand, factoring pollution costs in when deciding on future oil extraction will bring large environmental benefits, valued at 1.52 trillion US\$, that come with an increased private cost of about 0.53 trillion US\$

$(= 1.52 - 0.99)$. This reflects that reserves as of 2019 are abundant and differ significantly in their private extraction costs and carbon intensities. Second, this reduction of 7.64 $GtCO_2$ is close to the 6.66 $GtCO_2$ reduction over the same period (2019-2050) obtained when optimal recomposition starts in 1992. In other words, the correction of carbon misallocation in the past would not preclude the large gains from the recomposition of current and future supply. This reflects that lower-carbon emission oil is relatively abundant. The third, and related, comment is that future emission reductions are much lower than the emissions drop of 17.66 $GtCO_2$ from carbon pricing starting in 1992. In other words, past environmental mistakes remain significant even if the best oil assets are eventually used in the future in place of dirtier but cheaper oil. Again, as good resources are relatively abundant, the opportunity cost of using clean resources in the past is small and does not prevent large gains later on in the extraction sequence. The missed opportunities of carbon mitigation in the past are then truly lost.

Lower bound of the gains over 1992-2018. Now, what is the value of these missed opportunities, i.e. what would have been the "early-action gains" from starting optimal extraction in 1992 rather than 2019? These early-actions gains are the opportunities we missed irreversibly as they cannot be mitigated by post-2018 optimal extraction. They represent a lower bound of misallocation costs over the 1992-2018 period. We calculate them by decomposing the gains from optimal extraction over the whole 1992-2050 period as follows, denoting x^*_Z as the solution of $\mathcal{P}_1(T_0 = Z, T_f = 2050, \mu)$:

$$\begin{aligned}\mathcal{MC}(\mu, x^*_{1992}, 1992, 2050) = \; & \underbrace{\mathcal{MC}(\mu, x^*_{1992}, 1992, 2050) - \mathcal{MC}(\mu, x^*_{2019}, 2019, 2050)}_{\text{Early-action gains}} \\ & + \underbrace{\mathcal{MC}(\mu, x^*_{2019}, 2019, 2050)}_{\text{future gains}} \end{aligned} \tag{8}$$

These early-action gains amount to 7.82 trillion US\$ $(= 8.81 - 0.99)$, and the corresponding emissions gains are 10.02 $GtCO_2$ $(= 17.66 - 7.64)$. The wrong selection of assets over 1992-2018 was thus responsible for, at least, 10.02 $GtCO_2$.

Figure 3 shows the emission reductions in the *Optimum* and *Clean future* counterfactuals as a function of the social cost of carbon (SCC). Emission reductions from supply recomposition rise with the SCC, but are very stable over a large SCC range. At \$100, the emission reductions from the *Optimum* and the *Clean future* are about 3/4 of those from the main exercise with a \$200 SCC. The misallocation due to the 1992-2018 period as defined in (8), represented by the gap between the two curves, is remarkably constant: it varies from 7 to 12.5 $GtCO_2$ as the SCC rises from \$50 to \$400/tCO_2. These results are important, as they indicate that most of the emission reductions in our main analysis would be worth doing even

for a SCC figure as low as \$50 and for the whole range of SCC discussed in the literature (see Appendix C.6).

Is imperfect competition the source of carbon misallocation? One striking result is that the *Optimum* scenario over the 1992-2050 period produces a lower total cost of 8.81 trillion US\$ relative to the baseline (the first column and first row in Table 1), of which 5.28 trillion US\$ corresponds to private extraction costs and 3.53 trillion US\$ to environmental costs. The environmental gains come with large private economic gains. Do the lower extraction costs show that clean oil is also the cheapest? That there is little correlation between private extraction costs and carbon intensities for all reserves available in 1992, as can be seen in Figure 2(b), suggests that this is not so. To demonstrate more rigorously that solving extraction-cost misallocation alone is not the principal source of environmental gains, we consider another counterfactual in which private extraction costs are minimized over the whole time path, absent any carbon pricing, i.e. the solution of $\mathcal{P}_1(1992, 2050, 0)$. We label this counterfactual *Minimal private costs*. We then compare this counterfactual to the baseline. Calling x_{dt}^{pc} the extraction of deposit d at time t in this counterfactual, we calculate the social gains of the cost-effective supply as

$$\mathcal{MC}((\mu_t), (x_{dt}^{pc}), 1992, 2050) \equiv \sum_{1992}^{2050} \sum_{d} (c_d + \theta_d \mu_t)(\tilde{x}_{dt} - x_{dt}^{pc}) e^{-r(t-2018)}$$

with $\mu_t = 200e^{r(t-2018)}$ to account for pollution cost and its impact on CO_2 emissions as $\sum_{1992}^{2050} \sum_d \theta_d (\tilde{x}_{dt} - x^{pc})$. The social gains here appear in the third row of Table 1: total costs fall by 6.63 trillion US\$, of which 6.26 trillion US\$ refer to lower private extraction costs. The corresponding drop in carbon emissions is only 1.87 $GtCO_2$, i.e. about 10% of the *Optimum* figure. Overall, carbon misallocation has little to do with cost misallocation. Comparing the social gains in the *Optimum* and the *Minimal private costs* counterfactuals (the first and third lines in the first column of Table 1), the specific gains from taking pollution into account instead of only minimizing private extraction costs amount to 2.18 trillion US\$ $(= 8.81 - 6.63)$.

Extraction order and the selection of resources. We know that the optimal production path differs from the baseline in two dimensions: the selection of resources and the extraction order. As far as pollution is concerned, the only way to reduce misallocation is to change some deposit's cumulative extraction as compared to the baseline, i.e., to extract more of the 'good' resources (that are not used, or not used enough, in the baseline) so as to avoid or reduce the use of 'bad' resources. Part of the misallocation in private extraction costs is also explained by the extraction of the wrong deposits in the past, and some from the wrong ordering of deposit use. To pin-down the cost of this wrong order, we consider an

alternative counterfactual in which the recomposition of supply is limited to deposit reshuffling (*Baseline reshuffling*). More precisely, we solve $\mathcal{P}_1(1992, 2050, 0)$ under the constraints that $\sum_{T_0}^{T_f} x_{dt} = \sum_{T_0}^{T_f} \tilde{x}_{dt}$ for all deposits d. Under this counterfactual, the cumulative extraction by deposit is left unchanged (as compared to the baseline) so that there is no possible environmental gain. The economic gain from this reordering is 4.65 trillion US$, over 88% of the gain in private extraction costs of 5.28 trillion US$ under the optimal counterfactual. The main source of extraction-cost misallocation can then be understood as the wrong order of asset use, whereas carbon misallocation only comes from the wrong selection of assets.

Feasibility constraint and other market failures. It can be argued that the environmental gains from the optimal extraction sequence would be difficult to obtain in practice as other sources of misallocation, such as market power, work in the opposite direction, or because countries would refuse to correctly price their domestic emissions were doing so to be to the detriment of their domestic oil industry.

We first address this issue in another counterfactual that constrains annual production in each OPEC member country to be equal to their historical value over the 1992-2018 period.[21] The results appear in the third and fourth columns of Table 1. Maintaining the annual productions of each OPEC country does not prevent significant emission reductions. We find environmental gains of carbon pricing of 17.78 $GtCO_2$, valued at 3.56 trillion US$: these are even slightly larger than the environmental gains estimated without the OPEC constraint. This constraint reduces total gains via increased private extraction costs: the gain in extraction costs falls to 3.53 trillion US$ ($= 7.09 - 3.56$), compared to 5.28 trillion US$ without the constraint.[22] Second, the difference between this constrained counterfactual and the optimum, which can be interpreted as the loss from OPEC's market power, is 1.72 trillion US$. By way of comparison, the difference between the optimum and the counterfactual that minimizes private extraction costs (absent any environmental costs) without the OPEC constraint is 2.18 trillion US$. This last difference can be interpreted as the gain from carbon pricing.[23] The gains from the removal of these two distinct market failures — imperfect competition and carbon misallocation — are of the same magnitude.

Supply recomposition can lead to large welfare changes across countries. Although the winners from optimal supply recomposition could in theory compensate adversely-affected countries, this compensation is politically difficult to establish. Countries may have a pref-

[21] We abstract from market-power considerations after 2018, as the recent literature has argued that OPEC market power has been considerably reduced (Huppmann and Holz, 2012) and modeling oil-market power is beyond the scope of this paper.

[22] The discounted profit of the OPEC over the 1992-2018 period increases in the optimum counterfactual, which partly alleviates political feasibility issues.

[23] The difference between these counterfactuals but with the OPEC constraint is 1.75 trillion US$.

erence for domestic production, for job-related, public-finance or energy-security reasons. These preferences may explain part of the cost misallocation we identify. In addition, country preferences may pose a problem of feasibility for any ambitious supply reallocation. We thus re-run our main exercise constraining counterfactual annual production in each country to either match observed production or to be greater than the minimum of their production and consumption in two distinct exercises.[24] The results are shown in Appendix Table F1. Recomposing supply still produces large social gains and emission reductions. When country-level productions are kept at their baseline levels (the last two columns), the emission reductions compared to the baseline are 17.21 $GtCO_2$, almost the same as the 17.66 $GtCO_2$ in the optimal counterfactual. In contrast, overall social gains fall to 6.28 (from 8.81 in Table 1), representing lower private economic gains of about 2.44 US$ trillion, from a figure of 5.28 US$ trillion (= 8.81-17.66*0.2: the economic gains from the optimum without the constraint in Table 1) to 2.84 US$ trillion (= 6.28-17.21*0.2: the economic gains with the constraint in Appendix Table F1). Within-country private-cost misallocations therefore account for about 54% of total extraction-cost misallocation (= 2.84/5.28). This is in line with the estimates in Asker et al. (2019) for the 1970-2014 period. While CO_2 total abatement is stable, the private economic gains are significantly reduced by the country-specific constraints. This reveals that there is relatively more within-country variation in carbon intensities than in private extraction costs.

4.2 Sensitivity analysis

Appendix Table F2 tabulates the estimated gains and emission reductions from a series of counterfactual productions when we change our model parameters. Postponing the end of the oil era to 2066 has a large positive impact on the gains from implementing carbon pricing in 2019 instead of never (*Clean future*), mostly because this implies a greater demand to satisfy in the future in both the baseline and the counterfactual. On the contrary, it has a relatively limited impact on the overall gains and emission reductions from starting supply recomposition in 1992. There are two elements to extending the time horizon. First, the greater the demand, the more opportunities there are to improve the baseline. Second, oil abundance is reduced: were oil demand sufficient to exhaust all deposits, supply recomposition could not generate environmental gains. With a time horizon of 2066, the first effect continues to dominate, with environmental gains over the whole path that are larger than with a 2050 time horizon. This is still the case if we postpone the end of oil even further. Setting this to 2080 produces larger environmental gains, while reducing the economic gains.

[24] This also implies that variations in oil-transportation costs between the new counterfactual and the baseline are considerably reduced.

Overall, the evidence indicates that cheap resources are relatively scarcer than less-polluting resources.

Reducing the discount rate from 3% to 1.5% lowers the overall gains from the *Optimum* counterfactual, via smaller economic gains: selecting cheaper resources in the past now brings lower discounted benefits and smaller gains from reordering.[25] A lower discount rate also reduces the fall in emissions in the optimal counterfactual, as it biases the post-2018 resource-selection trade-off towards cheaper resources (at the expense of pollution reduction). This seems to dominate the opposite effect on the resource-selection trade-off prior to 2018: the lower discount rate biases this latter trade-off towards less-polluting deposits (at the expense of cost savings) in the past.

We then relax the discovery constraint, and assume that all resources discovered after 1992 were available starting in 1992. This change reflects the situation in which resource exploration is sufficiently efficient to respond (at no cost) to carbon-pricing incentives and make resources discovered after 1992 immediately available when needed. Relaxing this constraint produces similar estimated gains and emission reductions.[26]

In another series of robustness checks, we modify the annual extraction-capacity from $\mathcal{P}_1$. New results are recorded in Appendix Table F3. We start by assuming that field production is capped by the maximum of (i) the field's highest observed production since 1970 and (ii) 5% or 15% of the 1970 reserves, instead of 10% as in the main specification. In a second step, we account for the fact that extraction from a field can be increasingly constrained by physical phenomenons, such as a drop in reservoir pressure (Anderson et al., 2018). We assume that a field's extraction rate (production-to-*current*-reserves ratio) cannot exceed 10% or the maximal extraction rate, in any year, for that field, if the latter is larger, as in Asker et al. (2019). We then keep extractive capacities as defined in our main approach but assume that only 75% of the reserves recorded in Rystad (or the cumulative production over the 1992-2018 period if the latter is greater) can be extracted. Overall, the gains and emission reductions are similar to those in Table 1.

We then consider alternative ways of estimating deposit carbon intensity. Appendix Table F4 shows the new results. We first allow for 10% less flaring in all fields where this is practiced, and re-estimate upstream carbon intensity accordingly. The new estimated gains in our counterfactuals stem from the comparison of gains from joint carbon pricing and flaring

[25] The gains from the reordering of baseline resource extraction sequence (*Baseline reshuffling*) are halved compared to those with a higher discount rate (see Table 1).

[26] For two reasons. First, the observed private extraction costs of new discoveries tend to rise over time. Second, even if the average resource found long after 1992 is used in the counterfactual, it would be used relatively late in the extraction sequence to benefit from discounting, even when discovery constraints are removed. Overall, the discovery constraint for this resource has little, if any, impact on the timing of its use.

reduction to a baseline that also features less flaring. This helps us to estimate the extra gains of carbon pricing compared to a field-level standard on flaring. The gains from carbon pricing and flaring reduction (the optimal counterfactual with flaring reduction) compared to the baseline supply (also re-estimated with 10% less flaring) are similar to those in the main specification without any flaring reduction. Second, we take into account that some gas is often lifted together with oil and may be sold on the market, displacing gas production elsewhere. The OPGEE model was run with the Co-Product Displacement approach (CPD), in which gas sold from an oil field produces emission credits that are deducted from the field's total CO_2 emissions.[27] Finally, we check that our main results are robust to field-level carbon intensities of extraction that vary by the field depletion rate, to dropping the part of emissions related to refining, and to adding downstream emissions to midstream and upstream emissions. Overall, the estimated gains from the different counterfactuals are robust to changes in carbon-intensity estimates.

We then change the way in which field-level private extraction costs are calculated. We swap our LCOE measures for average cost, or recalculate LCOEs excluding all production and costs before the optimization starting date (1992 for the *Optimum*, *Minimal private costs* and *Baseline reshuffling*, and 2019 for the *Clean future*); we last consider extraction costs that vary from year to year which allows us to account for changes in extraction inputs' costs. The social gains and emission reductions in Appendix Table F5 change only little.

Finally, we consider imperfect substitution between oils. First, we impose that the annual productions of each of three high-value petroleum products (gasoline, diesel, jet fuel) cannot be smaller than the observed productions while fixing product slates of each crude. Second, we split oil into two categories: the first consists of only light and regular oil, the second of all other types of oil resources. We constrain the annual production of each of these two categories in the counterfactual to be the same as in the baseline. Appendix Table F6 shows the new estimates. Overall, our results are robust to these changes.[28]

[27] The rationale here is that producing a similar amount of gas elsewhere would have emitted Greenhouse Gases. Carbon intensities using the CPD approach are similar to the main figures (Appendix Figure B4). In addition, we have checked that the quantity of gas produced from oilfields and sold on the market in the optimum is of the same magnitude as that in the baseline, so that oil-supply recomposition has a negligible impact on the gas market.

[28] Across all robustness checks, optimal reductions in CO_2 emissions over the whole 1992-2050 period lie between 15.4 (when 25% of the reserves are not exploitable) and 23.24 $GtCO_2$ (oil era ends in 2080). Future environmental gains lie between 5.47 (when 25% of the reserves are not exploitable) and 12.91 (oil era ends in 2080). Missed opportunities of the 1992-2018 period lie between 8.7 (when midstream pollution is discarded) and 12.3 (with time varying costs) $GtCO_2$. The reduction in pollution in the competitive counterfactual lies between -4.3% of the optimal reduction (i.e. pollution actually increases in the competitive counterfactual compared to the baseline, when field carbon intensity varies with depletion) and 27.6% of the optimal reduction (with time varying costs).

4.3 Stranded assets: past and future

The environmental gains from the optimal counterfactual come from extracting cleaner oil deposits. Table 2 shows the country implications as the change in cumulative 1992-2018 production of the main oil producers when pollution starts to be accounted for in 1992 rather than 2019. These changes can be interpreted as their carbon debts or credits as of 2019. Had carbon been priced properly and production been optimal, 51.5% of the oil that Russia extracted between 1992 and 2018 should have stayed underground. In contrast, Saudi Arabia should have increased its extraction by 179.4% compared to its actual extraction figure. The Annex B countries, the advanced economies that committed to reduce their emissions in the Kyoto Protocol, over-extracted oil in the past: they should have extracted 66.0% less oil than they actually did, while the Non-Annex B countries should have extracted 30.7% more.

We cannot change the past, but we can act on the future. Where are the stranded assets in 2019, and how should their breakdown change if pollution is accounted for in 2019? The first column of Table 3 lists the stranded assets — the share of resources that will be left untouched forever — in the *Baseline future*, i.e. when carbon is not factored in but private extraction costs are minimized, and column two the stranded assets in the *Clean future* scenario, i.e. when oil is optimally extracted from 2019 onwards. In both scenarios, 69% of oil reserves should stay underground due to the shrinking of future demand. The share of stranded resources varies greatly across countries. If the future is clean, the country with the fewest stranded assets is Kuwait, with a percentage figure of only 15.3%, while 97.4% of Canadian resources are stranded. The stranded-assets percentage is similar in most countries for the clean future and baseline future. The UAE, Iraq, Norway, and Algeria are exceptions, as they have oil that ranks well in one dimension—extraction costs or pollution contents—but badly in the other. For instance, Norway has expensive but not very polluting oil: it thus has fewer stranded assets in the optimal scenario than in the competitive scenario. On the contrary, Algeria has cheap but polluting oil; it thus has more stranded assets in the optimal future than in the baseline. In the future, optimal taxes that reflect carbon-intensity heterogeneity rather than uniform oil taxation thus tackle important redistribution problems for only a few countries. Overall, there is significant room today for welfare-improving supply recomposition within countries, which partly alleviates political-feasibility issues.

4.4 Missed windows of opportunity: 1970-2018

The 1992 Earth Summit was not the only window of opportunity for the implementation of ambitious worldwide carbon mitigation in the oil industry.[29] We consider alternative dates of carbon-mitigation onset since 1970 to measure the gains from starting carbon mitigation one year earlier. The estimates of these gains appear in Figure 4. The red curve (circles) depicts the supplementary gains from starting optimal carbon mitigation (*Optimum*) one year earlier. The blue curve (squares) represents the pure economic gains from starting the minimization of private extraction costs one year earlier, when the environmental gains and losses are not accounted for in the cost-minimization program (*Minimal private costs*). The green curve (crosses) represents the supplementary social gains from the same counterfactual, but valuing unlooked-for environmental gains or losses at US$200 per ton of CO_2 in 2018. Last, the purple curve (diamonds) plots the economic gains from reshuffling the deposits used in the baseline (*Baseline reshuffling*).

The area below the red curve between 1992 and 2018 represents the social gain from starting optimal production in 1992 rather than 2019: this is 7.82 trillion US$ (the first row minus the second row in the first column of Table 1). These social gains can be decomposed into four parts. The first is the area below the purple curve, representing the gains from reshuffling the baseline deposits; these gains are only due to the discounting of extraction costs. The second is the area between the purple and blue curves, measuring the gains from selecting a new pool of deposits to reduce private extraction costs. The third is the area between the blue and green curves, the environmental co-benefit from private-cost minimization. Last, the fourth part is the area between the red and green curves, which is the gain associated with the optimal selection of deposits, rather than the selection of deposits only to minimize private extraction costs.

Figure 4 brings three main insights into missed mitigation opportunities. First, the additional gains from starting regulation earlier are always large, even as far back in time as the 1970s. About two-thirds of these remote gains come from the reshuffling of the baseline (purple curve). The resources used in the 1970s were not the cheapest: due to discounting, reshuffling these over a long time period yields gains of about 150 billion US$ for each extra year included in the reshuffling. Over one quarter of the 1970-1975 gains can be attributed to the counterfactual regulation (the area between the red and green curves), indicating that the pool of available lower-emitting resources is large and opportunity costs due to the

[29] Building on accumulated scientific evidence that stressed the anthropic origins of climate change, policy-makers discussed carbon mitigation as early as the 1960s (e.g., U.S. President Lyndon B. Johnson's Science Advisory Committee, 1965). After the Rio Summit, a series of major international negotiations (e.g., the Kyoto Protocol voted in 1997, the Doha Amendment voted in 2012, and the COP21 in 2015) could have led to more-ambitious mitigation policies. Appendix E provides more details on the carbon-policy context.

scarcity of good deposits, although not absent, are only of second order.

A second insight is that these additional gains are very large when optimization starts during the 2009-2019 period, due in part to the sharp increase in supply from 2009 to 2015 (the bottom panel of Appendix Figure F2). The corresponding gains normalized by annual production increase at a much slower rate (Appendix Figure F4). Another reason is baseline quality: observed extraction costs rose between 2009 and 2019 (the middle panel of Appendix Figure F2), mainly due to the US Shale Oil Revolution[30] and the Oil Sands boom in Canada. The largest share of the gains comes from switching from the baseline to the minimization of private extraction costs (the blue curve), rather than switching from the minimization of extraction costs to optimal supply (the difference between the blue and red curves).

A third insight is that the 'Oil Counter-Shock' (1980s) is the source of large carbon misallocation. Potential additional gains are relatively larger between 1979 and 1992, and in particular between 1982 and 1990. This is even clearer when considering gains per barrel to avoid any effect of the size of baseline demand (Appendix Figure F4). The large benefits (about 275 billion US$ for each extra year of production optimization) mainly come from the composition of baseline production. Over most of the 1980s, the combination of high carbon intensities and high private extraction costs explains the large gains per extracted barrel in the optimal counterfactual as against the baseline.[31]

5 Conclusions

This paper has explored a supply-side approach to the mitigation of carbon emissions in the oil industry. As oil demand can be satisfied by plentiful deposits that differ in private extraction costs and carbon intensity, the industry's carbon footprint could be reduced by pumping barrels from lower-carbon intensity deposits. In our setting, these changes in cumulative deposit use are the only source of environmental gains. We have identified carbon misallocation by comparing the baseline deposit-level supplies to counterfactual production that factors in pollution costs but leaves aggregate demand unchanged. Our approach thus

[30] The average barrel of US Shale Oil extracted over the period 2009-2018 is about twice as expensive and 4% less polluting than the median oil barrel (but is more polluting than the average conventional-oil barrel).

[31] Over the 1979-1985 period, extraction costs increased (Appendix Figure F2, middle panel). This is partly explained by the drop in Iranian oil production after the Iranian Revolution of 1978-1979 and the reduced productions of the belligerents in the Iran-Iraq War (1980-1988) (Appendix Figure F3). While extraction became costlier, the environmental quality of the baseline improved before 1982, as both Iraqi and Iranian oils are more polluting than average. However, between 1982 and 1985 higher extraction costs were accompanied by a rise in the average barrel's carbon intensity. This is partly due to the fact that Saudi Arabia, whose oil is both cleaner and cheaper than average, voluntarily shut down 3/4 of its production between 1981 and 1985 (Appendix Figure F3) to prevent a slump in oil prices. Part of this drop in production was compensated by greater production in Russia, where oil is more polluting and more expensive to extract.

contrasts with current policies that aim to reduce oil consumption. Even though these policies are necessary, they significantly reduce consumer surplus, as the low price-elasticity of transport demand is compounded by the scarcity of clean substitutes for oil in this sector.

Our findings contribute to the ongoing debate about the decarbonization of the World economy. The main takeaway is that the missed opportunities for carbon mitigation in the oil industry are large: optimal oil-deposit reallocation would have reduced emissions by at least 10.02 $GtCO_2$ over the 1992-2018 period. This is economically significant as compared to the remaining carbon budget (Mengis et al., 2018; IPCC, 2014, 2018) or if translated into environmental costs. These inefficient extra emissions are robust to varying the social cost of carbon between US$50 and US$400. Our data also allow us to map supply-side ecological debts: We find that Annex B countries, which committed to mitigation targets in the Kyoto Protocol, over-extracted oil by 66% over the 1992-2018 period. Some non-Annex B countries, such as Algeria, Venezuela, Nigeria, Mexico, also over-extracted oil during this period.

The second takeaway is that past carbon misallocation is largely different from private-cost misallocation. We find large misallocation in private extraction costs, with expensive oil being extracted in place of cheaper oil. However, solving this latter market failure alone produces emission reductions that are 10 times smaller than those from optimal supply. We have shown that even were carbon intensities and private extraction costs to be perfectly correlated, cost-efficient extraction (that ignores pollution) may differ from the optimal extraction path. The difference between these two paths is obviously even larger in real life. Using our field-level data, we have provided evidence that private extraction costs and carbon intensities are poorly correlated, which makes carbon misallocation empirically very distinct from private-cost misallocation.

The third takeaway concerns what can still be changed. We evaluate the gains from optimally extracting available resources, as compared to a competitive future supply with identical annual demand but in which pollution is ignored. Starting to extract oil optimally in 2019 reduces emissions by 7.64 $GtCO_2$. Last, we estimate countries' stranded reserves as of 2019 under an optimal future-extraction scenario. There is great heterogeneity in stranded assets across countries, with figures varying from 15.3% for Kuwait to 97.4% in Canada.

This brings into question the political feasibility of first-best supply. Although optimal supply comes with both environmental and private economic gains, so that the winners could compensate the losers, these transfers may be difficult to put in place. However, we have shown that recomposing supply while constraining the changes in some countries' productions still leaves large potential gains from supply recomposition. This partly alleviates political-feasibility concerns.

How can these recommended deposit-level supplies be implemented? A tax in the past

chosen over a relatively-large range would have led to emission reductions in the past of the same order. The existence of relatively low-carbon emitting resources that are also cheap to extract implies that even a small tax in the US$50-100 range leads to significant emission reductions. However, an effective tax might actually be larger than the true carbon price to account for the ability of oil producers to sacrifice some rent and absorb part of the tax (Heal and Schlenker, 2019). Carbon pricing may raise opposition: for instance, some countries may refuse to implement carbon pricing in order to carry on extracting domestic dirty resources. Consumer countries from a 'Green' coalition could set border carbon adjustments (McLure, 2014) or simply ban imports from non-cooperative countries with these dirty deposits. To durably prevent any country from consuming dirty oil, the 'Green' coalition could also buy the oil deposits in a supply-side policy *à la* Harstad (2012). Taking this approach, can we find a simple rule to lower emissions as in the optimal supply? Political feasibility sometimes rhymes with simplicity: precluding extraction from the 'worst oils' can be effected by categorizing high carbon-intensity deposits via the oil type and flaring levels. In detail, buying all of the deposits of bitumen, extra-heavy or heavy oils, and deposits in the top 18% of the flaring-to-oil ratio distribution in 1992 to prevent their exploitation, and then extracting the other deposits in a cost-effective way without any further pollution considerations would have generated the same emission reduction as over the optimal path (about 17.66 $GtCO_2$ over the 1992-2050 period). This is, however, significantly costlier than the optimal policy, as it reduces the associated private economic gains to US$ 3.62 trillion, as compared to 5.28$ trillion over the optimal supply path.

References

Agrawala, Shardul. "Context and early origins of the Intergovernmental Panel on Climate Change." *Climatic Change* 39, 4: (1998) 605–620.

Anderson, Soren T., Ryan Kellogg, and Stephen W. Salant. "Hotelling under Pressure." *Journal of Political Economy* 126, 3: (2018) 984–1026.

Andrade de Sá, Saraly, and Julien Daubanes. "Limit pricing and the (in)effectiveness of the carbon tax." *Journal of Public Economics* 139: (2016) 28–39.

Anthoff, David, and Richard S.J. Tol. "The uncertainty about the social cost of carbon: A decomposition analysis using fund." *Climatic Change* 117, 3: (2013) 515–530.

Asker, John, Allan Collard-Wexler, and Jan De Loecker. "(Mis)Allocation, Market Power, and Global Oil Extraction." *American Economic Review* 109, 4: (2019) 1568–1615.

Baum, Rudy M. (Sr). "The first climate change believer." Distillations, Science History Institute, 2016. https://www.sciencehistory.org/distillations/future-calculations#:~:text=The%20first%20climate%20change%20believer.&text=Danish%20painter%20P.S.%20Kr%C3%B8yer's%20The,machines%20would%20increase%20global%20temperatures.

Benchekroun, Hassan, Gerard van der Meijden, and Cees Withagen. "OPEC, unconventional oil and climate change - On the importance of the order of extraction." *Journal of Environmental Economics and Management* 104: (2020) 102,384.

Borenstein, Severin, James B. Bushnell, and Frank A. Wolak. "Measuring Market Inefficiencies in California's Restructured Wholesale Electricity Market." *American Economic Review* 92, 5: (2002) 1376–1405.

BP. "BP Statistical Review of World Energy, 68th edition." Technical report, British Petroleum, 2019.

Brandt, Adam R., and Alexander E. Farrell. "Scraping the bottom of the barrel: greenhouse gas emission consequences of a transition to low-quality and synthetic petroleum resources." *Climatic Change* 84, 3-4: (2007) 241.

Brandt, Adam R., Mohammad S. Masnadi, Jacob G. Englander, Jonathan Koomey, and Deborah Gordon. "Climate-wise choices in a world of oil abundance." *Environmental Research Letters* 13, 4: (2018) 044,027.

Brandt, Adam R., Yuchi Sun, and Kourosh Vafi. "Uncertainty in regional-average petroleum ghg intensities: countering information gaps with targeted data gathering." *Environmental Science & Technology* 49, 1: (2015) 679–686.

Budyko, Mikhail I. "The effect of solar radiation variations on the climate of the Earth." *Tellus* 21, 5: (1969) 611–619.

Calel, Raphael, and Paasha Mahdavi. "Opinion: The unintended consequences of antiflaring policies—and measures for mitigation." *Proceedings of the National Academy of Sciences* 117, 23: (2020) 12,503–12,507.

Calel, Raphael, and David A. Stainforth. "On the physics of three integrated assessment models." *Bulletin of the American Meteorological Society* 98, 6: (2017) 1199–1216.

Calel, Raphael, David A. Stainforth, and Simon Dietz. "Tall tales and fat tails: the science and economics of extreme warming." *Climatic Change* 132, 1: (2015) 127–141.

Callendar, G.S. "Temperature fluctuations and trends over the earth." *Quarterly Journal of the Royal Meteorological Society* 87, 371: (1961) 1–12.

CFA. "The Economics of Petroleum Refining." Discussion papers, Canadian Fuels Association, 2013.

Chakravorty, Ujjayant, Michel Moreaux, and Mabel Tidball. "Ordering the Extraction of Polluting Nonrenewable Resources." *American Economic Review* 98, 3: (2008) 1128–1144.

Chavan, Chetan, Mihir Jha, Manjit Kumar Singh, and Ratan Singh. "Selection and Successful Application of Jet Pumps in Mangala Oil field: A Case Study." In *SPE Artificial Lift Conference and Exhibition*. Society of Petroleum Engineers, 2012.

Correa, Juan A., Marcos Gómez, Andrés Luengo, and Francisco Parro. "Environmental Misallocation in the Copper Industry." Technical report, Mimeo, 2020.

Coulomb, Renaud, and Fanny Henriet. "The Grey Paradox: How fossil-fuel owners can benefit from carbon taxation." *Journal of Environmental Economics and Management* 87: (2018) 206–223.

Covert, Thomas, Michael Greenstone, and Christopher R. Knittel. "Will we ever stop using fossil fuels?" *Journal of Economic Perspectives* 30, 1: (2016) 117–38.

Creutzig, Felix, Patrick Jochem, Oreane Y. Edelenbosch, Linus Mattauch, Detlef P. van Vuuren, David McCollum, and Jan Minx. "Transport: A roadblock to climate change mitigation?" *Science* 350, 6263: (2015) 911–912.

Dietz, Simon, and Nicholas Stern. "Endogenous growth, convexity of damage and climate risk: how Nordhaus' framework supports deep cuts in carbon emissions." *Economic Journal* 125, 583: (2015) 574–620.

Elvidge, Christopher, Mikhail Zhizhin, Kimberly Baugh, Feng-Chi Hsu, and Tilottama Ghosh. "Methods for global survey of natural gas flaring from visible infrared imaging radiometer suite data." *Energies* 9, 1: (2016) 14.

European Commission. "Kyoto 1st commitment period (2008–12)." European Commission, 2020. https://ec.europa.eu/clima/policies/strategies/progress/kyoto_1_en.

European Council. "Conclusions of 12 December 2019." European Council, 2019. https://www.consilium.europa.eu/en/press/press-releases/2019/12/12/european-council-conclusions-12-december-2019/.

Farina, Michael F. "Flare Gas Reduction: Recent global trends and policy considerations." Technical report, General Electric Company, 2011.

Financial Accountability Office of Ontario. "Cap and Trade: A Financial Review of the Decision to Cancel the Cap and Trade Program." Technical report, Financial Accountability Office of Ontario, 2018.

Fischer, Carolyn, and Stephen W. Salant. "Balancing the carbon budget for oil: The distributive effects of alternative policies." *European Economic Review* 99: (2017) 191–215.

Gates, Ian D., and Stephen R. Larter. "Energy efficiency and emissions intensity of SAGD." *Fuel* 115: (2014) 706–713.

Gillingham, Kenneth, William Nordhaus, David Anthoff, Geoffrey Blanford, Valentina Bosetti, Peter Christensen, Haewon McJeon, and John Reilly. "Modeling uncertainty in integrated assessment of climate change: a multimodel comparison." *Journal of the Association of Environmental and Resource Economists* 5, 4: (2018) 791–826.

Gordon, Deborah, Adam R. Brandt, Joule Bergerson, and Jon Koomey. *Know your oil: creating a global oil-climate index*. Carnegie Endowment for International Peace Washington, DC, 2015.

Greene, Suzanne, Haiying Jia, and Gabriela Rubio-Domingo. "Well-to-tank carbon emissions from crude oil maritime transportation." *Transportation Research Part D: Transport and Environment* 88: (2020) 102,587.

Guner, Nezih, Gustavo Ventura, and Yi Xu. "Macroeconomic implications of size-dependent policies." *Review of Economic Dynamics* 11, 4: (2008) 721–744.

Gupta, Joyeeta. "A history of international climate change policy." *Wiley Interdisciplinary Reviews: Climate Change* 1, 5: (2010) 636–653.

Hansen, Petter Vegard, and Lars Lindholt. "The market power of OPEC 1973–2001." *Applied Economics* 40, 22: (2008) 2939–2959.

Harstad, Bård. "Buy coal! A case for supply-side environmental policy." *Journal of Political Economy* 120, 1: (2012) 77–115.

Heal, Geoffrey, and Wolfram Schlenker. "Coase, Hotelling and Pigou: The Incidence of a Carbon Tax and CO_2 Emissions." Working Paper 26086, National Bureau of Economic Research, 2019.

Herfindahl, Orris C. *"Depletion and Economic Theory" In Extractive Resources and Taxation ed. Mason Gaffney, 63-90.* University of Wisconsin Press, 1967.

Höök, Mikael, Simon Davidsson, Sheshti Johansson, and Xu Tang. "Decline and depletion rates of oil production: a comprehensive investigation." *Philosophical Transactions of the Royal Society A: Mathematical, Physical and Engineering Sciences* 372, 2006: (2014) 20120,448.

Hopenhayn, Hugo. "Firms, misallocation, and aggregate productivity: A review." *Annual Review of Economics* 6, 1: (2014) 735–770.

Hopenhayn, Hugo, and Richard Rogerson. "Job Turnover and Policy Evaluation: A General Equilibrium Analysis." *Journal of Political Economy* 101, 5: (1993) 915–938.

Hotelling, Harold. "The Economics of Exhaustible Resources." *Journal of Political Economy* 39, 2: (1931) 137–175.

Hsieh, Chang-Tai, and Peter J. Klenow. "Misallocation and manufacturing TFP in China and India." *The Quarterly Journal of Economics* 124, 4: (2009) 1403–1448.

Huppmann, Daniel, and Franziska Holz. "Crude Oil Market Power – A Shift in Recent Years?" *The Energy Journal* 33, 4: (2012) 1–22.

IEA. *World Energy Outlook 2008.* International Energy Agency, Paris, 2008.

———. "IEA Refinery Margins: Methodology Notes." Discussion papers, International Energy Agency, Oil Industry and Markets Division, 2012.

———. "The Future of Petrochemicals." Technical report, International Energy Agency, 2018a.

IEA, Christophe McGlade, Glenn Sondak, Mei Han. "Whatever happened to enhanced oil recovery?" International Energy Agency, November 28, 2018b. https://www.iea.org/newsroom/news/2018/november/whatever-happened-to-enhanced-oil-recovery.html.

IPCC. "Climate Change 2014: Synthesis Report. Contribution of Working Groups I, II and III to the Fifth Assessment Report of the Intergovernmental Panel on Climate Change [Core Writing Team, R.K. Pachauri and L.A. Meyer (eds.)].", 2014.

———. "An IPCC Special Report on the impacts of global warming of 1.5°C above pre-industrial levels and related global greenhouse gas emission pathways, in the context of strengthening the global response to the threat of climate change, sustainable development, and efforts to eradicate poverty [V. Masson-Delmotte, P. Zhai, H. O. Pörtner, D. Roberts, J. Skea, P.R. Shukla, A. Pirani, W. Moufouma-Okia, C. Péan, R. Pidcock, S. Connors, J. B. R. Matthews, Y. Chen, X. Zhou, M. I. Gomis, E. Lonnoy, T. Maycock, M. Tignor, T. Waterfield (eds.)].", 2018.

Jing, Liang, Hassan M. El-Houjeiri, Jean-Christophe Monfort, Adam R. Brandt, Mohammad S. Masnadi, Deborah Gordon, and Joule A. Bergerson. "Carbon intensity of global crude oil refining and mitigation potential." *Nature Climate Change* 10: (2020) 526–532.

Knaus, Christopher. "Mining firms worked to kill off climate action in Australia, says ex-PM." The Guardian, October 10, 2019. https://www.theguardian.com/environment/2019/oct/10/mining-firms-worked-kill-off-climate-action-australia-ex-pm-kevin-rudd.

Lamp, Stefan, and Mario Samano. "(Mis)allocation of Renewable Energy Sources." Technical report, TSE Working Paper, n° 20-1103, 2020.

Le Treut, Hervé, Ulrich Cubasch, and Myles Allen. "Historical Overview of Climate Change Science." *Notes* 16.

Lemoine, Derek. "The Climate Risk Premium: How Uncertainty Affects the Social Cost of Carbon." *Journal of the Association of Environmental and Resource Economists* 8, 1: (2021) 27–57.

Lenton, Timothy M., and Juan-Carlos Ciscar. "Integrating tipping points into climate impact assessments." *Climatic Change* 117, 3: (2013) 585–597.

Lipton, Eric. "Behind the Coal Industry's Trump-Era Lobbying War." The New York Times, October 5, 2020. https://www.nytimes.com/2020/10/05/us/politics/coal-trump-industry-lobbying.html.

Malins, Chris, Sebastian Galarza, Anil Baral, Gary Howorth, and Adam Brandt. "The Development of a Greenhouse Gas Emissions Calculation Methodology for Article 7a of the Fuel Quality Directive. Report to the European Commission Directorate-General for Climate Action." Technical report, Washington D.C.: The International Council on Clean Transportation (ICCT), 2014a.

Malins, Chris, Stephanie Searle, Anil Baral, Sebastian Galarza, and Haifeng Wang. "The reduction of upstream greenhouse gas emissions from flaring and venting. Report to the European Commission Directorate-General for Climate Action." Technical report, Washington D.C.: The International Council on Clean Transportation (ICCT), 2014b.

Masnadi, Mohammad S., and Adam R. Brandt. "Climate impacts of oil extraction increase significantly with oilfield age." *Nature Climate Change* 7, 8: (2017) 551–556.

Masnadi, Mohammad S., Hassan M. El-Houjeiri, Dominik Schunack, Yunpo Li, Jacob G. Englander, Alhassan Badahdah, Jean-Christophe Monfort, James E. Anderson, Timothy J. Wallington, Joule A. Bergerson, Deborah Gordon, Jonathan Koomey, Steven Przesmitzki, Inês L. Azevedo, Xiaotao T. Bi, James E. Duffy, Garvin A. Heath, Gregory A. Keoleian, Christophe McGlade, D. Nathan Meehan, Sonia Yeh, Fengqi You, Michael Wang, and Adam R. Brandt. "Global carbon intensity of crude oil production." *Science* 361, 6405: (2018) 851–853.

McCollum, David, Nico Bauer, Katherine Calvin, Alban Kitous, and Keywan Riahi. "Fossil resource and energy security dynamics in conventional and carbon-constrained worlds." *Climatic change* 123, 3-4: (2014) 413–426.

McGlade, Christophe, and Paul Ekins. "Un-burnable oil: An examination of oil resource utilisation in a decarbonised energy system." *Energy Policy* 64: (2014) 102–112.

———. "The geographical distribution of fossil fuels unused when limiting global warming to 2C." *Nature* 517, 7533: (2015) 187–190.

McLure, Charles E. (Jr). "Selected international aspects of carbon taxation." *American Economic Review* 104, 5: (2014) 552–56.

Meinshausen, Malte, Nicolai Meinshausen, William Hare, Sarah C.B. Raper, Katja Frieler, Reto Knutti, David J. Frame, and Myles R. Allen. "Greenhouse-gas emission targets for limiting global warming to 2°C." *Nature* 458, 7242: (2009) 1158–1162.

Mengis, Nadine, Jonathan Jalbert, Antti-Ilari Partanen, and H. Damon Matthews. "1.5°C carbon budget dependent on carbon cycle uncertainty and future non-CO_2 forcing." *Scientific Reports* 5831.

Michielsen, Thomas O. "Brown backstops versus the green paradox." *Journal of Environmental Economics and Management* 68, 1: (2014) 87–110.

Mui, Simon, Luke Tonachel, and E. Shope. "GHG emission factors for high carbon intensity crude oils." *Natural Resources Defense Council* 2.

Murray, Brian, and Nicholas Rivers. "British Columbia's revenue-neutral carbon tax: A review of the latest "grand experiment" in environmental policy." *Energy Policy* 86: (2015) 674–683.

Nordhaus, William D. "The 'DICE' model: Background and structure of a dynamic integrated climate-economy model of the economics of global warming." Technical report, Cowles Foundation for Research in Economics, Yale University, 1992.

———. *Managing the global commons: the economics of climate change*, volume 31. MIT Press Cambridge, MA, 1994.

———. "A review of the Stern review on the economics of climate change." *Journal of Economic Literature* 45, 3: (2007) 686–702.

———. "Revisiting the social cost of carbon." 114, 7: (2017) 1518–1523.

Pindyck, Robert S. "Climate change policy: What do the models tell us?" *Journal of Economic Literature* 51, 3: (2013) 860–72.

———. "The social cost of carbon revisited." *Journal of Environmental Economics and Management* 94: (2019) 140–160.

Replogle, Michael, Ramiro Alberto Ríos Flores, Christopher Porter, Wendy Tao, María Pia Iannariello, and Gautam Dutt. "Mitigation Strategies and Accounting Methods for Greenhouse Gas Emissions from Transportation." Technical report, Inter-American Development Bank, 2013.

Restuccia, Diego, and Richard Rogerson. "Policy distortions and aggregate productivity with heterogeneous establishments." *Review of Economic Dynamics* 11, 4: (2008) 707–720.

Revesz, Richard L., Peter H. Howard, Kenneth Arrow, Lawrence H. Goulder, Robert E. Kopp, Michael A. Livermore, Michael Oppenheimer, and Thomas Sterner. "Global warming: Improve economic models of climate change." *Nature News* 508, 7495: (2014) 173.

Rogelj, J., D. Shindell, K. Jiang, S. Fifita, P. Forster, V. Ginzburg, C. Handa, H. Kheshgi, S. Kobayashi, E. Kriegler, L. Mundaca, R. Séférian, and M.V. Vilariño. "Mitigation Pathways Compatible with 1.5°C in the Context of Sustainable Development. In: Global Warming of 1.5°C. An IPCC Special Report on the impacts of global warming of 1.5°C above pre-industrial levels and related global greenhouse gas emission pathways, in the context of strengthening the global response to the threat of climate change, sustainable development, and efforts to eradicate poverty [V. Masson-Delmotte, P. Zhai, H. O. Pörtner, D. Roberts, J. Skea, P.R. Shukla, A. Pirani, W. Moufouma-Okia, C. Péan, R. Pidcock, S. Connors, J. B. R. Matthews, Y. Chen, X. Zhou, M. I. Gomis, E. Lonnoy, T. Maycock, M. Tignor, T. Waterfield (eds.)]." Technical report, 2018.

Rogelj, Joeri, Piers M. Forster, Elmar Kriegler, Christopher J. Smith, and Roland Séférian. "Estimating and tracking the remaining carbon budget for stringent climate targets." *Nature* 571: (2019) 335–34.

Sawarkar, Ashish N., Aniruddha B. Pandit, Shriniwas D. Samant, and Jyeshtharaj B. Joshi. "Petroleum residue upgrading via delayed coking: A review." *The Canadian Journal of Chemical Engineering* 85, 1: (2007) 1–24.

Sellers, William D. "A global climatic model based on the energy balance of the earth-atmosphere system." *Journal of Applied Meteorology* 8, 3: (1969) 392–400.

Sexton, Steven E., A. Justin Kirkpatrick, Robert Harris, and Nicholas Z. Muller. "Heterogeneous Environmental and Grid Benefits from Rooftop Solar and the Costs of Inefficient Siting Decisions." NBER working papers, National Bureau of Economic Research, 2018.

Sharma, Ambrish, Jun Wang, and Elizabeth Lennartson. "Intercomparison of MODIS and VIIRS fire products in Khanty-Mansiysk Russia: Implications for characterizing gas flaring from space." *Atmosphere* 8, 6: (2017) 95.

Sims, R., R. Schaeffer, F. Creutzig, X. Cruz-Núñez, M. D'Agosto, D. Dimitriu, M.J. Figueroa Meza, L. Fulton, S. Kobayashi, O. Lah, A. McKinnon, P. Newman, M. Ouyang, J.J. Schauer, D. Sperling, , and G. Tiwari. "Transport. In: Climate Change 2014: Mitigation of Climate Change. Contribution of Working Group III to the Fifth Assessment Report of the Intergovernmental Panel on Climate Change [Edenhofer, O., R. Pichs-Madruga, Y. Sokona, E. Farahani, S. Kadner, K. Seyboth, A. Adler, I. Baum, S. Brunner, P. Eickemeier, B. Kriemann, J. Savolainen, S. Schlömer, C. von Stechow, T. Zwickel and J.C. Minx (eds.)].", 2014.

Snasiri, Fatemah, Eman Abdulrazzaq, Naween Tirkey, Rohit Kotecha, Naz H. Gazi, Mohammad

Al-Othman, Salem Al-Sabea, and Farida Ali. "Excellent Stimulation Results in Deep Carbonate Reservoir in Marrat Formation in Magwa Structure in Greater Burgan Field Kuwait." In *SPE Kuwait Oil and Gas Show and Conference, Mishref, Kuwait*. Society of Petroleum Engineers, 2015.

Solomon, Susan, Dahe Qin, Martin Manning, Kristen Averyt, and Melinda Marquis. *Climate change 2007-the physical science basis: Working group I contribution to the fourth assessment report of the IPCC*, volume 4. Cambridge university press, 2007.

Solow, Robert M. "The Economics of Resources or the Resources of Economics." *The American Economic Review* 64, 2: (1974) 1–14.

Stanhill, Gerald. "The Growth of Climate Change Science: A Scientometric Study." *Climatic Change* 48: (2001) 515–524.

Stern, Nicholas. "The Economics of Climate Change." *American Economic Review* 98, 2: (2008) 1–37.

Tol, Richard S.J., Kenneth J. Arrow, Maureen L. Cropper, Christian Gollier, Ben Groom, Geoffrey Heal, Richard G. Newell, William D. Nordhaus, Robert S. Pindyck, William A. Pizer, Paul R. Portney, Thomas Nils Samuel Sterner, and Martin L. Weitzman. "How Should Benefits and Costs Be Discounted in an Intergenerational Context?" Working papers, Department of Economics, University of Sussex, 2013.

United Nations. "United Nations Framework Convention on Climate Change." United Nations, 1992. http://unfccc.int/files/essential_background/background_publications_htmlpdf/application/pdf/conveng.pdf.

———. "Kyoto Protocol - Targets for the first commitment period." United Nations, 2020. https://unfccc.int/process-and-meetings/the-kyoto-protocol/what-is-the-kyoto-protocol/kyoto-protocol-targets-for-the-first-commitment-period.

U.S. Energy Information Administration. "Oil and petroleum products explained: Refining crude oil." U.S. Energy Information Administration, 2020a. https://www.eia.gov/energyexplained/oil-and-petroleum-products/refining-crude-oil-the-refining-process.php.

———. "Oil and petroleum products explained: Where our oil comes from." U.S. Energy Information Administration, 2020b. https://www.eia.gov/energyexplained/oil-and-petroleum-products/where-our-oil-comes-from.php.

———. "What countries are the top producers and consumers of oil?" U.S. Energy Information Administration, 2020c. https://www.eia.gov/tools/faqs/faq.php?id=709&t=6.

U.S. President Lyndon B. Johnson's Science Advisory Committee. "Restoring the Quality of Our Environment: Report of The Environmental Pollution Panel President's Science Advisory Committee." Technical report, The White House, 1965.

Van Den Bergh, Jeroen C.J.M., and Wouter J.W. Botzen. "A lower bound to the social cost of CO_2 emissions." *Nature Climate Change* 4, 4: (2014) 253.

Van der Meijden, Gerard, Karolina Ryszka, and Cees Withagen. "Double limit pricing." *Journal of Environmental Economics and Management* 89: (2018) 153–167.

Van der Ploeg, Frederick, and Cees Withagen. "Too much coal, too little oil." *Journal of Public Economics* 96, 1: (2012) 62–77.

Vimmerstedt, Laura, Austin Brown, Emily Newes, Tony Markel, Alex Schroeder, Yimin Zhang, Peter Chipman, and Shawn Johnson. "Transformative Reduction of Transportation Greenhouse Gas Emissions. Opportunities for Change in Technologies and Systems." Technical report, National Renewable Energy Laboratory (NREL), Golden, CO (United States), 2015.

Weitzman, Martin L. "On modeling and interpreting the economics of catastrophic climate change." *Review of Economics and Statistics* 91, 1: (2009) 1–19.

———. "Fat-Tailed Uncertainty in the Economics of Catastrophic Climate Change." *Review of Environmental Economics and Policy* 5, 2: (2011) 275–292.

———. "GHG targets as insurance against catastrophic climate damages." *Journal of Public Economic Theory* 14, 2: (2012) 221–244.

Wood Mackenzie. "Global Oil Cost Curves and Pre-FID Breakevens – updated H2 2018." Technical report, Wood Mackenzie, 2019.

World Bank. "Carbon Pricing Dashboard." World Bank, 2020. https://carbonpricingdashboard.worldbank.org/map_data.

Figures and Tables (Body of the Article)

Figure 1: Heterogeneity in upstream and midstream carbon intensities.

(a) Carbon intensity by oil type: 1992-2018

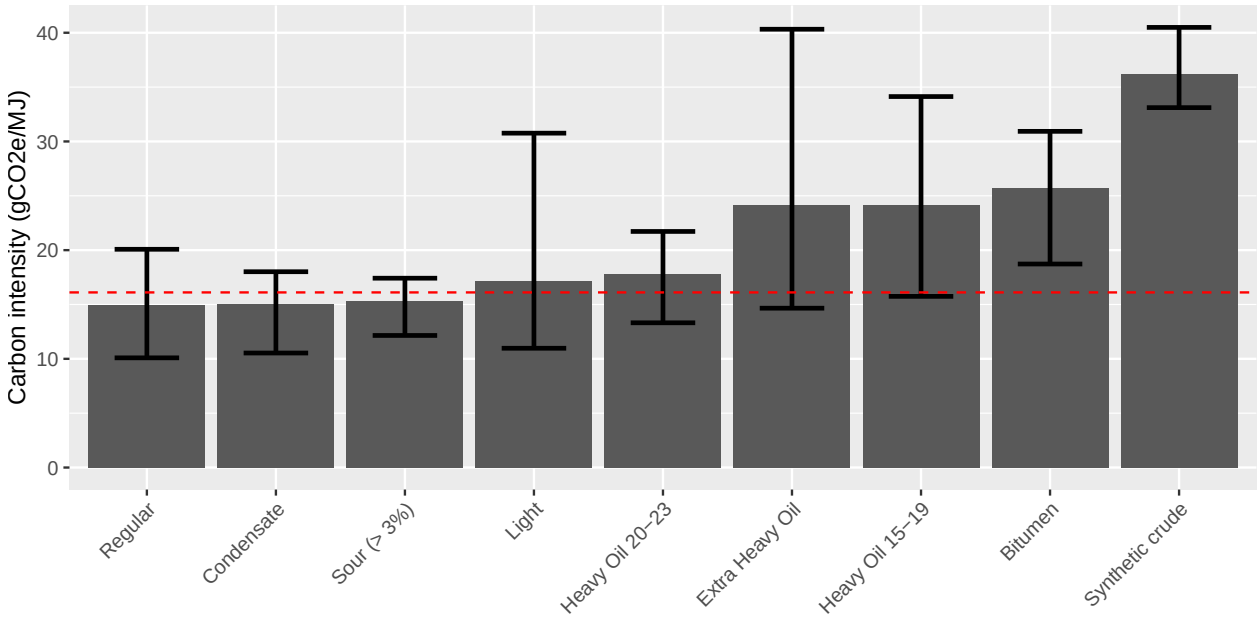

(b) Carbon intensity by country: 1992-2018

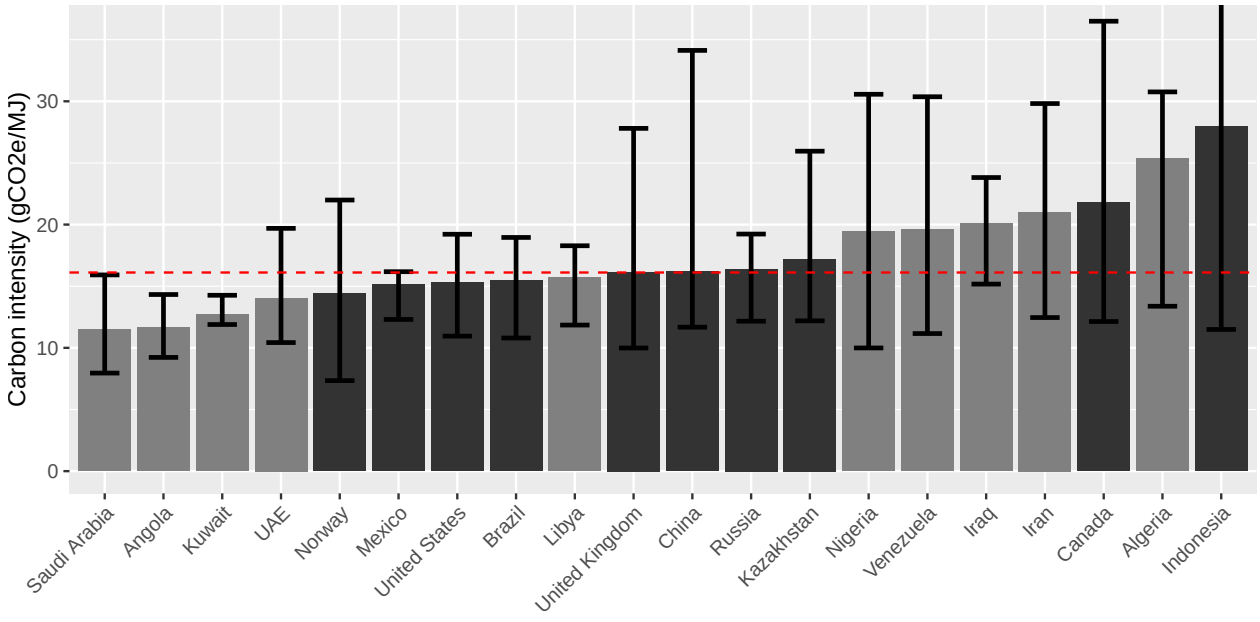

Notes: Panels (a) and (b) represent the combined upstream-midstream carbon intensity per megajoule (MJ) based on observed production over the 1992-2018 period by oil type and producing country respectively. The bar height represents the average (weighted by production), and the extremities of the lines the 10% and 90% deciles. The construction of carbon intensity is described in Section 2.3 and Appendix B. In Panel (b), only the top 20 oil producers over the period are represented, and OPEC country carbon intensity bars appear in light grey. The red dashed line corresponds to the World average figure. OPEC, as of 2019, included Algeria, Angola, Congo, Ecuador, Equatorial Guinea, Gabon, Iran, Iraq, Kuwait, Libya, Nigeria, Saudi Arabia, the UAE, Venezuela, and the Neutral Zone shared by Kuwait and Saudi Arabia.

Figure 2: Oil cumulative supply curves.

(a) Carbon-intensity-based oil supply: as of 1992.

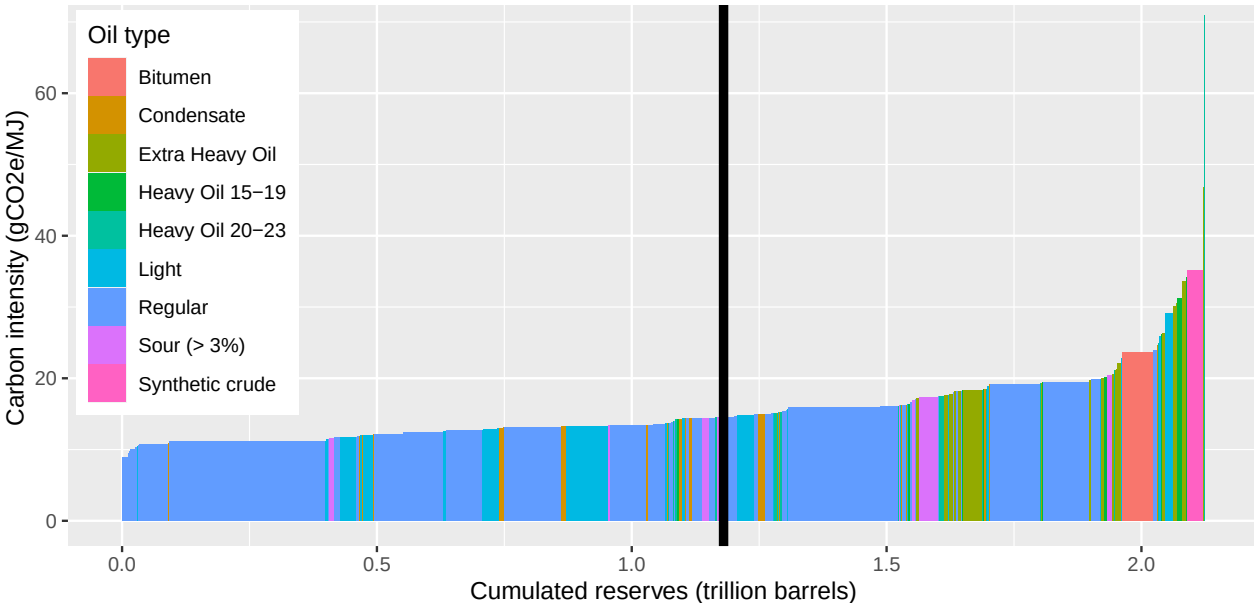

(b) Cost-based cumulative oil supply: as of 1992

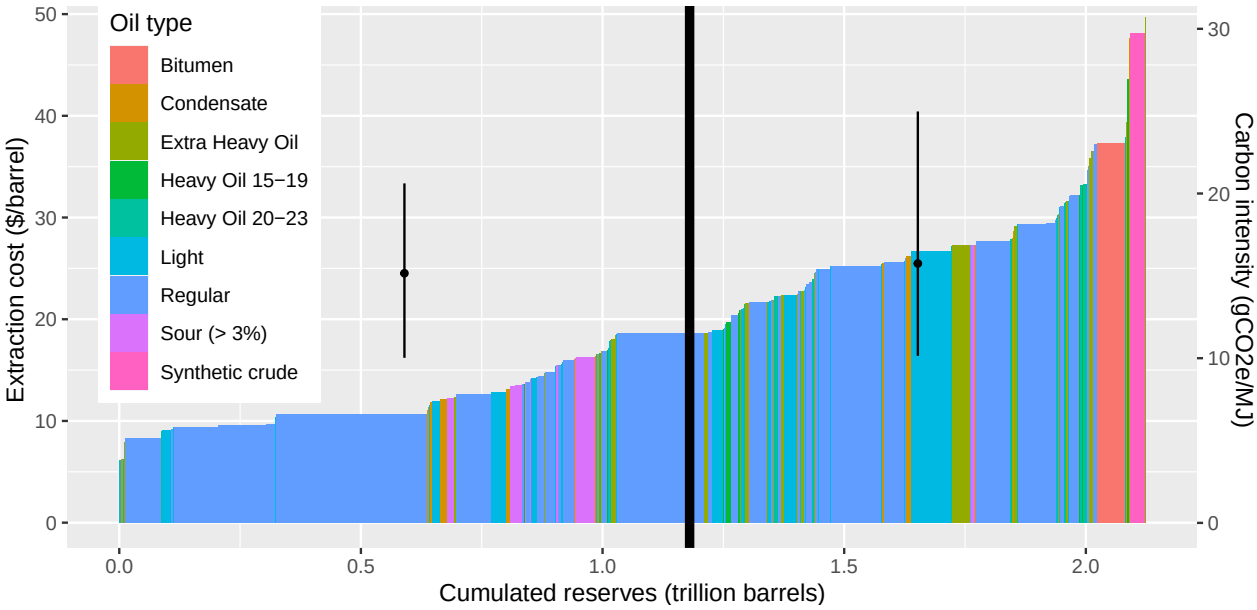

Notes: Panel (a) displays the carbon intensities of the available reserves in 1992, aggregated by oil type and country for visibility. Panel (b) depicts the extraction cost (colored bars, left-hand axis) of the available reserves in 1992 aggregated by oil type and country for visibility, and the average carbon intensities (dots and lines, right-hand axis) of resources on the left and on the right of the vertical line (aggregate demand). The dots represent the mean barrel carbon intensity, while the extremities of the lines represent the 10% and 90% deciles. Reserves are resources that are economically and technologically recoverable over the post-1991 extraction sequence using the Rystad definition. Some extra-heavy reserves such as Venezuela and Canada's main reserves are de facto excluded from this figure, as they are not economically recoverable according to Rystad. The vertical line represents the cumulative oil demand to satisfy over the 1992-2050 period. Section 2.3 and Appendix B describe the estimation of carbon intensities, and Appendices B–C the reserves data, post-1992 demand and the estimation of the costs.

Figure 3: The emission reductions from starting optimal supply recomposition in 2019 or 1992, as a function of the social cost of carbon.

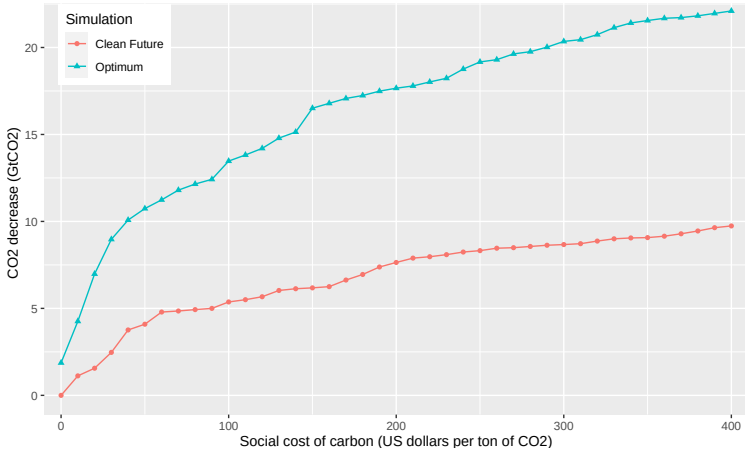

Notes: This figure displays the emission reductions (in $GtCO_2$) in the two counterfactuals, *Optimum* (blue curve, triangles) and *Clean future* (red curve, circles), for different values of the social cost of carbon (in 2018 US dollars). *Optimum*: the extraction path is optimized over the 1992-2050 period, factoring in pollution costs. *Clean future*: the extraction path is optimized over the 2019-2050 period, factoring in pollution costs, and pre-2019 production is the same as in the baseline.

Figure 4: The gains from starting supply recomposition one year earlier: 1970-2018.

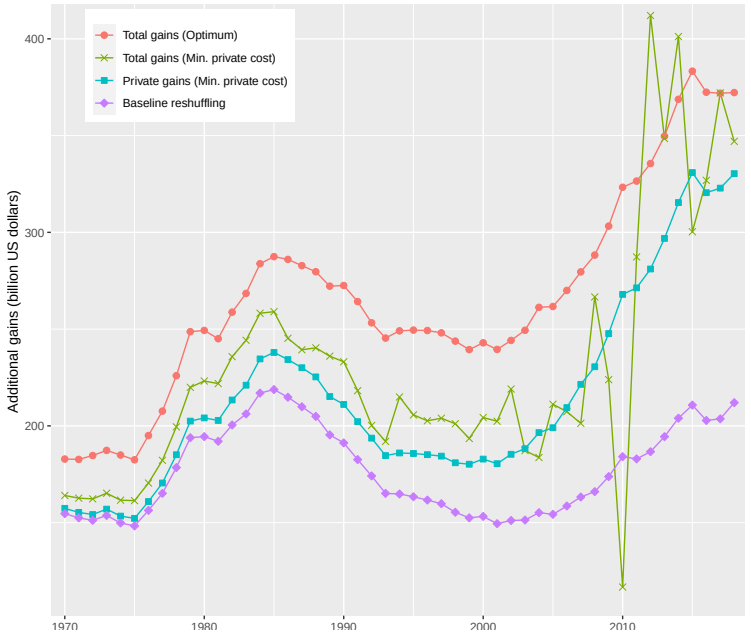

Notes: This figure displays the additional gains (in billions of US Dollars) of starting supply recomposition at date t instead of $t+1$, for t between 1970 and 2018, or equivalently the misallocation cost of starting optimal supply in $t+1$ instead of date t. Three distinct supply recompositions are considered. *Optimum*: the extraction path is optimized in t instead of $t+1$, factoring in pollution costs (red curve, circles). *Minimal private costs*: a cost-efficient extraction path that ignores pollution starts in t instead of $t+1$. Using this counterfactual, two series of additional gains are calculated: the blue curve (squares) depicts the associated additional gains when considering only private gains, i.e. extraction costs; the green curve (crosses) depicts the associated social gains, i.e., the sum of the private gains and the unlooked-for environmental gains or losses. *Baseline reshuffling*: cumulative extractions by deposit are unchanged. Only oil barrels that are actually extracted in the baseline are used, but are reshuffled so as to minimize the sum of discounted private extraction costs (purple curve, diamonds).

Table 1: Total gains and emission reductions from supply recomposition.

	No OPEC constraint		OPEC constraint	
	Total gains (trillion US$)	CO_2 decrease ($GtCO_2$)	Total gains (trillion US$)	CO_2 decrease ($GtCO_2$)
Optimum	8.81	17.66	7.09	17.78
Clean future	0.99	7.64	–	–
Minimal private costs	6.63	1.87	5.34	3.69
Baseline reshuffling	4.65	0	2.65	0

Notes: Each row refers to a distinct counterfactual supply and the columns *Total gains* (in trillions of US Dollars) and *CO_2 decrease* (in gigatons of CO_2) are calculated relative to the baseline. *Optimum*: the extraction path is optimized over the 1992-2050 period, factoring in pollution costs. *Clean future*: the extraction path is optimized over the 2019-2050 period, factoring in pollution costs, and pre-2019 production is the same as in the baseline. *Minimal private costs*: the sum of discounted extraction costs is minimized over the 1992-2050 period (pollution costs are ignored). *Baseline reshuffling*: Only oil extracted in the baseline is used (cumulative extractions by deposit are unchanged), but is reshuffled so as to minimize the sum of discounted extraction costs. *Total gains* are calculated as the lower discounted extraction costs (2018 value) plus the environmental gains, each ton of CO_2 being valued at US$ 200 in 2018. In the last two columns *OPEC constraint*, annual productions in each OPEC country are equal to their baseline values over the 1992-2018 period. OPEC (as of 2019) included Algeria, Angola, Congo, Ecuador, Equatorial Guinea, Gabon, Iran, Iraq, Kuwait, Libya, Nigeria, Saudi Arabia, the UAE, Venezuela, and the Neutral Zone shared by Kuwait and Saudi Arabia.

Table 2: Production changes in the Top-15 producing countries.

	Baseline production 1992-2018 (% of global production)	Change in production 1992-2018 (% of 1992-2018 baseline production)	
		Optimum	Min. private costs
Saudi Arabia	13.7	179.4	165.4
Russia	11.5	-51.5	-54.5
United States	9.7	-61.4	-64.2
Iran	5.3	46.5	91.6
China	5.0	-96.1	-96.1
Mexico	4.2	-59.7	-96.9
UAE	3.7	122.6	106.8
Venezuela	3.5	-49.0	-40.5
Canada	3.5	-77.0	-80.7
Iraq	3.2	211.7	210.9
Norway	3.2	-92.4	-96.4
Kuwait	3.0	202.0	189.4
Nigeria	3.0	-76.0	-64.9
United Kingdom	2.3	-99.9	-99.9
Algeria	2.2	-39.1	13.3
OPEC	43.3	88.7	90.7
Annex B	31.7	-66.0	-68.9
Non-Annex B	68.3	30.7	32.0

Notes: The *Baseline production 1992-2018* column shows the share of world cumulative production over the 1992-2018 period for each of the Top-15 oil producers. Column *Change in production 1992-2018: Optimum* lists the change in cumulative production over the 1992-2018 period when production is optimal over the whole 1992-2050 period, compared to the baseline. Column *Change in production 1992-2018: Minimal private costs* shows the change in cumulative production over the 1992-2018 period, when the sum of discounted private extraction costs is minimized over the whole 1992-2050 period (pollution is ignored), compared to the baseline. OPEC (as of 2019) included Algeria, Angola, Congo, Ecuador, Equatorial Guinea, Gabon, Iran, Iraq, Kuwait, Libya, Nigeria, Saudi Arabia, UAE, Venezuela, and the Neutral Zone shared by Kuwait and Saudi Arabia. Annex B countries are Australia, Austria, Belarus, Belgium, Bulgaria, Canada, Croatia, Cyprus, the Czech Republic, Denmark, Estonia, Finland, France, Germany, Greece, Hungary, Iceland, Ireland, Italy, Japan, Latvia, Liechtenstein, Lithuania, Luxembourg, Malta, Monaco, Netherlands, New Zealand, Norway, Poland, Portugal, Romania, the Russian Federation, Slovak Republic, Slovenia, Spain, Sweden, Switzerland, Turkey, Ukraine, the United Kingdom, and the United States of America.

Table 3: Countries' stranded reserves (% of 2019 reserves): Baseline and Clean future.

	Baseline	Clean future
Saudi Arabia	28.7	28.9
Russia	84.7	81.9
United States	95.0	92.6
Iran	50.1	65.3
China	98.3	94.0
Mexico	92.2	93.4
UAE	52.3	34.1
Venezuela	94.0	96.5
Canada	98.2	97.4
Iraq	50.5	89.0
Norway	99.3	46.6
Kuwait	26.7	15.3
Nigeria	95.1	91.3
United Kingdom	100.0	97.3
Algeria	51.1	75.3
OPEC	45.2	51.1
Annex B	92.9	88.4
Non Annex B	58.2	60.2
World	69.0	69.0

Notes: This table lists the share of the reserves of each of the Top-15 producers over the 1992-2018 period that should stay forever underground (as a % of the observed reserves in 2019) under two distinct scenarios over the 2019-2050 period. *Baseline*: the sum of discounted extraction costs is minimized over the 2019-2050 period (pollution costs are ignored). *Clean future*: the extraction path is optimal over the 2019-2050 period, factoring in pollution costs. In both scenarios, pre-2019 production is the observed production. OPEC (as of 2019) included Algeria, Angola, Congo, Ecuador, Equatorial Guinea, Gabon, Iran, Iraq, Kuwait, Libya, Nigeria, Saudi Arabia, the UAE, Venezuela, and the Neutral Zone shared by Kuwait and Saudi Arabia. Annex B countries are Australia, Austria, Belarus, Belgium, Bulgaria, Canada, Croatia, Cyprus, Czech Republic, Denmark, Estonia, Finland, France, Germany, Greece, Hungary, Iceland, Ireland, Italy, Japan, Latvia, Liechtenstein, Lithuania, Luxembourg, Malta, Monaco, Netherlands, New Zealand, Norway, Poland, Portugal, Romania, Russian Federation, Slovak Republic, Slovenia, Spain, Sweden, Switzerland, Turkey, Ukraine, the United Kingdom, and the United States of America.

APPENDIX

A Field-level data

A.1 Rystad upstream database

Our empirical investigation employs one of the most-comprehensive datasets on oil and gas fields, the Rystad Upstream Database (UCube).[32] This database covers World oil production since 1900, with over 65,000 oil and gas assets. It brings together precise field-level data on oil and gas production,[33] exploitable reserves, resource discoveries, capital and operational expenditures from exploration to field decommission, current governance (ownership and operating companies), field development dates (discovery, license, start-up, and production end), oil types, and reservoir characteristics (water depth, basin, and location), among others. The data sources include governments and companies' operation reports.

A.2 Flaring data

Since only a minority of countries and companies collect and publish data on flared gas, nearly 95% of the fields in Rystad have missing flaring data. We overcome this using satellite data from the National Oceanic and Atmospheric Administration (NOAA). This lists all flared gas that was detected by the VIIRS instrument (Visible Infrared Imaging Radiometer Suite) between 2012 and 2016, along with the corresponding geographic coordinates. Flaring volumes were calculated from satellite observations using the VIIRS Nightfire (VNF) algorithm, which is recognized as the most effective for the task (Sharma et al., 2017).[34]

The matching of the flares identified by VIIRS to the Rystad field data based on exact geographic coordinates has a number of limitations due to inaccuracies in flare detection,[35] thus flaring averages were computed at the "Area" level. These Areas are geographic units defined in the Rystad dataset: 1,437 Areas in the World produced oil between 2012 and 2016, with an average of 24.3 fields per Area. Province-level averages were attributed to

[32] Information on this database is available at https://www.rystadenergy.com/products/EnP-Solutions/ucube.

[33] All productions are expressed in energy-equivalent barrels, using Brent Crude as the benchmark.

[34] For additional information on flaring-estimations methods using VIIRS, and data access, see Elvidge et al. (2016).

[35] We cannot conclude that no field flared gas in locations where no gas flares were spotted by VIIRS, due to detection inaccuracies. Despite its acclaimed precision, the VIIRS instrument cannot detect all flares, especially those that are small or with low temperature. Moreover, as noted in Elvidge et al. (2016): A "second shortcoming arises from the temporal sampling limitations of the VIIRS instrument. VIIRS collects global data every night, but the dwell time of VIIRS on a flaring site is a fraction of a second. For steady and continuous flares, this temporal sampling appears to be adequate. However, VIIRS under-samples intermittent or rarely active flares. This under-sampling lowers the probability of detection and decreases the accuracy of flared gas estimates for flares with highly variable flared gas volumes".

oil fields in Areas with substantial gas production.[36] These Provinces are geographic units defined in the Rystad dataset: 458 Provinces produced oil any time between 2012 and 2016, and the average Province contains 112 fields.

B Estimating carbon intensities

B.1 Upstream carbon intensities

The OPGEE. To estimate upstream emissions, we rely on the *Oil Production Greenhouse Gas Emissions Estimator* (OPGEE) developed by Adam Brandt (Stanford University).[37] The OPGEE measures GhG emissions in grams of CO_2 equivalent (gCO_2eq)[38] in a field and then divides it per megajoule (MJ) of energy extracted. In most oil fields, associated gas is extracted together with oil and is sometimes sold on the market. It is therefore necessary to decide how to account (or not) for the associated gas production. The same remark applies for on-site produced electricity and Natural Gas Liquids (NGL), to a lesser extent. The OPGEE model was run with the two following approaches.

- *Energy-based allocation* (EBA). Oil carbon intensity is $CI_{EBA} = \frac{E_{field}}{Prod_{oil}+Prod_{gas}}$. Total carbon emissions of the field, E_{field}, are calculated and then assigned to oil and gas proportionally to their respective productions in megajoules, $Prod_{oil}$ and $Prod_{gas}$.
- *Co-product displacement* (CPD). Oil carbon intensity is $CI_{CPD} = \frac{E_{field}-Prod_{gas}.\overline{CI}_{gas}}{Prod_{oil}}$, with $\overline{CI}_{gas}$ the carbon intensity of the displaced system producing gas, and E_{field} the total pollution of the field, i.e. the pollution of the joint production of oil and gas, $Prod_{oil}$ and $Prod_{gas}$. With the CPD approach, any by-product (gas or electricity) that is not used in situ but is sold gives rise to carbon-emission credits that are equal to the amount of gas (or electricity) sold multiplied by an estimate of the average carbon intensity of gas production in the World, $\overline{CI}_{gas}$. The carbon intensity of the displaced

[36] Those with an average gas-to-oil ratio (GOR) above 10,200 Standard Cubic Foot per Barrel (scf/bbl). This cut-off is similar to the Rystad cut-off to separate oil from gas fields and is consistent with Masnadi et al. (2018), who use a GOR threshold of 10,000 scf/bbl.

[37] To access the model and its documentation, see https://eao.stanford.edu/research-areas/opgee. For a detailed description of the model, see Gordon et al. (2015).

[38] "A CO_2 equivalent [...] is a metric measure used to compare the emissions from various greenhouse gases on the basis of their global-warming potential, by converting amounts of other gases to the equivalent amount of carbon dioxide with the same global warming potential" (Eurostat). The global warming potential of a gas represents the combined effect of the time the gas remains in the atmosphere and its relative effectiveness in absorbing outgoing thermal infrared radiation, integrated over a given time horizon. The values for each gas in OPGEE are taken from Solomon et al. (2007), which uses global-warming potentials over a 100 year-time frame according to the Kyoto Protocol method.

system is calculated from the CA-GREET model[39] and is fixed for all fields. With the CPD approach, the field is credited the amount of pollution that would have been emitted to produce this quantity of gas elsewhere.

The EBA approach was selected for the baseline carbon-intensity estimation. Figure B4 illustrates that the two approaches produce very similar carbon-intensity estimates. In a robustness check, we also reproduce the main outcomes of our analysis using carbon intensities estimated via the CPD approach.

Running OPGEE. Masnadi et al. (2018) provide a sample of 958 large fields, with data formatted to be used as inputs in OPGEE (values of 2015). 12 fields out of 958 were discarded due to missing data or production termination in 2015, resulting in imprecise carbon estimates from OPGEE.[40]

The data for the 946 remaining fields were checked and a small number of improvements were made. We first corrected missing or erroneous values of the On-Offshore variable for 81 fields with data available in the Rystad database, and re-checked on the Internet (http://abarrelfull.wikidot.com/). Second, missing 2015 production values were added using Rystad data.[41] In addition, field production in 2013 or 2014 was assigned to fields in the production phase but not yet producing in 2015 for maintenance or cost reasons. Last, the CO_2 proportion of the "Mangala" field (India) was corrected using Chavan et al. (2012), and the shares of other gases were calculated proportionally to the default composition. The correction was made to avoid a bug due to missing data when running OPGEE. For 19 UK fields, flaring values were inconsistent with the associated gas-to-oil ratios. Associated gas-production values were checked from UK government data,[42] and flaring ratios set at OPGEE default values consistent with the observed GOR values.

Matching OPGEE and Rystad fields We match the 946 publicly-available OPGEE fields with those from the Rystad dataset using field name and location. 184 fields out of 946, mostly Californian fields that represent only a marginal share of US production (jointly producing 133 kbbl/d, i.e. 1.4% of US oil production and 0.16% of World production in 2015) were unmatched. The 762 OPGEE fields were matched with 1,173 fields from the Rystad dataset. The difference in these figures is due to some fields in one dataset (either Rystad or OPGEE dataset) being represented by more than one field in the other dataset. Despite

[39]The model is available at https://greet.es.anl.gov.

[40]The missing data was for Dagmar (DN), Regnar (DN), Rob Roy (UK), Scampton (UK), Brynhild (UK), Hutton North (UK) and Sedgwick (UK). The "Beatrice" field (UK) was ignored as production stopped in February 2015. Fields with duplicated names in one dataset (Rystad or OPGEE) or imprecise names were discarded: Tomoporo (VE), Columba B and D (UK), and South Russia (Russia).

[41]The Kuwaiti "Magwa" field is part of the Burgan-Magwa-Ahmadi field in Rystad, thus only joint production is available in Rystad. Production was replaced by an estimate from Snasiri et al. (2015).

[42]Available at: https://itportal.ogauthority.co.uk/pprs/full_production.htm.

representing only 8% of producing fields, these 1,173 fields account for over 54% of 2015 World oil production. This subsample includes most oil-producing countries, although wells located in the UK and the US are over-represented. The OPGEE sample is representative of the rest of the Rystad oil assets in the dimensions that matter for the estimation of upstream and midstream carbon intensity. There are however some differences. The fields operated by Major companies are over-represented in the OPGEE sample, as are fields extracting Bitumen and Synthetic crudes, those employing steam injection, and Offshore fields. The GOR tends to be larger for fields in the OPGEE sample, but the difference is not statistically significant. The OPGEE sample consists of relatively larger fields, although field size has no significant impact on carbon intensity per barrel when added to the set of explanatory variables.

Estimation model. The existing literature (Brandt and Farrell, 2007; Mui et al., 2010; Masnadi et al., 2018) has highlighted a number of deposit characteristics that help explain upstream GhG emissions: The American Petroleum Institute (API) gravity, the gas-to-oil ratio (GOR), the flaring-to-oil ratio (FOR), and the steam-to-oil ratio (SOR). We briefly discuss below how these deposit characteristics relate to GhG emissions.

- The American Petroleum Institute (API) gravity is a measure of oil density. Together with oil viscosity (a measure of the fluid's resistance to flow), this is used to characterize the main oil types. The U.S. Geological Survey[43] uses the following classification: *light oil* has an API gravity over 22° and viscosity under 100 centipoise (cP); *Heavy oil* is an asphaltic, denser oil type with an API gravity under 22° and a viscosity of at least 100 cP; *Extra heavy oil* is a type of heavy oil with an API gravity below 10°. Heavier oils require more energy to be brought up to the surface by traditional well-based extraction methods. Their extraction thus generates more carbon emissions, all else equal.

- Gas-to-oil ratio (GOR, in scf/bbl): when oil is extracted, natural gas is also brought up to the surface. Deposits differ in terms of the quantity of gas that comes with each oil barrel. The extraction of high-GOR deposits can generate large emissions depending on how this gas is handled. Gas can be either sold on the gas market, reinjected underground, flared, or directly vented into the atmosphere.

- Flaring-to-oil ratio (FOR, in scf/bbl): gas flaring, i.e. the on-site combustion of gas (or part of it), helps control the pressure in the well and the plant equipment. This technology is largely tied to the oil reservoir's specificity (e.g. GOR) and the distance

[43] https://pubs.usgs.gov/fs/fs070-03/fs070-03.html.

to the gas market (field localization). Flaring is a major contributor of upstream carbon intensity.[44]

- Steam-to-oil ratio (SOR, in bbl of water/bbl of oil): steam injection concerns mostly heavy oils and bitumen. Injecting steam heats the oil and thereby reduces its viscosity, enabling oil to flow toward the extraction wells. Steam injection requires vast amounts of energy, and therefore produces substantial GhG emissions.

After attributing the OPGEE-calculated carbon intensities to the corresponding Rystad fields, we specify a regression model to explain the across-field variation in carbon intensity using the variables from the Rystad dataset. Only oil fields (those with gas-to-oil ratios below 10,200 scf/bbl following conventions and the Rystad classification) were retained for the analysis. Finally, 664 OPGEE fields are used for the model estimation, corresponding to 1,077 Rystad assets. We refer to these fields as the "OPGEE sample".

Models with all potential explanatory variables, at different orders (up to cubic) with multiple interactions were tested. Variables with little explanatory power were then dropped one by one to avoid data over-fitting. The selected model[45,46] includes the main CI explanatory variables found in the literature: oil-type dummies, GOR and FOR, and a steam-injection dummy. We also add a dummy for Offshore fields and a dummy for fields operated by "Majors", which are the seven major private companies in terms of size (ExxonMobil, BP, Shell, Chevron, Total, ConocoPhillips, ENI; this classification is from Rystad).

[44]It is still however preferable to venting—the direct release of methane into the atmosphere without burning. Gas combustion transforms methane into carbon dioxide, and the latter has a 25-times smaller global-warming potential over a 100-year time horizon (Solomon et al., 2007). Unfortunately, very little data is available on the amount of vented gas in the World, as this is not systematically and truthfully reported by corporations or governments, and is extremely difficult to detect using remote sensors (Calel and Mahdavi, 2020).

[45]For the sake of parsimony, we selected a unique regression model for the two approaches (EBA, CPD). Using approach-specific estimation models would provide similar regression models and ultimately similar CIs. Deposits with a high water-to-oil ratio tend to have higher carbon intensities. We do not include the water-to-oil ratio for two reasons. First, this variable is not in the Rystad dataset. Second, the WOR mostly explains within-field changes over time in carbon intensity (mostly due to depletion). We assume constant deposit carbon intensities in our main approach, and are thus mostly interested in time-invariant carbon-intensity heterogeneity across deposits related to WOR. The *Major* dummy captures part of the time-invariant WOR heterogeneity that can affect CIs (e.g., investments to reduce the volume of produced water). Fields operated by Majors tend to have lower water-to-oil ratios, despite being older on average. In the OPGEE sample, the average WOR figure is 2.45 bbl water/bbl in Major companies' fields, as against 4.61 in the other fields, with analogous age figures of 27 and 22 years.

[46]To account for some OPGEE fields being matched to more fields in the main database (due to differences in field definitions between the OPGEE and Rystad datasets), weights were added in the regression so that all OPGEE fields have equal weight.

The selected model is:

$$\begin{aligned} CI_f^{OPGEE,C} &= \sum_0^8 \beta_i^C OilType_{i,f} + \beta_9^C GOR_f + \beta_{10}^C FOR_f \\ &+\beta_{11}^C SteamInjection_f + \beta_{12}^C Offshore_f + \beta_{13}^C Major_f + \epsilon_f, \end{aligned} \tag{9}$$

where f denotes a field, C a configuration of the OPGEE model (either EBA or CPD), $OilType_i$ oil-type dummies (e.g., Extra Heavy, Light, Regular, Bitumen), GOR the ratio of the gas quantity (in standard cubic feet, scf) to the oil quantity (in barrels, bbl) in the reservoir, FOR the ratio between flared gas and extracted oil, also in scf/bbl, *Steam Injection* a dummy for steam injection being used in the reservoir, *Offshore* a dummy for the asset being located offshore, and *Major* a dummy for the operator being a Major company.

For each field in the Rystad dataset, we then predict the carbon intensity using variables from the Rystad dataset and the estimated coefficients from equation (9):

$$\begin{aligned} CI_f^{Upstream,C} &= \sum_0^8 \widehat{\beta}_i^C OilType_{i,f} + \widehat{\beta}_9^C GOR_f + \widehat{\beta}_{10}^C FOR_f \\ &+\widehat{\beta}_{11}^C SteamInjection_f + \widehat{\beta}_{12}^C Offshore_f + \widehat{\beta}_{13}^C Major_f \end{aligned} \tag{10}$$

Regression results. The regression results for CI calculated with the EBA or CPD approaches appear in Table B1. The estimation model explains most of the CI variation (an R-squared of 94% for EBA). All coefficients — except for those on GOR and the Major dummy — are significant at the 1% level. The intercept values for the oil types range from 4.0 gCO_2eq/MJ for bitumen to 9.9 gCO_2eq/MJ for extra heavy oil for the CI calculated with EBA (the CPD CI yields similar results). The intercept value for synthetic crude is particularly high (25.6 gCO_2eq/MJ), due to the upgrading process in the upstream phase to transform bitumen into synthetic oil. Apart from condensate and bitumen, the intercepts are larger as API gravity falls, i.e. as oil gets denser. This is expected as denser oils require more energy to be lifted. The high condensate value reflects its gassy nature; a small share of the GOR effect is captured by this dummy. The particularly low value for bitumen is due to all bitumen-extracting fields in our sample using steam injection (94% in the Rystad database), so that the average Bitumen oil has a very high CI. The coefficients for FOR are the same in the two methods, and their size confirms this variable's importance in explaining CI heterogeneity. Despite not being significant at conventional levels, the sign of the GOR coefficient is consistent with the way in which gas production is accounted for in the EBA and CPD approaches. Steam injection plays, as expected, an important role in carbon intensity due to the considerable amounts of energy it requires (Gates and Larter, 2014). Although all bitumen fields in our dataset use steam injection, this technique is also employed in some non-bitumen heavy oil fields. Last, the Offshore and Major dummies have little explanatory

power. The Offshore coefficient is negative, as offshore extraction is not accompanied by land-use transformation, such as deforestation, that generates GhG emissions. As expected, fields operated by Major companies have lower carbon intensities, all things equal. This may reflect the technological advancement of Major companies, in particular concerning the handling of water in oil fields, or unobserved field characteristics. However, operator type has only a very small impact compared to oil types, indicating that technology, as proxied by Major companies, has little impact apart from flaring and steam-injection techniques that are both largely related to the deposit's exogenous characteristics (e.g., GOR, oil viscosity, and distance to gas market).

The final field-level upstream dataset of carbon intensities contains the CIs estimated using OPGEE models for fields common to the OPGEE and Rystad datasets, and the CI predicted using the regression above for the remaining Rystad fields.

Robustness checks. The overall performance of our estimation model is illustrated in Figure B1. In Panel (a) there is a strong correlation between the carbon intensities predicted using equation (10) (CI^{Rystad}) and those directly calculated in OPGEE (CI^{OPGEE}). We then consider the sensitivity of the estimated coefficients of specification (9) to specific observations, and re-estimate it multiple times removing the fields in our main estimation sample one by one. Panel (b) presents the resulting correlation coefficients. Each grey line corresponds to a different estimation, and the thick red line to the original correlation coefficient in the full OPGEE sample. In Figure B2 we show the estimated coefficients before each explanatory variable. Overall, these robustness checks indicate that estimated parameters of equation (9) are robust to changes in the estimation sample of deposits.

We then look at the robustness of our estimates to the exclusion of the most influential observations. For a given variable, we define the n most-influential observations as those with the n largest Cook's distances (CD), with $CD_i = \sum_{j=1}^{N} \left(\widehat{y}_j - \widehat{y}_{j(i)}\right)^2 / ps^2$, where $\widehat{y}_j$ and $\widehat{y}_{j(i)}$ are the fitted response values from using the full sample and after excluding field i, respectively; s^2 is the mean squared error of the regression model, p the number of coefficients, and N the number of observations. We re-estimate equation (9) after dropping the 1, 5, or 10 most-influential observations by this definition, and list the new estimates in Table B2. Overall, the coefficients on the explanatory variables are stable.

Last, we show that our approach is suitable for out-of-sample prediction. Masnadi et al. (2018) provide *anonymized* OPGEE deposit-level CIs for 2015. Figure B3 plots the distribution of our estimated CI and the OPGEE-calculated CI for the fields producing in 2015 (using the CPD approach, as this is the only one available for the disaggregated list of OPGEE-calculated CIs in their paper). The two distributions are very similar: our carbon intensities are very close to those in Masnadi et al. (2018).

B.1.1 Alternative measures used in sensitivity analysis

Flaring. Part of an oil's carbon intensity comes from the extraction technology, and flaring is of particular importance. Although operating companies may react to a carbon policy that covers flaring-related emissions, the true emission abatement is particularly difficult to predict.[47] Instead of being flared, gas could be re-injected into the reservoir, sold, or vented into the atmosphere, with the firm's best option differing across fields depending on the local context. The existing literature offers contrasting estimates of flaring-abatement costs (see Malins et al. 2014b). These are likely large, explaining why flaring regulation seems to be globally ineffective (Farina, 2011). As noted in Calel and Mahdavi (2020) "Even outright bans—as in Algeria in 2005 and Ghana in 2010—have not been followed by reductions in flaring [...], nor, where offered, have site-level financial incentives to curb emissions decreased flaring".

More importantly, flaring regulation could be counterproductive if non-flared methane is directly vented into the atmosphere. As noted in Calel and Mahdavi (2020), "Because flaring is easily detected with high-resolution satellites whereas measurements of venting are either imprecise (conducted with medium resolution satellites) or prohibitively costly at scale (done with aerial monitoring), restrictions on flaring can push oil producers toward greater venting": Calel and Mahdavi (2020) note that gas that is vented instead of flared has a global-warming potential that is 16.2 times larger. As such, even were only 7% of non-flared methane to be vented following some policy, the overall field CO_2eq emissions would actually rise, making regulation counterproductive.

Due to the data limitations regarding the field-level costs of abating flaring emissions, and the difficulty in relating less flaring to true emission reductions, our main specification assumes fixed field flaring-to-oil ratios. In a robustness check, we update the upstream carbon intensity accordingly using equation (10), but with field-level FOR reduced by 10% (at no cost and with no rise in venting).

Carbon intensities varying with field's depletion. In our main specification, we have assumed that field-level carbon intensities do not vary with the depletion of the field. This is a simplification, as recent literature has shown that the per-barrel carbon intensity can change along an oil field's life cycle due to for instance an accrued use of Enhanced Oil Recovery techniques or the increase in the field's water-to-oil ratio. Using a set of 25 large oilfields, Masnadi and Brandt (2017) provide evidence of a doubling of (per barrel) upstream carbon intensity over 25 years using an engineering-based approach that relies on the use of

[47] Estimating the emission-abatement costs of flaring would require a great deal of data (distance to the nearest gas pipeline, field depth, the cost of setting up a new well, etc., together with more-readily accessible data such as the gas-to-oil ratio) and an adequate model.

the OPGEE model, which they interpret as the effect of increased depletion.

Building on this evidence, we construct alternative measures of carbon intensities that vary with depletion as follows. For each field, we consider its reserves at the discovery date, and we split a deposit's initial reserves into two bins of similar size. We assume that the most polluting bin is k times more polluting to extract than the least polluting bin, while keeping the average carbon intensity of the field the same as in our main specification. We label scenarios as "low", "medium" and "'high" for $k = 1.2$, $k = 1.4$ and $k = 1.6$ respectively. Extracting from a deposit can be seen as extracting from its bins, starting with the first bin (the average CI when the depletion rate is below 50%) and then moving to the second (the average CI when the depletion rate is above 50%) once the first bin is exhausted.

We then rerun our main exercise swapping the deposits for their bins. The extraction costs for each bin in a field are the same. As of 1992, the reserves of a bin equal half of the initial reserves of the master deposit, amputated from pre-1992 production from the deposit (assuming that past production is first affected to the first bin and then to the second bin, but only after cumulative ante-1992 production reaches the size of the first bin). The capacity constraint is rewritten so that the sum of productions from the bins that compose a deposit is each year below the deposit's extractive capacities. The solution of $\mathcal{P}_1(T_0, T_f, \mu)$ with the deposits' bins used instead of deposits leads to never extracting the second bin of a deposit before the first bin is exhausted.

B.2 Midstream carbon intensities

PRELIM. The *Petroleum Refinery Life-Cycle Inventory Model* (PRELIM),[48] developed by Joule Bergerson (University of Calgary), is an engineering-based model to estimate energy use, refining yields and GhG emissions from crude-oil refining. Three types of refinery (hydroskimming, medium conversion, and deep conversion) appear in the model. PRELIM selects the refining type based on the crude's API gravity and sulfur content as follows: deep conversion for heavy crudes (under 22 API) with any sulfur content; medium conversion for medium crudes (22-32 API) and for light sour crude (over 32 API and 0.5% sulfur content by weight); and hydroskimming for light sweet crude (over 32 API and below 0.5% sulfur content by weight).

PRELIM runs with two refining configurations, "(delayed) coking" and "hydrocracking", relating to the way in which bottom-of-the-barrel residues are transformed into valuable products. This mostly concerns the refining of heavy oils, as lighter oils have fewer residues so that there is little difference between delayed coking and hydrocracking. We use delayed coking as

[48] The model and documentation is available at www.ucalgary.ca/lcaost/prelim.

the baseline in our midstream CI estimations, as thermal conversion processes (among which delayed coking is the most popular) represent 62.7% of World residue-processing capacities. By comparison, the analogous figure for hydrocracking is only 18.4%, and is naturally limited by its high consumption of hydrogen and the limited hydrogen supply (Sawarkar et al., 2007).

The Rystad dataset contains only a subset of the crude properties required to run PRELIM. To the best of our knowledge, there is no systematic collection of crude assays for global oil production.[49] We thus run PRELIM with 149 assays — from companies, specialized websites and past research — that are publicly available in the PRELIM 1.3 Assay Inventory. In this sample, Canadian and US crudes are over-represented as the assays of most of their domestically-produced crudes are publicly disclosed.[50] We run PRELIM and obtain the carbon intensities for these 149 assays for both the "coking" and "hydrocracking" processes.

Linking PRELIM's crude assays and Rystad's fields. PRELIM crudes were linked to the Rystad fields using operator name, crude name, and location information. 11 of the 149 PRELIM crudes were disregarded, as they are no longer produced, and 107 crudes out of the remaining 138 were matched to producing fields in the Rystad database. For some fields (mostly in Canada), the extracted oil was split into different refined crudes, depending on the company. For these fields, the weighted averages were calculated when data on the use of each field's oil was available.[51] Otherwise, weighted averages using the companies' shares[52] in the fields were calculated. Simple averages were calculated when the company shares were not available. 953 fields in Rystad were finally matched to 107 PRELIM crude values. The imbalance is due to some crudes being produced from oil extracted in a number of fields: for example, Siberian Light, Western Texas Intermediate, and Brent.

Estimation model. After matching the PRELIM crude assays to the corresponding fields in the Rystad dataset, we regress midstream carbon intensities on key variables from the Rystad dataset that can impact the refining process in this sample of 953 fields.[53] As

[49]Some major companies such as ExxonMobil and Chevron make publicly available some of their crude assays, but do not however match the PRELIM input requirements.

[50]This data is available at http://www.crudemonitor.us/ and http://www.crudemonitor.ca/.

[51]For example, 85% of the oil from Christina Lake (Canada) is refined as "Christina Dilbit Blend", while the remaining 15% is blended with other oils and refined as "Western Canadian Select". Data on the use of each field's oil is available at https://www.oilsandsmagazine.com/projects/.

[52]For instance, there are two crudes in the American field "Thunder Horse" (one from BP and another from ExxonMobil). It was assumed that as ExxonMobil owns 75% of the field, 75% of the production was refined by ExxonMobil (and so 25% by BP). Data on companies' shares come from Rystad.

[53]This sample is representative of the remainder of the Rystad oil assets in the dimensions that matter for the estimation of midstream carbon intensity. For the Rystad assets matched to the PRELIM assays, mean API is 37.0, 18% contain over 1% of sulfur, and 12% are operated by Major companies. The Rystad dataset assets that are unmatched to PRELIM oil assays, with positive reserves in 1992, have analogous figures of

discussed above, the PRELIM model automatically selects the best refinery configuration for a crude based on its API gravity and sulfur content: heavy and sour crudes require complex deep conversion refineries that emit more carbon. We also add a Major company dummy, as these blend oil crudes to create specific oil crudes with stable chemical and physical properties for refining. Note that we are interested in explaining only the part of midstream carbon intensity that relates to oil characteristics, so that a change in deposit extraction could reduce the carbon footprint of refining. We consider refineries as fixed, and abstract from heterogeneity in midstream emissions that relate to refinery particularities independent of the oil type. We estimate the following model:

$$\begin{aligned} CI_f^{PRELIM} &= \beta_0 + \beta_1 API_f + \beta_2 API_f^2 + \beta_3 API_f^3 + \beta_4 API_f^4 \\ &+ \beta_5 Sour_f + \beta_6 Major_f + \epsilon_f, \end{aligned} \tag{11}$$

where CI^{PRELIM} is the midstream carbon intensity of crude f, API crude API gravity, *Sour* a dummy for the crude having over 1% sulfur, and *Major* a dummy for the operator being a Major company. We run the econometric specification separately for the PRELIM CIs calculated using the "coking" and "hydrocracking" refining configurations.

For each field in the Rystad dataset, we then predict the refining carbon emissions of its oil:

$$\begin{aligned} CI_f^{Midstream} &= \widehat{\beta}_0 + \widehat{\beta}_1 API_f + \widehat{\beta}_2 API_f^2 + \widehat{\beta}_3 API_f^3 + \widehat{\beta}_4 API_f^4 \\ &+ \widehat{\beta}_5 Sour_f + \widehat{\beta}_6 Major_f \end{aligned} \tag{12}$$

Regression results. The estimates of (11) appear in Table B3. Despite the small number of explanatory variables, our model explains over half of the variance in the midstream carbon intensities of crudes (for both the "coking" and "hydrocracking" refining configurations). This reflects the link between the refining process (deep or medium conversion, and hydroskimming) and the API gravity and sulfur content. There is significant CI variation between heavy and light oils, with bitumen refining being the most polluting. The Sour dummy also captures the particularities of the refining process. The Major dummy coefficient is not significant at conventional levels when considering hydrocracking refining.

The final field-level midstream dataset of carbon intensities contains the CIs estimated using PRELIM for crudes that are common to the PRELIM and Rystad datasets, and the CIs predicted using the regression (12) for the remainder of the Rystad fields.

Robustness checks. We compare the carbon intensities of both the coking and hydrocracking refining processes. In Panel (a) of Figure B5, we plot the distributions of the CIs calculated in PRELIM using the 146 crude assays available in PRELIM (3 out of the initial

33.5, 24% and 8%.

sample of 149 assays could not be run in PRELIM). The CI distribution is very similar for these two refining methods. In Panel (b), we plot the distribution of the CIs calculated in PRELIM for the Rystad fields matched to the PRELIM crude assays and those predicted using (11) for the remainder of the Rystad fields in the two configurations. The CI distributions from the two refining processes are again similar.

B.3 Downstream emissions

The downstream sector represents the transport of refined products to end consumers, and their use (mostly combustion). Downstream emissions do not vary much across the original crudes. Oil-product combustion represents most of their life-cycle carbon emissions (75.68 gCO_2eq/MJ on average), but combustion emissions do not vary across oil crudes for a given composition of final products (e.g. gasoline, kerosene etc.) that we take as given, as our focus is on supply rather than demand. Greene et al. (2020) show that the carbon emissions from well-to-tank seaborne transportation vary between 5 and 27 gCO_2eq per liter (i.e. between 0.13 and 0.7 gCO_2eq/MJ), with an average figure of 10 gCO_2eq per liter (0.26 gCO_2eq/MJ). Even the difference between the two extreme values, 0.57 gCO_2eq/MJ, is small compared to the standard deviation of carbon intensity in our dataset (8.96 for observed production over the 1992-2018 period). We also take as given the quantity of oil used in the petrochemical industry (about 12% according to IEA 2018a), for which downstream emissions are small.

In a robustness check, we allow the composition of petroleum products to vary with crude origin: this generates variation in combustion-related emissions per barrel of crude oil. We use the *Oil Products Emissions Module* (OPEM) model from the Oil-Climate Index to compute downstream carbon intensity of petroleum products for each crude assay, we then match these crude assays with Rystad fields using a matching approach identical to that used for midstream emissions. OPEM was developed by Deborah Gordon, Eugene Tan, Jonathan Koomey, and Jeffrey Feldman. See the Oil-Climate Index (OCI) Website at https://oci.carnegieendowment.org/.

Figure B1: The correlation between predicted and OPGEE-calculated carbon intensities.

(a) Predicted and OPGEE-calculated CIs: OPGEE sample

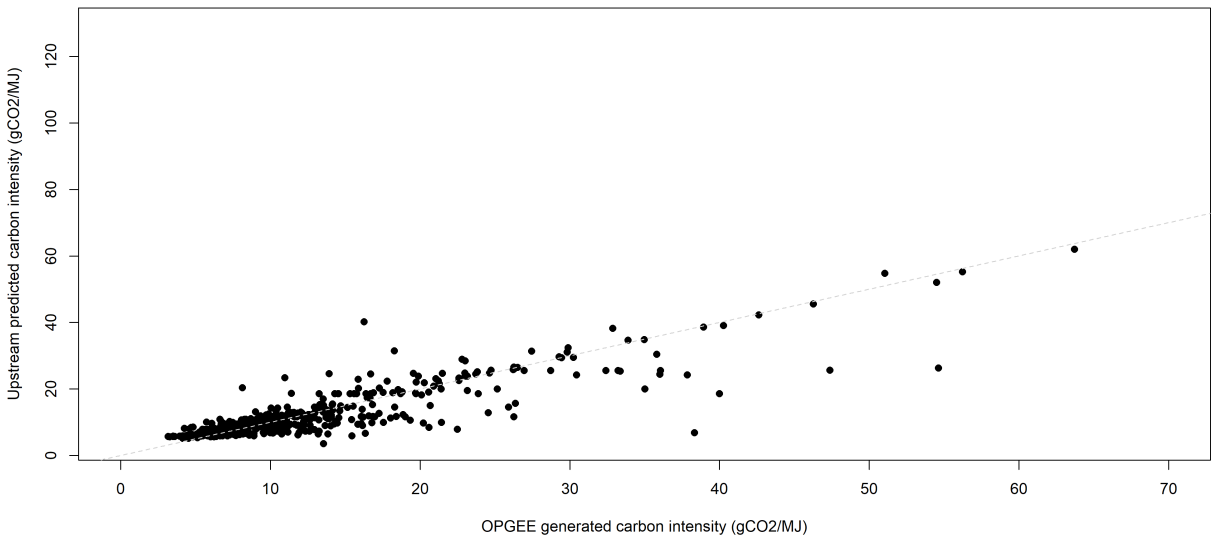

(b) Correlation coefficients of predicted and OPGEE-calculated CIs: OPGEE sample

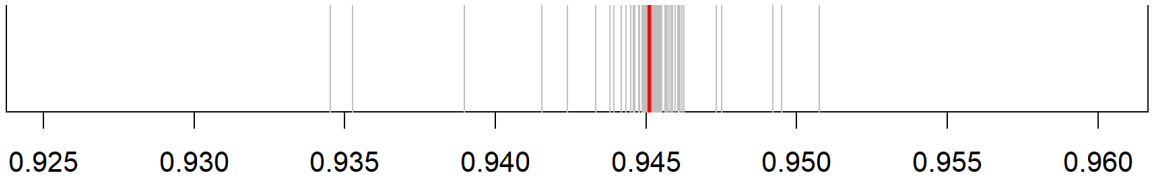

Notes: Panel (a) plots the predicted CIs from equation (9) and the calculated CIs in OPGEE for the sample of publicly-available fields provided with OPGEE ("OPGEE sample"). Each point represents a distinct field, and the dashed line is the best linear fit. Panel (b) displays the correlation coefficients between the CIs calculated in OPGEE and the CIs obtained when replicating regression (9) removing OPGEE fields one-by-one from the "OPGEE sample". Each grey line corresponds to a different estimation with the same number of observations: $N(OPGEE_{sample}) - 1$. The thick red line shows the original correlation coefficient from the comparison of the predicted CIs and the CIs calculated in OPGEE with the full OPGEE sample.

Figure B2: Upstream CI estimation: Estimates of the coefficients on the explanatory variables removing the OPGEE fields one-by-one.

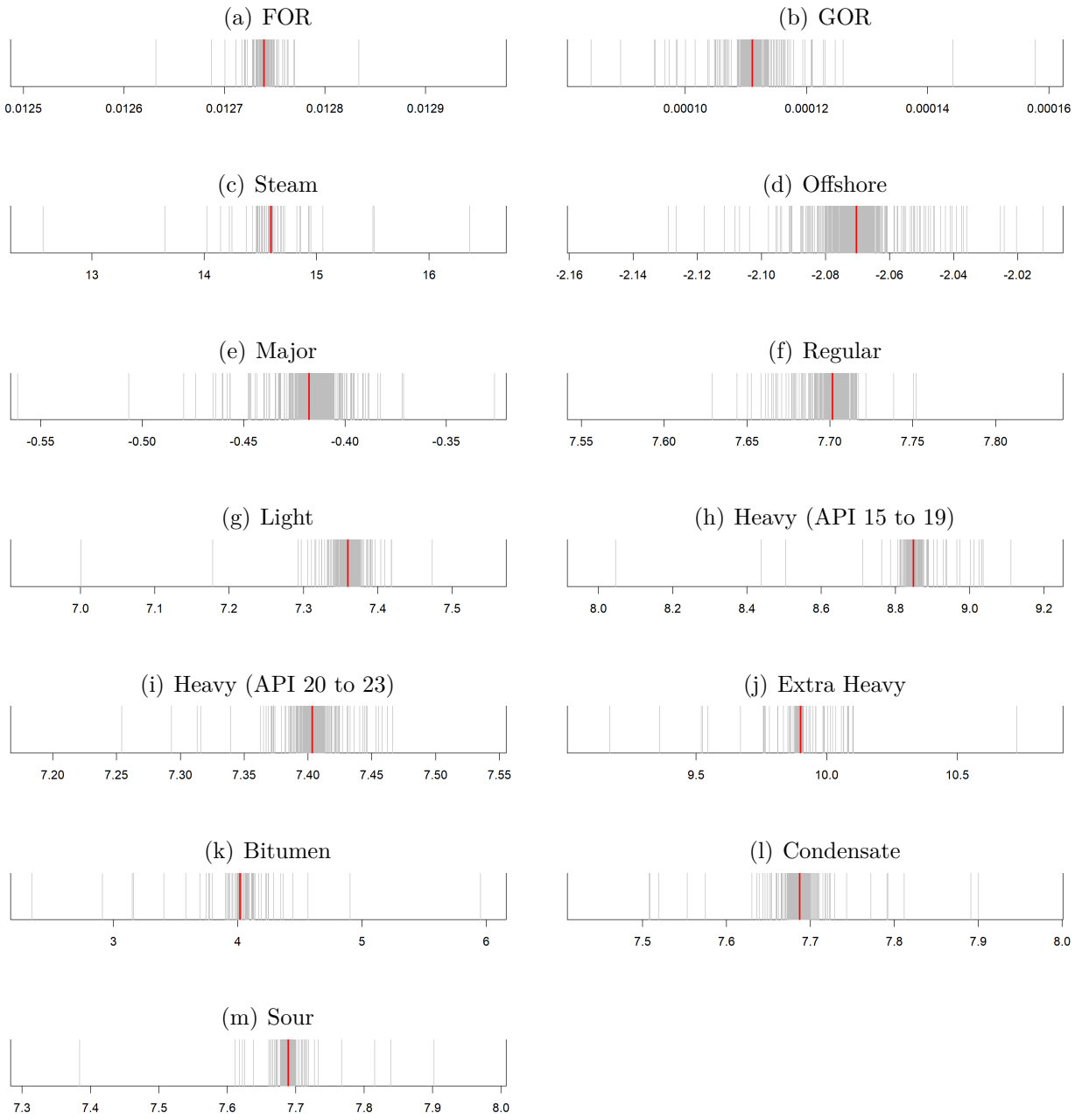

Notes: These panels show the estimated coefficients on each of the explanatory variables in equation (9) removing OPGEE fields one-by-one. Each grey line corresponds to a different estimation with the same number of observations: $N(OPGEE_{sample}) - 1$. The thick red lines show the original estimates obtained with the full sample of OPGEE publicly-available fields (OPGEE sample).

Figure B3: Predicted CIs and OPGEE-calculated CIs: 2015 World production.

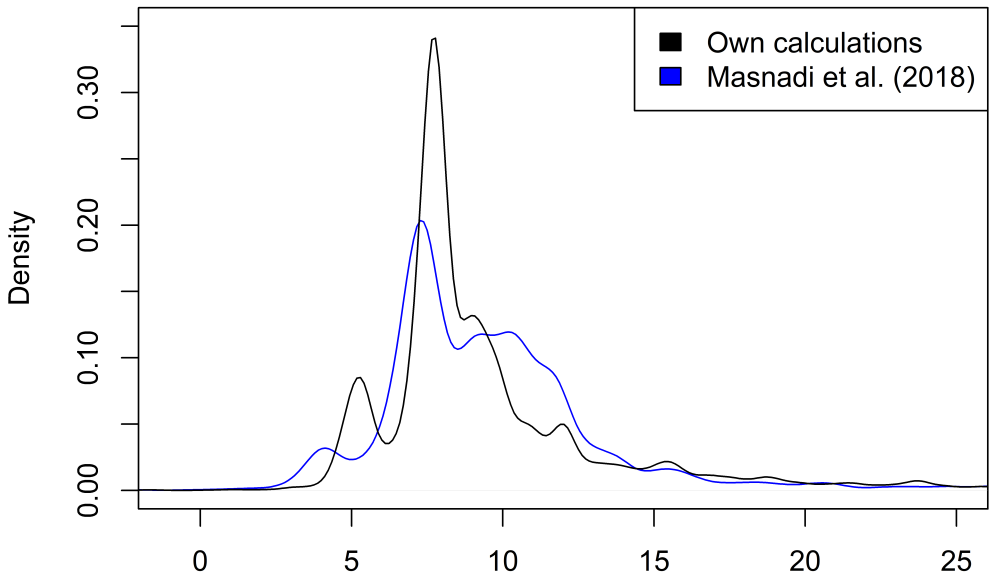

Notes: The figure plots the distributions of our estimated upstream CIs using equation (9) for fields producing in 2015 (black) and those from Masnadi et al. (2018) (blue). These distributions are based on the CPD approach, as the only publicly-available deposit-level CIs in Masnadi et al. (2018) for fields covering the entire 2015 production are those calculated using the CPD approach. On the horizontal axis, CI are in grams of CO_2eq per megajoule (gCO_2eq/MJ).

Figure B4: The distribution of upstream carbon intensities: EBA and CPD.

(a) OPGEE-sample fields

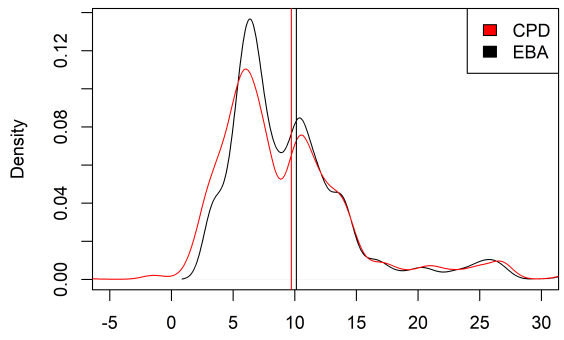

(b) All producing fields 1992-2018 (Rystad)

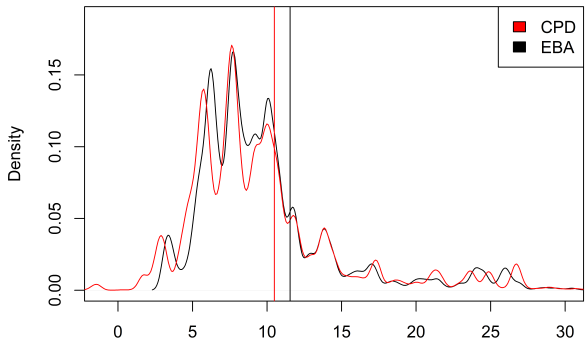

Notes: Panel (a) plots the production-weighted distributions of upstream CIs (2015 production) calculated in OPGEE for fields in the OPGEE sample using the EBA (black) and CPD (red) methods ($GOR < 10,200$). See Appendix B for the description of these methods. On the horizontal axis, CIs are in grams of CO_2eq per megajoule (gCO_2eq/MJ). The vertical bars are the CI means weighted by 2015 production. Panel (b) plots the production-weighted distributions of predicted CIs (using equation (9) and Rystad data) and those calculated in OPGEE when possible with the EBA (black) and CPD (red) methods for all fields producing oil between 1992 and 2018 with $GOR < 10,200$. On the horizontal axis, CIs are in grams of CO_2eq per megajoule (gCO_2eq/MJ). The vertical bars are the CI means weighted by 1992-2018 productions. We exclude fields with $CI > 32$ for visibility reasons.

Figure B5: The distribution of midstream carbon intensities: Coking and hydrocracking.

(a) PRELIM crude assays

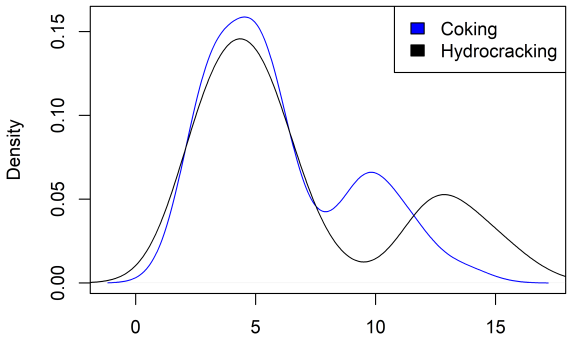

(b) All producing fields 1992-2018 (Rystad)

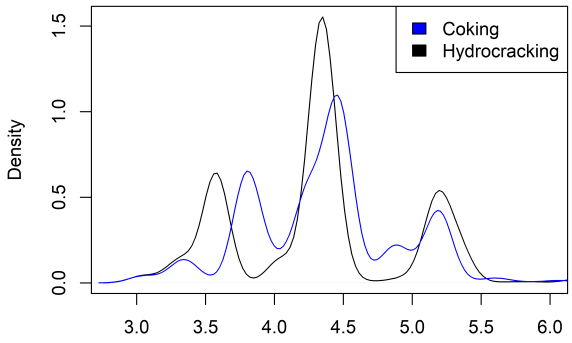

Notes: Panel (a) plots the distributions of midstream carbon intensities for PRELIM crude assays calculated in PRELIM with either the coking (blue) or hydrocracking (black) configuration. Panel (b) plots the distributions of predicted CIs and those calculated in PRELIM when possible for all fields producing oil between 1992 and 2018. On the horizontal axis, CIs are in grams of CO_2eq per megajoule (gCO_2eq/MJ). In Panels (a) and (b), we exclude the crudes with $CI > 17$ and $CI > 6$, respectively, for visibility reasons.

Table B1: Regression results from upstream carbon-intensity estimations.

	Energy-Based Allocation	Co-Product Displacement
Synthetic	25.584***	25.706***
	(1.218)	(1.273)
Bitumen	4.017***	4.704***
	(1.005)	(1.05)
Extra Heavy	9.899***	9.776***
	(0.628)	(0.657)
Heavy (15-19)	8.848***	8.962***
	(0.759)	(0.794)
Heavy (20-23)	7.403***	7.464***
	(0.608)	(0.635)
Regular	7.701***	7.751***
	(0.223)	(0.233)
Light	7.359***	7.261***
	(0.384)	(0.402)
Condensate	7.687***	7.387***
	(0.956)	(0.999)
Sour (> 3%)	7.689***	7.985***
	(1.056)	(1.104)
Offshore	-2.07***	-2.383***
	(0.245)	(0.256)
Steam Injection	14.593***	13.979***
	(0.782)	(0.817)
Major	-0.418	-0.56**
	(0.266)	(0.278)
GOR (kscf/bbl)	0.111	-0.098
	(0.071)	(0.074)
FOR (kscf/bbl)	12.739***	13.454***
	(0.156)	(0.163)
R-squared	0.949	0.945
Adjusted R-squared	0.948	0.944

Notes: *p<0.1; **p<0.05; ***p<0.01. The dependent variable is the upstream carbon intensity in gCO_2eq/MJ calculated in OPGEE. Columns 1 to 2 display the estimated coefficients from equation (9) with carbon intensities calculated in OPGEE via the EBA, and CPD approaches respectively: see Appendix B for the explanation of the different approaches. *Synthetic*, ..., *Sour (> 3%)* are dummy variables for each oil type. *Sour (> 3%)* represents oil with a sulfur content of over 3%. *Offshore* is a dummy for the field being offshore. *Steam Injection* is a dummy for steam being used in the reservoir to extract oil. *Major* is a dummy for the operator being an Oil Major. *GOR* is the ratio between the quantity of gas in Thousands of cubic feet (kscf) and the quantity of oil in barrels in the reservoir. *FOR* is the ratio between the quantity of gas flared and the quantity of oil extracted, also in kscf/bbl. See Appendix B for the definition of these variables.

Table B2: Robustness checks: Excluding influential observations for upstream CI estimation (Cook's distance).

	Synthetic	Bitumen	Condensate	Extra-Heavy	Heavy 15-19
1	30.377*** (1.274)	2.343** (0.981)	7.648*** (0.919)	9.17*** (0.608)	8.712*** (0.73)
5	30.377*** (1.053)	4.25*** (0.843)	7.704*** (0.759)	9.75*** (0.509)	8.957*** (0.603)
10	29.031*** (1.302)	3.112*** (0.859)	7.744*** (0.727)	8.786*** (0.5)	8.923*** (0.578)
	Heavy 20-23	Light	Regular	Sour	Offshore
1	7.373*** (0.584)	7.324*** (0.369)	7.65*** (0.214)	7.661*** (1.014)	-2.02*** (0.235)
5	7.404*** (0.483)	6.967*** (0.306)	7.65*** (0.177)	7.705*** (0.838)	-2.051*** (0.195)
10	7.43*** (0.462)	7*** (0.293)	7.709*** (0.17)	7.698*** (0.803)	-1.998*** (0.187)
	Steam Injection	Major	GOR	FOR	
1	16.361*** (0.773)	-0.457* (0.256)	0.121* (0.068)	12.74*** (0.150)	
5	13.097*** (0.672)	-0.434** (0.212)	0.097* (0.056)	12.78*** (0.124)	
10	14.322*** (0.715)	-0.604*** (0.204)	0.094* (0.054)	12.79*** (0.119)	

Notes: *p<0.1; **p<0.05; ***p<0.01. Each line represents the coefficient on the variable indicated at the column head when estimating equation (9) excluding the n most-influential observations from the OPGEE sample. The number n appears in the first column. We define the n most-influential observations as those with the n-largest Cook's distances (CD). The Cook's distance of observation i is $CD_i = (1/ps^2)\sum_{j=1}^{N}\left(\widehat{y}_j - \widehat{y}_{j(i)}\right)^2$, where $\widehat{y}_j$ is the fitted response value obtained with the full sample and $\widehat{y}_{j(i)}$ that after excluding i, s^2 the mean squared error of the regression model, p the number of coefficients, and N the number of observations in the OPGEE sample. See Appendix B for the definition of these variables and the note to Table B1.

Table B3: Regression results from midstream carbon-intensity estimations.

	Coking	Hydrocracking
(Intercept)	-14.838***	-24.198***
	(1.221)	(1.613)
API	4.135***	6.22***
	(0.234)	(0.309)
API^2	-0.236***	-0.36***
	(0.014)	(0.019)
API^3	5.15e-03***	7.96e-03***
	(5.15e-03)	(7.96e-03)
API^4	-3.86e-05***	-6.04e-05***
	(-3.86e-05)	(-6.04e-05)
Sour (> 1%)	0.731***	0.855***
	(0.149)	(0.197)
Major	-0.45***	-0.293
	(0.156)	(0.206)
R-squared	0.517	0.552
Adjusted R-squared	0.514	0.549

Notes: *p<0.1; **p<0.05; ***p<0.01. This table shows the estimates from equation (11). The dependent variable is the midstream carbon intensity in gCO_2eq/MJ computed in PRELIM using the coking (Column 1) or hydrocracking (Column 2) configurations. *API* is the American Petroleum Institute (API) gravity index, a measure of oil density. *Sour (> 1%)* is a dummy for the sulfur content being over 1%. *Major* is a dummy for the operator being an Oil Major. See Appendix B for the definition of these variables.

C Modeling and parameter choices

C.1 The selection of deposits

For each exercise, we retain fields with positive reserves at the beginning of the period of interest of each exercise of at least one of the following oil types: "Condensate", "Light", "Regular", "Sour (> 3%)", "Extra Heavy Oil", "Heavy Oil 15-19", "Heavy Oil 20-23", "Bitumen", and "Synthetic crude" (the numbers for heavy oils represent the API gravity range). In line with the Rystad categorization of oil and gas fields, those with a gas-to-oil ratio of over 10,200 scf/bbl are considered to be gas fields, and are excluded from our sample.

C.2 Reserves

The reserve estimates are from the Rystad UCube dataset. A deposit reserve is defined as its economically-recoverable volume, assuming an oil price of US$ 120 per barrel (scenario

"Resources High Case"). Current World reserves amount to 1,517 billion barrels in the Rystad dataset, as against 1,729 billion barrels for World proven reserves according to BP (2019). The difference in these numbers mostly reflects that the Rystad dataset does not record the proven reserves for some bitumen and extra heavy oils that are too expensive to be profitable, even in the long run. For instance, in Rystad, Canada and Venezuela have reserves estimated respectively at 101 and 34 billion barrels at the end of 2018; the analogous figures in BP (2019) are 167 and 303 billion barrels. The resources not in the Rystad dataset are in general not only too expensive to be extracted but also very polluting. As a consequence, they would not be used in counterfactual scenarios in which extraction costs are minimized and pollution costs factored in. Overall, using a less-restrictive definition of reserves in our analysis would have little impact on our findings.

C.3 Extraction costs

C.3.1 The field-level levelized cost of extraction (LCOE)

We use precise annual field-level data on capital (CAPEX) and operational expenditures (OPEX) from the Rystad UCube database to calculate the per barrel private extraction cost. For each field, we calculate the barrel extraction cost as the discounted levelized cost of extraction (LCOE) of the field over the 1970-2099 period, with an annual discount rate of 3%. Denoting by x_{dt} and c_{dt} the annual deposit production and cost, and r the annual discount rate, the unitary cost c_d of deposit d is:

$$c_d = (\sum_{1970}^{2099} c_{dt} e^{-rt}) / (\sum_{1970}^{2099} x_{dt} e^{-rt})$$

We measure annual costs as the sum of "well" and "facility" CAPEX, and the "selling, general and administrative", "transportation" and "production" OPEX. According to the Rystad definitions, "well CAPEX is capitalized costs related to well construction, including drilling costs, rig lease, well completion, well stimulation, steel costs and materials." Facility CAPEX includes development CAPEX ("costs to develop, install, maintain and modify surface installations and infrastructure"), exploration CAPEX ("costs incurred to find and prove hydrocarbons"), and abandonment costs ("costs associated with shutting down and dismantling the surface and subsea facilities"). Production OPEX is "operational expenses directly related to the production activity. The category includes materials, tools, maintenance, equipment-lease costs and operation-related salaries. Depreciation and other non-cash items are not included." Transportation OPEX includes "the costs of bring the oil and gas from the production site/processing plant to the pricing point (only upstream transportation)".

We convert Rystad nominal-cost values into 2018 dollars using the World Bank US GDP deflator.[54] For post-2018 years, we estimated costs and production provided by Rystad UCube based on the 120$-per-barrel price scenario.

In our main analysis, we assume that the present value aggregate cost $C(.)$ of extracting a stream of oil $\mathbf{x_d} \equiv (x_{dt})_t$ for a deposit d starting extraction at date t_1 and ending extraction at date t_2 is:

$$C(\mathbf{x_d}) = \sum_{t_1}^{t_2} c_d x_{dt} e^{-rt}$$

where c_d is specific to the deposit. We also assume that this present-value aggregate cost can be in practice spread over multiple time periods. Take the following example: consider an extraction stream (x_1, x_2) occurring at dates 1 and 2. To extract these quantities, an oil company, that owns a deposit d with $c_d = 2$, can either spend $2x_1$ US$ at date 1 and $2x_2$ US$ at date 2, or spend $2x_1 + 2e^{-r}x_2$ US$ at date 1 and 0 US$ at date 2, or even $2x_1e^r + 2x_2$ US$ at date 2. In all three cases, it can extract the stream (x_1, x_2) only if the present value of its payment at date 1 is $2x_1 + 2e^{-r}x_2$.

This cost function reflects that some of the expenditures required for production at a given date do not necessarily take place at the date of production. For instance rig lease, included in Rystad Capital expenditures, can be paid in advance or may include an upfront payment which depends on the achievable production each year (x_1, x_2).

Taking this form of the cost function, the constant-cost equivalent c_d can be estimated from the observed expenditures at date t, c_{dt}, and observed production x_{dt}, as long as the whole extraction path from the deposit is observed, which is the case in our data. The estimate $\hat{c}_d$ is:

$$\hat{c}_d = (\sum_{1970}^{2099} c_{dt} e^{-rt}) / (\sum_{1970}^{2099} x_{dt} e^{-rt})$$

Note that the cost function can entail time inconsistencies if costs are paid before extraction takes place. However we assume that, in the Rystad data, producers commit to a whole stream of production before the deposits start to produce. In addition, in our counterfactual we assume that costs are paid at the year of production. Note that when the counterfactual starts in $T_0 > 1970$, we could remove from the calculation of the equivalent constant extraction cost c_d the costs paid pre-T_0 but that can be attributed to production post-T_0. In detail, assume a deposit d for which the equivalent constant extraction cost estimated over the whole 1970-2099 period is $\hat{c}_d$. Now if $(\sum_{1970}^{T_0} c_{dt} e^{-rt}) / (\sum_{1970}^{T_0} x_{dt} e^{-rt}) > \hat{c}_d$, some of the cost paid during the 1970-T_0 period was for future production. More precisely, calling $\hat{c}_{d,T_0}$ the

[54] Available at https://data.worldbank.org/indicator/NY.GDP.DEFL.ZS?locations=US, accessed on October 16^{th} 2019.

extraction costs that should be considered in any counterfactual starting at date T_0:

$$\hat{c}_{d,T_0} = (\sum_{T_0}^{2099} c_{dt}e^{-rt})/(\sum_{T_0}^{2099} x_{dt}e^{-rt})$$

we can check that whenever $(\sum_{1970}^{T_0} c_{dt}e^{-rt})/(\sum_{1970}^{T_0} x_{dt}e^{-rt}) > \hat{c}_d$, we have $\hat{c}_{d,T_0} < \hat{c}_d$.

In our main analysis, we assume that c_d is always equal to the LCOE constructed from the data over the whole 1970-2099 period, as adding more years (data points) makes the estimation more precise if the measurement errors are uncorrelated. However, we also carry out a robustness check in which only the costs that occur after the starting date of optimization are considered for the calculation of the constant equivalent extraction costs, i.e. we calculate $\hat{c}_{d,T_0}$ (see the approach *Only future costs* below). We find very similar results.

C.3.2 Other approaches

We consider three alternative approaches for the calculation of deposit-extraction costs.

The first is average costs, which are calculated as: $c_d = (\sum_{t_1}^{t_2} c_{dt})/(\sum_{t_1}^{t_2} x_{dt})$. We call this approach *Average costs*.

The second consists in removing from the calculation of the LCOE the production stream and the costs paid before the starting date of the optimization, $\hat{c}_{d,T_0}$. We call this approach *Only future costs*.

The last approach builds on the construction of extraction costs in Asker et al. (2019) and accounts for observed shocks in extraction costs each year, such as changes in extraction-input prices. This is as follows. First, we assume that the private costs of extraction take the form: $c_{dt} = c_d\mu_{dt}$, in which μ_{dt} is governed by an exogenous Martingale process such that $\mathbb{E}(\mu_{dt+k}|\mu_{dt}) = \mu_{dt}$ for $k \geq 1$. We assume furthermore that c_d can be estimated from the cost data assuming that $c_d\mu_{dt} = c_d\mu_{st}exp(\epsilon_{dt})$, where s indexes the onshore or offshore deposits and ϵ_{dt} is a measurement error. The year and on- or off-shore specific cost shift μ_{st} is estimated as $\ln\hat{\mu}_{st} = \sum_{d\in s} \kappa_{dt} \ln c_{dt}$, where κ_{dt} is the quantity weight of a field in a given year's total output. The time-invariant marginal cost, c_d, is then estimated, allowing for measurement error, using the following (within-deposit) regression: $\ln c_{dt} - \ln\hat{\mu}_{st} = ln\hat{c}_d + \epsilon_{dt}$. Consider now the optimization of production starting at some date t. A deposit that did not produce before date t in the Rystad data cannot produce at date t in our counterfactual, but can produce later on in the counterfactual, starting from its first production date in the data. Considered from date t, the expected private cost of the extraction of deposit d at date $t+k$ is $c_d\mu_{st}$. The counterfactual starting at date t is built by optimizing production over the whole $[t, T_f]$ period, taking $c_d\mu_{st}$ as the constant extraction cost of deposit d. Once

the counterfactual starting at date t is calculated using cost estimates as above, we move to $t+1$ and re-apply the same algorithm: we reconstruct the private costs of extraction and re-optimize the supply sequence post-$t+1$. The unitary extraction cost of a deposit varies over time but this extraction path is consistent with the assumption that $\mathbb{E}(c_{d,t+k}) = c_{d,t}$, for all $k \geq 1$. We call this approach *Time-varying costs*.

C.3.3 Refining and transportation costs

As explained above, we use precise field-level data on capital (CAPEX) and operational expenditures (OPEX) from the Rystad UCube database to calculate the per barrel private extraction cost. We consider these as production costs, i.e. we abstract from refining costs and assume that these latter are the same for all crudes. In reality, refining costs vary across crudes according to their density and sulfur content: heavier crudes and those with a high sulfur content are more costly to refine into diesel and gasoline (CFA, 2013). Including refining costs in the analysis would increase our gains from supply recomposition, as the most-polluting resources have higher refining costs. Refining-cost data is difficult to obtain. Operational costs are mostly available for US refineries, and to a lesser extent in Europe; in Asia, refineries are often State-owned and their operating costs are rarely disclosed. The estimates are US$ 3.8 per barrel in the US (2011, Valero refineries) and US$ 3.3-4.2 in Europe (2011, Petroplus refineries) according to IEA (2012). These costs, and their variations across oils, are small compared to the standard deviation of crude-extraction costs (10.8 in our dataset when weighted by observed production over the 1992-2018 period). We also abstract from transportation costs, as these are also small compared to crude-extraction costs. According to the OECD-Stats (Maritime Transport Costs for Crude oil) available at https://stats.oecd.org/Index.aspx?DataSetCode=MTC, the average cost of shipping a barrel from Saudi Arabia, UAE, and Kuwait to the US over the 2002-2007 period was US$ 1.8, 2.5, and 2.0 respectively.

Figure C1: Heterogeneity in deposit extraction costs.

(a) The private cost of extraction by oil type: 1992-2018

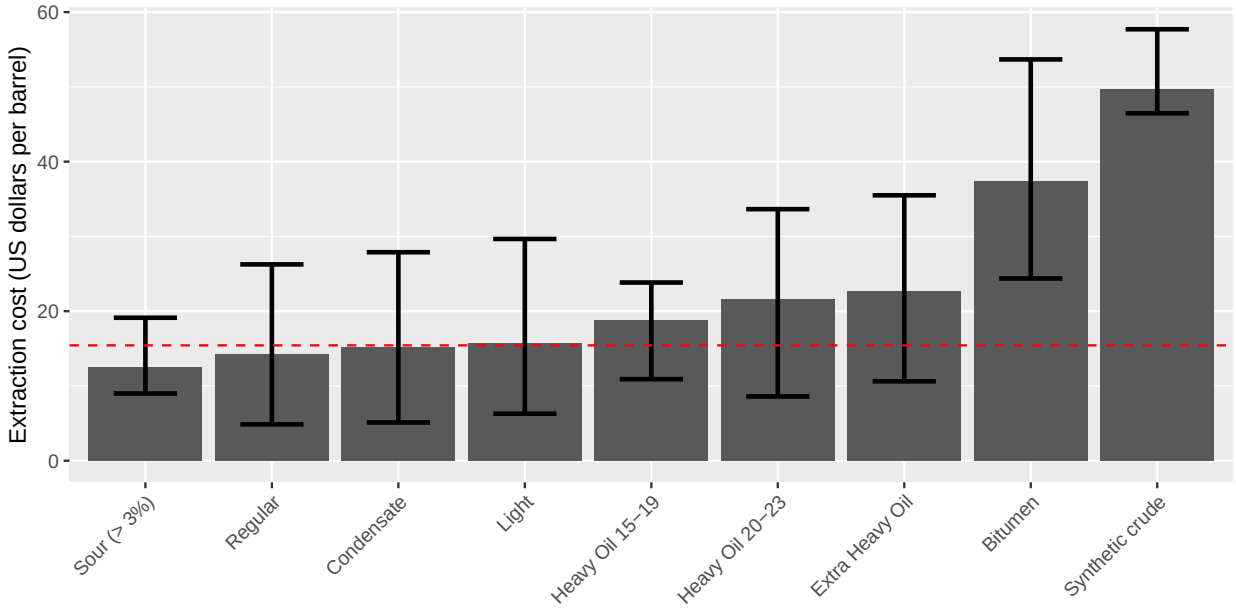

(b) The private cost of extraction by country: 1992-2018

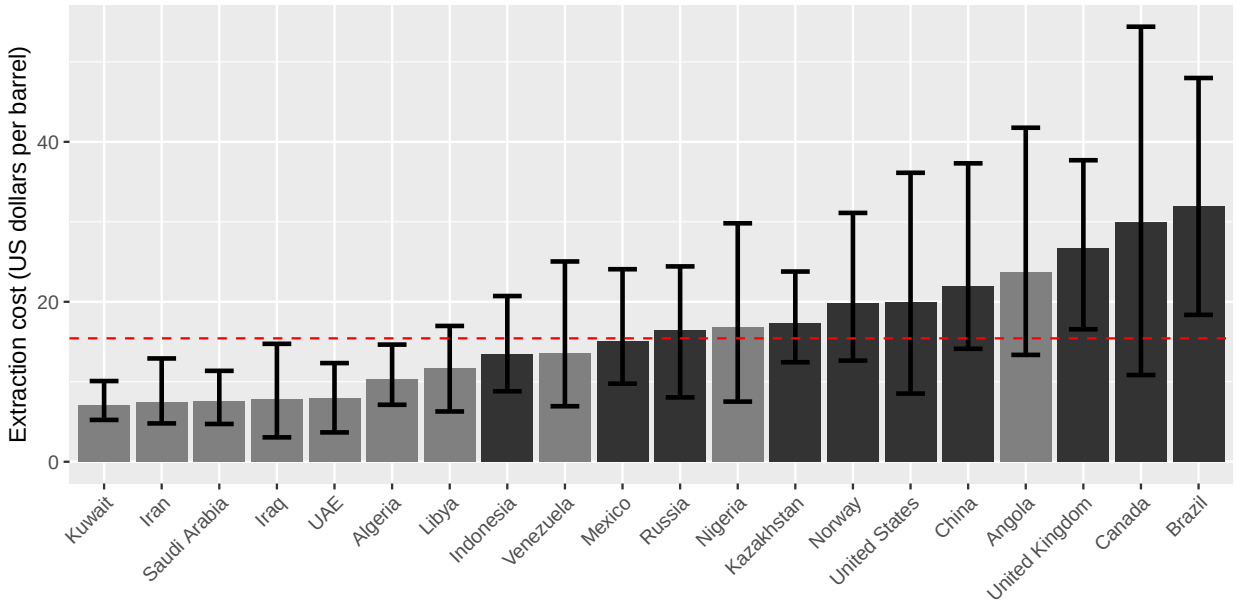

Notes: Panels (a) and (b) show the extraction cost per barrel based on observed production over the 1992-2018 period by oil type and producing country respectively. The bar represents the mean (weighted by deposit production) and the extremities of the lines the 10% and 90% deciles. The construction of extraction costs is described in Appendix C. In Panel (b), only the Top-20 oil producers over the period are depicted, and OPEC country carbon-intensity bars appear in light grey. The red dashed line corresponds to the World average figure. OPEC, as of 2019, included Algeria, Angola, Congo, Ecuador, Equatorial Guinea, Gabon, Iran, Iraq, Kuwait, Libya, Nigeria, Saudi Arabia, the UAE, Venezuela, and the Neutral Zone shared by Kuwait and Saudi Arabia.

C.4 Discovery years

For each field, Rystad UCube provides two dates: the discovery and approval years. The first corresponds to the year the deposit oil reserves were found to be extractable, while the second indicates the year when local authorities approved exploitation. We assume that a field can produce starting from its discovery year.

C.5 Post-2018 demand

In most of our analysis, we assume that future demand falls linearly from 2018 to zero in 2050 ('strict' carbon neutrality in the oil industry). This horizon matches countries' decarbonization pledges. At the UN Climate Action Summit held in 2019, 70 countries and major sub-national economies such as California endorsed an objective of zero net emissions by 2050, with 75 other countries committed to present plans to reach carbon neutrality by 2050. The objective of carbon neutrality by 2050 was endorsed by the European Union (European Council, 2019), Canada, Chile, Costa Rica, Fiji, the Marshall Islands, Norway, New Zealand, South Korea, Switzerland and the United Kingdom, among others, in line with the Paris Agreement.[55] This horizon is also consistent with the IPCC understanding that "global net human–caused emissions of carbon dioxide (CO_2) would [reach] net zero around 2050" to limit global warming to 1.5°C (Rogelj et al., 2018).

In our sensitivity analysis, we consider an alternative post-2018 demand in which "net" carbon neutrality is reached overall by 2050. Under this scenario, some emissions — that need to be compensated by CO_2 removal from the atmosphere to reach "net" carbon neutrality — persist in 2050 in the oil sector. In this case, we consider that oil-related emissions in 2050 represent 34% of 2020 World emissions. This is in line with the IPCC scenario "Below–1.5C and 1.5C– low-OS pathway" in which oil demand falls by 66% (Solomon et al., 2007). This corresponds to oil demand of 9.9 billion barrels in 2050. In this alternative post-2018 future demand scenario, we consider that, starting in 2018, demand falls linearly to 9.9 billion barrels in 2050. Assuming the same linear decrease post-2050, the oil era ends in 2066 in this robustness check. In a second robustness check, we consider that the oil era ends in 2080 and that demand falls linearly from 2018 to reach zero in 2080.

[55]The full list of countries sharing this ambition appears at https://www.climatechangenews.com/2019/06/14/countries-net-zero-climate-goal/ and https://www.carbon-neutrality.global/wp-content/uploads/2019/09/CNC-Fact-Sheet.pdf.

C.6 The social cost of carbon

The development of Integrated Assessment Models (IAMs) in the 1990s — e.g., the Dynamic Integrated Climate and Economy (DICE, developed by William Nordhaus and used e.g., in Nordhaus 1994, 1992), the Policy Analysis of the Greenhouse Effect (PAGE, developed by Chris Hope, and used in e.g., Stern 2008), and the Climate Framework for Uncertainty, Negotiation, and Distribution (FUND, developed by Richard Tol and used e.g. in Anthoff and Tol, 2013), see Calel and Stainforth (2017) for a comparison of these IAMs — constituted a turning point in the estimates of the social cost of carbon (SCC). These models describe interactions between carbon-dioxide concentration, the climate, damage from climate change, and human activities that produce carbon-dioxide emissions. Although criticisms about the limitations of IAM remain (e.g., Pindyck, 2013, 2019, which stress arbitrary modelling choices, the deterministic nature of most IAMs, and the exclusion of catastrophes), the IAM estimates have been widely discussed in the public debate.

The SCC estimates from IAMs vary greatly, in particular depending on the choice of the social discount rate (Nordhaus, 2007; Stern, 2008; Tol et al., 2013), the coverage of damage, and the modeling (if any) of uncertainty (Weitzman, 2009, 2011; Calel et al., 2015; Gillingham et al., 2018). A growing body of literature argues that social costs of carbon, such as those used by the U.S. Government Interagency Working Group, that are based on simulations from the DICE, PAGE and FUND models underestimate the true social costs, as they ignore key uncertainties, some climate-change related damage, irreversibilities and acceleration factors, such as the possibility of tipping points, and usually keep the valuation of ecosystems constant despite their rarefaction (for a summary of these criticisms, see e.g., Revesz et al., 2014; Van Den Bergh and Botzen, 2014).

Nordhaus (2017) finds a SCC of 36.7 US$ in 2020 (in 2010 US$) along the optimized emission path, which jumps to 87 US$ with a discount rate of 3%. In the baseline parameterization of the DICE2016R, constraining the increase in temperature over the next 100 years as compared to 1900 to be under 2.5°C increases the SCC to 229.1 US$ per tCO_2 (in 2010 US$). Dietz and Stern (2015) bring three main changes to the 2010 version of the DICE model: (i) Climate change negatively affecting the accumulation of physical, technological and intellectual capital; (ii) Modifying the function translating temperature increases into GDP loss to account for possible tipping points (Weitzman, 2012; Lenton and Ciscar, 2013); (iii) The "climate-sensitivity" parameter, which links atmospheric concentrations of greenhouse gases to (expected) temperature increases, being updated to account for new climate-science knowledge, although Nordhaus' discount rate is left unchanged (at twice the level of that preferred by Stern). They find a carbon price in the \$32-103/tCO_2 range (2012 prices) in 2015. Lemoine (2021) estimates a 200-year social cost of carbon in 2014 of \$362

per tCO_2 in a calibration exercise accounting for uncertainty about both warming and the impact of warming on consumption, and including stochastic shocks to consumption growth.

Overall, our choice of a SCC of 200 US$ per tCO_2 in 2018 is consistent with the SCC in DICE2016R when the temperature increase is kept strictly below 2.5°C over the next 100 years. In our sensitivity analysis, we vary the SCC value between $0 and $400.

C.7 Cost minimization

The numerical analysis is carried out in R (version 3.6.0) using the following packages: data.table, Matrix, slam, gurobi, pryr, ggplot2, Hmisc, and rio. Optimization is carried out using the linear-programming solver Gurobi Optimizer available at https://www.gurobi.com/products/gurobi-optimizer/.

D The optimal extraction path: resource selection and extraction order

Proof of Lemma 1.

The first claim is trivial. With total oil reserves exceeding total demand, if the cheapest resource is polluting enough, its social cost will be high enough to prevent its use.

2. Deviations from the "least-cost first" principle. Even if pollution is ignored, the optimal extraction sequence does not boil down to a simple deviation from the rule in Herfindahl (1967). This "least-cost first" rule can be described by the following algorithm, similar to that employed in Asker et al. (2019): start with the first year of the period, t_0. Consider the pool of resources available for extraction that year (positive reserves, with discovery dates equal or anterior to t_0) and label the resources $R1$, $R2$, ..., RN such that $c_1 < c_2 < ... < c_N$, where N is the number of available resources that year. Satisfy demand with the cheapest resource in that pool $R1$, then move to the next-cheapest resource $R2$ only if the previous resource is exhausted or its capacity-constraint binds and demand in year t_0 is not yet satisfied, and then repeat moving up in the resource ranking until demand at t_0 is fulfilled. Then, redefine the pool of resources available for extraction at the beginning of $t_0 + 1$, as well as the reserves as of the beginning of $t_0 + 1$ and each resource capacity constraint, and relabel the resources by their ranks in the updated (increasing) order of extraction costs. Repeat this process until the end of the period of interest is reached.

We show below that, since some resources are not exhausted in the long run (oil is abundant in a carbon-constrained world), a cost-effective or optimal extraction sequence is not incompatible with a resource being extracted in a year despite there being a cheaper

resource (used in the future) available for extraction that year, i.e. the "least-cost first" algorithm described above usually does not provide the solution to the social planner's cost-minimization problem.

Consider the cost-minimization program of (6) in the following resource context. The oil era lasts two years, with T_0 and T_f the first and last years. Annual oil demand is two barrels per year. Three resources, $R1$, $R2$, $R3$, are available with extraction costs and pollution contents ordered as $c_1 < c_2 < c_3$ and $\theta_1 < \theta_2 < \theta_3$. The reserves for each resource at the beginning of T_0 are two barrels. All resource discovery dates are prior to T_0. The capacity constraints, and thus maximum annual extraction, for $R1$, $R2$ and $R3$ are two, one and two barrels per year respectively.

Assume that only economic costs matter. The "least-cost first" extraction sequence generalized to account for capacity constraints, $S1$, is:

- T_0: Two barrels of $R1$ ($R1$ exhausted);
- T_f: One barrel of $R2$ and one barrel of $R3$ ($R2$ is not exhausted, as only one barrel of $R2$ is used due to the capacity constraint).

Consider the alternative allocation, $S2$ with:

- T_0: One barrel of $R1$, one barrel of $R2$.
- T_f: One barrel of $R1$, one barrel of $R2$.

Both sequences, $S1$ and $S2$, satisfy annual demands and the reserve and extraction-capacity constraints. The payoff of $S2$ compared to $S1$ (T_0 value) is $Cost(S1) - Cost(S2) = 2c_1 + (c_2 + c_3)/(1+r) - (c_1 + c_2)(1 + 1/(1+r))$, with r being the annual discount rate. It is trivial to check that for c_3 large enough, $S2$ is strictly preferred to $S1$.

Assume now that only pollution matters, i.e. we look for the lowest-possible cumulative emissions. The equivalent "least-cost first" rule — that consists in filling demand starting with the least polluting resource until a resource availability constraint binds (annual capacity or reserve size) — is not optimal. This produces a sequence similar to $S1$, as resource carbon contents are ranked similarly to their extraction costs in our example. The gains for implementing $S2$ instead of $S1$ are $Cost(S1) - Cost(S2) = \mu(\theta_3 + \theta_2 + 2\theta_1 - 2\theta_2 - 2\theta_1) = \mu(\theta_3 - \theta_2) > 0$, where μ is the social cost of carbon in T_0: $S2$ is thus always preferred.

In the above example, there is room to improve on extraction $S1$ as $R2$ is not exhausted at the end of the oil era in $S1$. Were all oil deposits to be exhausted in the long run, then the optimal extraction path could be found by implementing the amended "least-cost first" algorithm described above. In Asker et al. (2019), all reserves are exhausted in the

long run, so the "least-cost first" algorithm provides the solution to the social planner's cost-minimization problem.

3. The difference between cost-effective supply and optimal supply with perfectly-correlated private costs and carbon contents. We assume that $c_3 < \bar{c}$ with $\bar{c} = (c_1 + c_2)(2 + r) - 2c_1(1 + r) - c_2$. It is easy to verify that the sequence $S1$ actually corresponds to the cost-effective supply if pollution is ignored.

Now consider optimal supply: the social gains from the deviation from $S1$ to $S2$ are $Cost(S1) - Cost(S2) = 2c_1 + (c_2 + c_3)/(1 + r) - (c_1 + c_2)(1 + 1/(1 + r)) + \mu(\theta_3 - \theta_2)$.

Even if costs and carbon contents are perfectly correlated, it is trivial to see that for μ large enough the social gains of moving to $S2$ are strictly positive, and thus $S1$ is not the optimal supply. We have provided an example in which the cost-effective supply is distinct from optimal supply, even when carbon contents and extraction costs are perfectly correlated.

The optimal extraction sequence over a period and ulterior demand. Consider the resource context described above and assume that a third extraction year is added, t_3. The period is now composed of three years T_0, T_f, t_3 (in chronological order). Also assume that $c_3 > \bar{c}$. If demand in t_3 is zero, the optimal path will be S_2 (this is true for all values of μ). Now, if demand in t_3 is 2 barrels, all reserves will end up exhausted. In this case, it is trivial to see that the sequence $S1$ continued by an extraction of "one barrel of R_2 and one barrel of $R3$" in t_3 is optimal. The optimal sequence over $[T_0, T_f]$ varies with the size of the demand after year T_f, i.e. the demand in t_3.

In this simple case, we have shown that for a given set of costs, carbon intensities, reserve and capacity constraints, the horizon over which the optimization is carried out or the size of future demand affects optimal extraction over a sub-segment of the extraction path. In other words, the solutions of $\mathcal{P}_1(1992, X, \mu)$ and $\mathcal{P}_1(1992, Y, \mu)$ with $Y \neq X$, usually do not coincide over a given period.

E The carbon policy context

This Appendix provides an overview of the development in scientific knowledge on man-made climate change prior to the 1992 Earth Summit, describes the post-1992 international carbon policy context, and last presents evidence on the lack of significant attempts to regulate greenhouse gas (GhG) emissions from the oil industry.

E.1 Pre-1992 awareness of man-made climate change

Scientific recognition of the possibility of man-made climate change can be traced back to Svante Arrhenius' work published in 1896.[56] Observing the rising demand for coal, he calculated the extent to which changes in atmospheric carbon dioxide would lead to global warming (Baum, 2016). Arrhenius' calculations indicated that doubling the CO_2 concentration would increase average temperatures by about 4-5°C. However, the prevailing consensus over the next 60 years was that human activities could not sufficiently affect the abundance of CO_2 in the atmosphere to change the Earth's climate.

In 1955, casting doubt on the consensus at that time, Hans Suess' carbon-14 isotope analysis demonstrated that the oceans do not immediately absorb carbon dioxide from fossil-fuel combustion. In 1958, Charles David Keeling started recording the first continuous time series of CO_2 concentration in the atmosphere: this time series reveals a 29% increase in CO_2 concentration between 1958 and 2019. Other extensive CO_2-concentration datasets were constructed and published, showing a similar upward atmospheric CO_2 trajectory (e.g., Callendar, 1961) and climate-change modeling improved over the following decades (e.g., the introduction of the ice-albedo effect in Budyko, 1969; Sellers, 1969). The acceleration of scientific knowledge about climate change in the second part of the 20^{th} Century is best illustrated by the multiplication of academic articles on the topic: In the abstracting journal of the American Meteorological Society, Stanhill (2001) found that 95% of the literature on the causes and impacts of climate change was published between 1951 and 1997, with a doubling of output every 11 years.[57]

Scientists' concerns reached policy-makers' attention via reports starting in the 1960s (e.g., U.S. President Lyndon B. Johnson's Science Advisory Committee, 1965). The establishment of the Intergovernmental Panel on Climate Change (IPCC) in 1988 by the World Meteorological Organization represented a landmark in the process of providing policy makers with up-to-date scientific knowledge about climate change (see Agrawala 1998 for an analysis of IPCC creation). By 1990, all Organisation for Economic Co-operation and Development (OECD) countries, with the exception of the US and Turkey, had domestic targets for the stabilization of emissions (Gupta, 2010).

[56] In 1820s, Jean Fourier understood the Greenhouse Effect: the Earth's atmosphere retains part of heat radiation, making the Earth warmer. Building on Fourier's work and research carried by Claude Servais Pathias Pouillet and William Hopkins, among others, John Tyndall designed the first experiment to measure the radiant-heat absorption of different gases in 1859.

[57] See Le Treut et al. (2005) for an overview of major advancements in climate-change science.

E.2 The Earth Summit, the Kyoto Protocol, and the Doha Amendment

We here explain how the two cornerstones of the international carbon mitigation framework — countries have differentiated responsibilities and are free to choose their mitigation instruments and sectors to regulate — have de facto limited the coverage of carbon-mitigation initiatives.

The Earth Summit was held in Rio de Janeiro, Brazil, from June 3^{rd} to June 14^{th} 1992. This represented a major landmark in the development of global political awareness of climate-change risk and international mitigation efforts. Its main achievement was the adoption of the United Nations Framework Convention on Climate Change (UNFCCC), which entered into force on March 21^{st} 1994, and the creation of the Conferences of the Parties (COP), which annually brings together policy makers, experts, and NGOs to discuss objectives, methods, and courses of actions regarding climate-change mitigation and adaptation. At the Earth Summit, UNFCCC Parties argued in favor of a "stabilization of greenhouse gas concentrations in the atmosphere at a level that would prevent dangerous anthropogenic interference with the climate system" (United Nations, 1992). The treaty acknowledged "[countries'] common but differentiated responsibilities and respective capabilities and their social and economic conditions". Quantitative mitigation targets were set out for industrialized countries (Annex B), which were expected to reduce GhG emissions to their 1990 levels by 2000.[58]

The Kyoto Protocol was adopted on December 11^{th} 1997, and entered into force on February 16^{th} 2005. This is a legally-binding international treaty under the UNFCCC with country-specific emission-reduction targets. Its first commitment period started in 2008 and ended in 2012.[59] Industrialized countries (Annex B) were expected to reduce GhG emissions over the 2008-2012 period by 5% compared to their 1990 levels on average (see Table E1). As many major emitters were not part of the agreement, this only covered about 18% of world emissions.

[58] Annex B countries are advanced economies or industrialized economies in transition to market economies. This covers Australia, Austria, Belarus, Belgium, Bulgaria, Canada, Cyprus, Denmark, the European Union, Estonia, Finland, France, Germany, Greece, Hungary, Iceland, Ireland, Italy, Japan, Latvia, Lithuania, Luxembourg, Malta, Netherlands, New Zealand, Norway, Poland, Portugal, Romania, the Russian Federation, Spain, Sweden, Switzerland, Turkey, Ukraine, the United Kingdom, and the United States of America. Croatia, the Czech Republic, Liechtenstein, Monaco, the Slovak Republic and Slovenia were added to Annex B by an amendment that entered into force on August 13^{th} 1998.

[59] Over this first period, the Protocol covered emissions of the six main greenhouse gases: Carbon dioxide (CO_2), Methane (CH_4), Nitrous oxide (N_2O), Hydrofluorocarbons (HFCs), Perfluorocarbons (PFCs), and Sulfur hexafluoride (SF_6). The Doha Amendment added nitrogen trifluoride (NF_3) to the list of greenhouse gases to be reported by the Parties, and modified the accounting of emissions related to land use and forestry.

The "Doha Amendment to the Kyoto Protocol" was adopted in Qatar on December 8^{th} 2012, creating a second commitment period from January 1^{st} 2013 to December 31^{st} 2020 with a new group of countries required to reduce their GhG emissions by at least 18% below their 1990 levels over the 2013-2020 period (see Table E1). As of October 28^{th} 2020, 147 Parties had deposited their instrument of acceptance, a figure above the threshold that triggers the entry into force of the Amendment.

The Earth Summit Convention, the Kyoto Protocol and then the Doha Amendment acknowledged countries' differentiated responsibilities regarding climate change. The consensus was that developing economies should not suffer economically from global GhG-mitigation efforts. As direct transfers between countries are politically difficult to implement, this recognition of differentiated responsibilities translated into binding carbon targets being set only for advanced economies.

The Earth Summit and the Kyoto Protocol acknowledged that emission reduction should be carried out in a cost-effective manner.[60] The Protocol leaves countries free to choose their mitigation instruments and the economic sectors to be regulated. In countries with binding carbon targets, emissions from some sectors were de facto not covered or inadequately covered by domestic regulation.

This has limited the coverage of mitigation schemes,[61] and as seen in the next subsection has led to the oil-industry emissions being mispriced since 1970.

E.3 Carbon policy and the oil industry

There are three main messages considering GhG regulations in the oil industry.

First, most major oil-producing countries do not have internationally-binding mitigation targets (Panel A of Table E1). Of the Top-10 oil producers in 2018, only the US and Russia belonged to the group of countries with emission-reduction targets in the Kyoto Protocol (Annex B). However, the US did not ratify the Kyoto Protocol, and Russia's target was to keep emissions over 2008-2012 at their 1990 level, a loosely binding constraint in the context of the post-USSR collapse in industrial production.

[60] The Clean Development Mechanism (CDM) offers the possibility for an Annex B Party to develop a project to reduce emissions outside of Annex B. By doing so, the Annex B party will earn certified emission-reduction credits, which can be counted towards meeting its Kyoto targets. The CDM is an instrument designed to exploit cheap abatement opportunities outside of Annex B countries, while in theory fostering local sustainable development in CDM projects host countries. This is an attempt to improve the overall cost-effectiveness of worldwide mitigation efforts in the context of asymmetric regulation across countries.

[61] Carbon pricing initiatives are scarce and relatively recent around the world. According to World Bank (2020), in 2019 these initiatives covered 11 $GtCO_2eq$, representing 20.1% of World GhG emissions. At the end of 1992, only Finland, Poland, Norway, Sweden, and Denmark had implemented some form of carbon pricing, representing about 0.25% of global GhG emissions as of 2012.

Second, in countries with some oil-emission regulations, these usually cover emissions related to oil combustion, ignoring upstream and midstream emissions. As oil heterogeneity in terms of CO_2 lies in these two sectors, current policies, such as taxing fuel, imposing fuel-efficiency standards or subsidizing oil alternatives, produce no incentives to extract oil from less-polluting deposits. Amongst the Top-10 oil producers in 2018 (Panel B of Table E1), only the US, China, and Canada have implemented a carbon tax or an emissions-trading system (ETS). However, these schemes do not cover upstream emissions, with the exception of that in Alberta Province in Canada.[62,63,64]

Third, these instruments do not always ensure correct carbon pricing (for instance, as non market-based instruments are used, or carbon prices differ across jurisdictions, or are too low compared to the social cost of carbon[65]). Carbon mispricing leads to the current situation where polluting oil types are extracted, refined and combusted instead of less-polluting alternatives.

[62]China developed a regional pilot ETS (planned to be developed into a nation-wide ETS). The ETS systems in Hubei, Shanghai, Tianjin, Beijing, Guangdong partly regulate emissions from the petrochemical sector. However, there is no significant oil extraction in these regions. More information on the Chinese pilot ETS is available at https://www.ncbi.nlm.nih.gov/pmc/articles/PMC6571708/.

[63]In the USA, some States have implemented carbon-pricing initiatives, including oil-producing States (e.g., California), but upstream and midstream emissions are not covered. None of the Top-5 US producing States (Texas, North Dakota, New Mexico, Oklahoma and Alaska, which jointly represent 68% of total US crude-oil production in 2018 according to U.S. Energy Information Administration 2020b) has set up a carbon-pricing scheme to price oil emissions as of 2019.

[64]In Alberta, Canada, under the Carbon Competitiveness Incentive Regulation (CCIR), since 2018 firms receive credits if their carbon intensity is below a product-specific threshold, and have to pay a levy per tonne of CO_2 above this threshold. The Alberta CCIR applies to GhG emissions from the industry, power generation and also to large oil-sands mines. The nominal carbon price was CAN\$30/tCO_2eq (US\$22/tCO_2eq) as of August 1^{st} 2019. In Ontario, a cap and trade system existed between 2017 and 2019, linked with California and Quebec within the Western Climate Initiative (WCI). The cap and trade system was canceled, with an effective end year of 2019. With a first compliance period starting in 2013, the Quebec ETS system initially covered electricity generation and industry, and after 2015 the distribution and import of fossil fuels (notably for transportation, building, and the small-business sectors). This includes industrial-process emissions. The Quebec ETS was linked in 2014 to that of California. Its price reached US\$18/tCO_2eq on August 1^{st} 2019. The Province of British Columbia implemented a carbon tax in 2008. All sectors are covered, with some exemptions for the industry, aviation, transport and agriculture sectors. Fugitive emissions, gas linked to extraction but not flared (most often methane), are not covered. The carbon price is US\$30/tCO_2eq (CAN\$40/tCO_2eq).

[65]For instance, the Chinese pilot ETS had carbon prices ranging from 6 to US\$13/tCO_2eq (from RMB39/tCO_2eq to RMB84/tCO_2eq) across the ETS as of August 1^{st} 2019.

Table E1: The global carbon-policy context.

Panel A: Kyoto and Doha emission-reduction targets by country

Country	Target* 2008-2012	Target* 2013-2020	Oil rank 2018
EU**	-8%	-20%	17
Switzerland	-8%	-15.8%	-
US$^{\diamond}$	-7%	NA	1
Canada$^{\diamond\diamond}$	-6%	NA	13
Japan	-6%	NA	72
Hungary	-6%	-20%	66
Poland	-6%	-20%	58
Croatia	-5%	-20%	67
Russia	0%	NA	3
Ukraine	0%	+24%	55
New Zealand	0%	NA	71
Norway	+1%	-16%	15
Australia	+8%	-0.5%	38
Iceland	+10%	-20%	-

Panel B: Carbon-pricing initiatives in the 10 largest oil producers as of 2018

Country	Share of world supply	Year (start-end)	Sectors
US ETS	18%		
RGGI†		2009-	power
Washington		2017-	industry, power, transport, waste, buildings
Massachusetts		2018-	power
California		2012-	power, road fuel distribution
Canada	5%		
Alberta		2007-17	industry, power
Alberta CCIR		2018-	industry, power, large oil-sands mines
Quebec ETS		2013-	power, industry, distribution, fossil-fuel imports
BC tax		2008-	all sectors except agriculture (from 2013)
Ontario CaT		2017-19	all sectors except agriculture, waste, aviation, marine transport
China ETS	5%		
Shanghai		2013-	power, petrochemicals, aviation, heavy industry
Shenzhen		2013-	power, manufacturing
Tianjin		2013-	petrochemicals, power, oil & gas, heavy industry
Guangdong		2013-	power, cement, steel, petrochemicals
Chongqing		2014-	power, heavy industry
Hubei		2014-	power, heavy industry, petrochemicals
Beijing		2013-	power, heavy industry, petrochemicals

Notes: In Panel A, *: The 1990 base year is for carbon dioxide (CO_2), methane (CH_4), and nitrous oxide (N_2O). Some Economies in Transition (EIT) have a baseline other than 1990 for the first commitment period: Bulgaria (1988), Hungary (the average of the years 1985–1987), Poland (1988), Romania (1989), and Slovenia (1986). The base year for hydrofluorocarbons (HFCs), perfluorocarbons (PFCs), and sulfur hexafluoride (SF_6) is 1995, except for Austria, Croatia, France, Italy, and Slovakia, in which it is 1990. **: EU-15, Bulgaria, Czech Republic, Estonia, Latvia, Liechtenstein, Lithuania, Monaco, Romania, Slovakia and Slovenia. The 15 EU States in 1997 adopted a joint 8% target, redistributed among themselves. The UK has a specific target for the second commitment period of −19%. $\diamond$: The US did not ratify the Kyoto Protocol. $\diamond\diamond$: On December 15^{th} 2011, Canada notified its withdrawal from the Kyoto Protocol. Data from United Nations (2020) and European Commission (2020). In Panel B, production includes the domestic production of crude oil, all other petroleum liquids, biofuels, and refinery processing gain. Data from U.S. Energy Information Administration (2020c) and World Bank (2020). For the British Columbia (BC) carbon tax and Ontario CaT, data are from Murray and Rivers (2015) and Financial Accountability Office of Ontario (2018) respectively. †: The Regional Greenhouse Gas Initiative (RGGI) covers Connecticut, Delaware, Maine, Maryland, Massachusetts, New Hampshire, New York, Rhode Island, and Vermont.

F Additional figures and tables

Figure F1: Deposit-level extraction costs and carbon intensities.

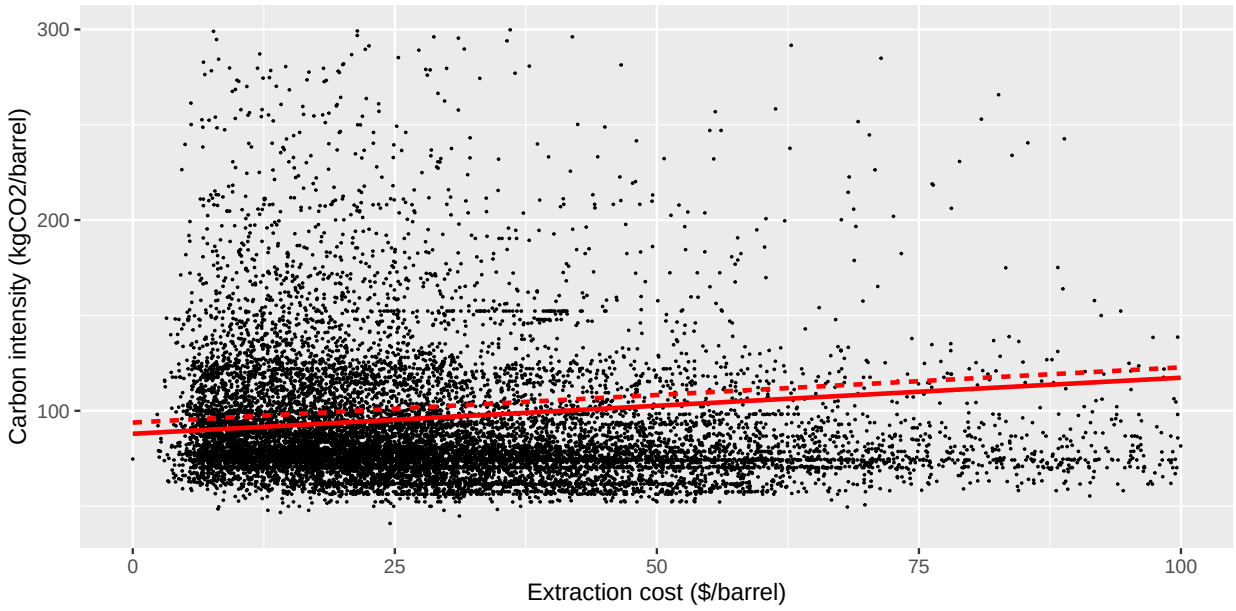

Notes: Each data point is a deposit with positive cumulative production over the 1992-2018 period. The unbroken red line represents the best linear fit when deposits are weighted by their 1992 reserves, and the dashed red line the best linear fit when deposits are weighted by their total production over 1992-2018. Section 2.3 and Appendix B describe the estimation of carbon intensities, and Appendix C the reserves data and the estimation of the costs. Fields with either carbon intensities above 300 or private extraction costs above 100 are excluded from the graph for visibility reasons.

Figure F2: Historical oil supply: 1970-2018.

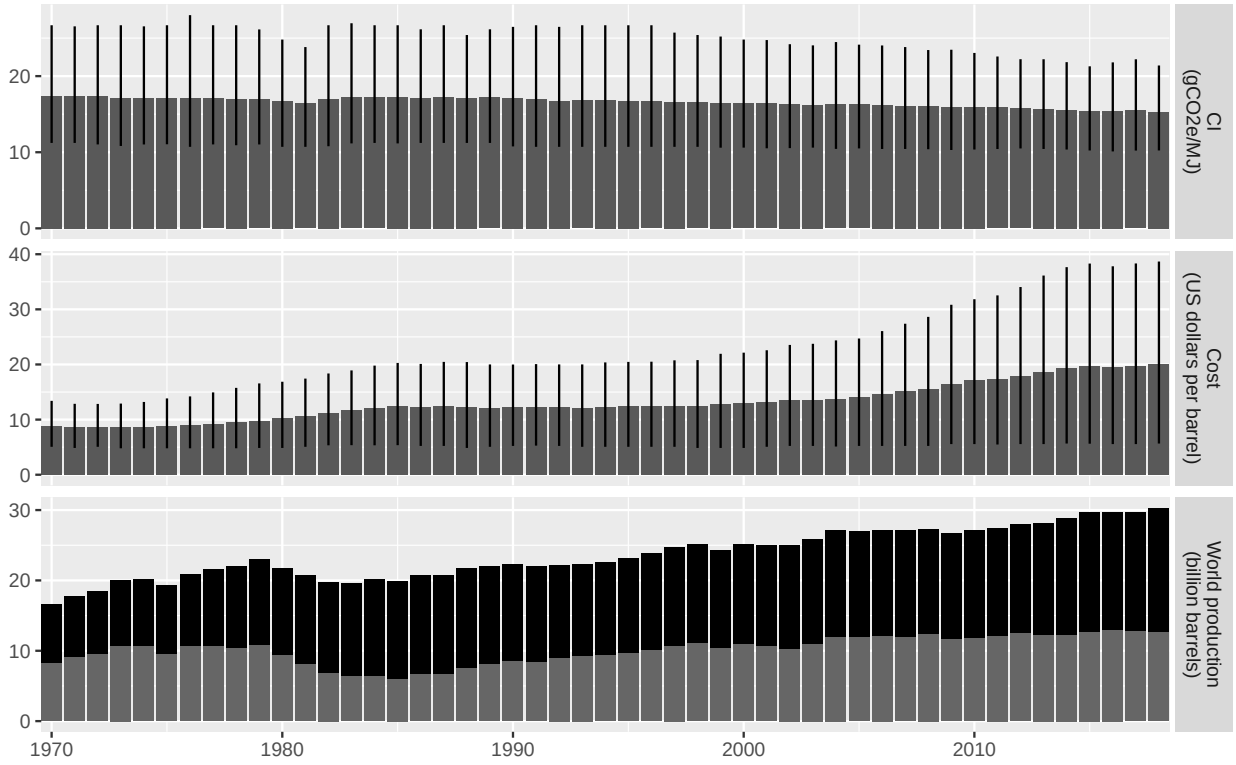

Notes: The top panel represents the annual average upstream-midstream carbon intensity (weighted by annual deposit productions, in grams of CO_2 per megajoule) of World oil supply from 1970 to 2018. The extremities of the lines represent the first and last deciles. The estimation of carbon intensity is described in Section 2.3 and Appendix B. The middle panel represents the annual average extraction cost (in 2018 US Dollars per barrel) of World oil supply from 1970 to 2018 (the average weighted by annual deposit production). The extremities of the lines represent the first and last deciles. The construction of extraction costs is described in Appendix C. The bottom panel shows annual World production (in billions of barrels) from 1970 to 2018, with OPEC production in grey. OPEC, as of 2019, included Algeria, Angola, Congo, Ecuador, Equatorial Guinea, Gabon, Iran, Iraq, Kuwait, Libya, Nigeria, Saudi Arabia, the UAE, Venezuela, and the Neutral Zone shared by Kuwait and Saudi Arabia.

Figure F3: Historical production in selected countries: 1970-2018.

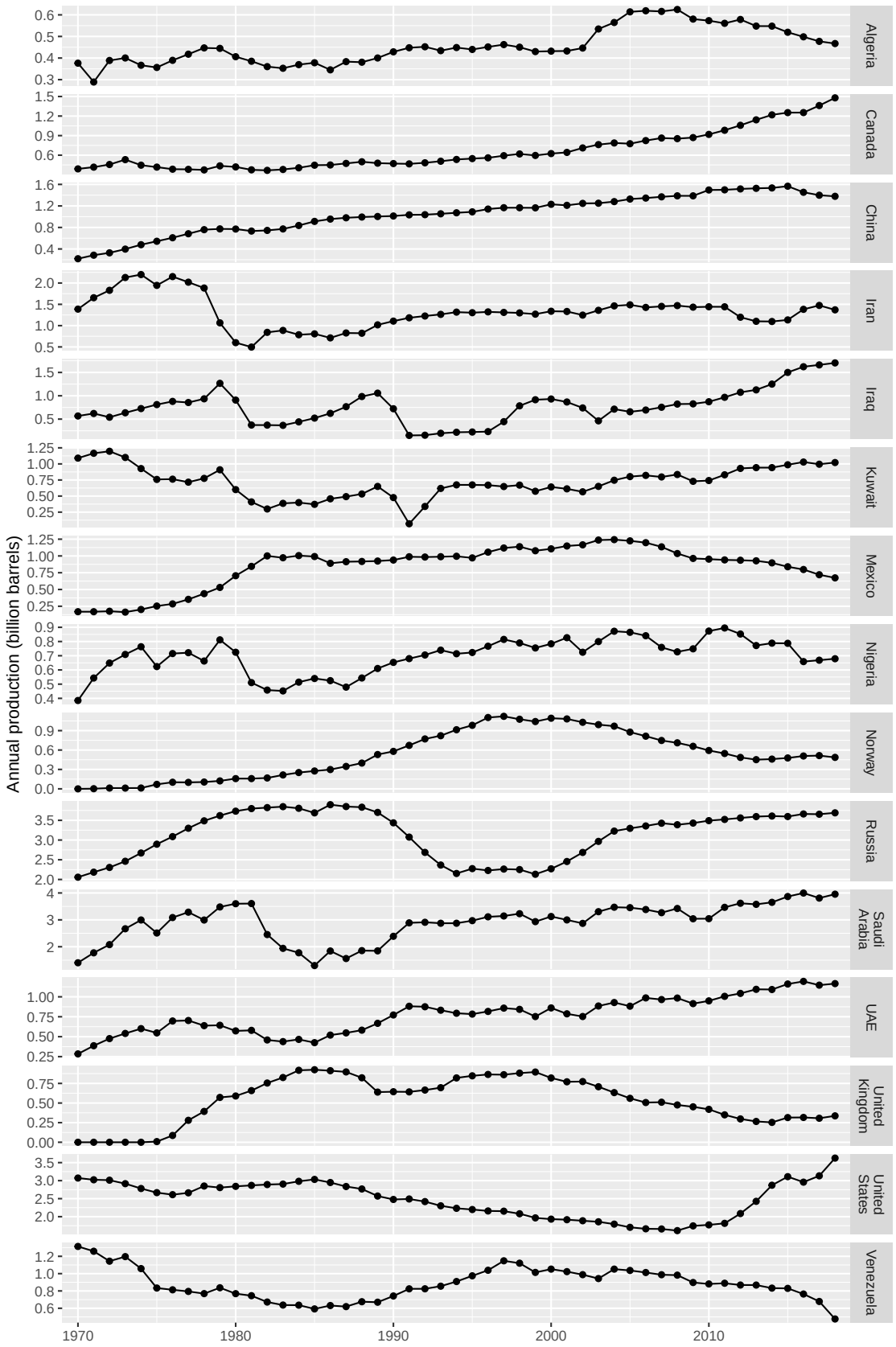

Notes: The figure displays historical annual productions in the Top 15-producing countries over the 1970-2018 period.

Figure F4: Bringing forward the beginning of supply recomposition, 1970-2018: Gains per barrel.

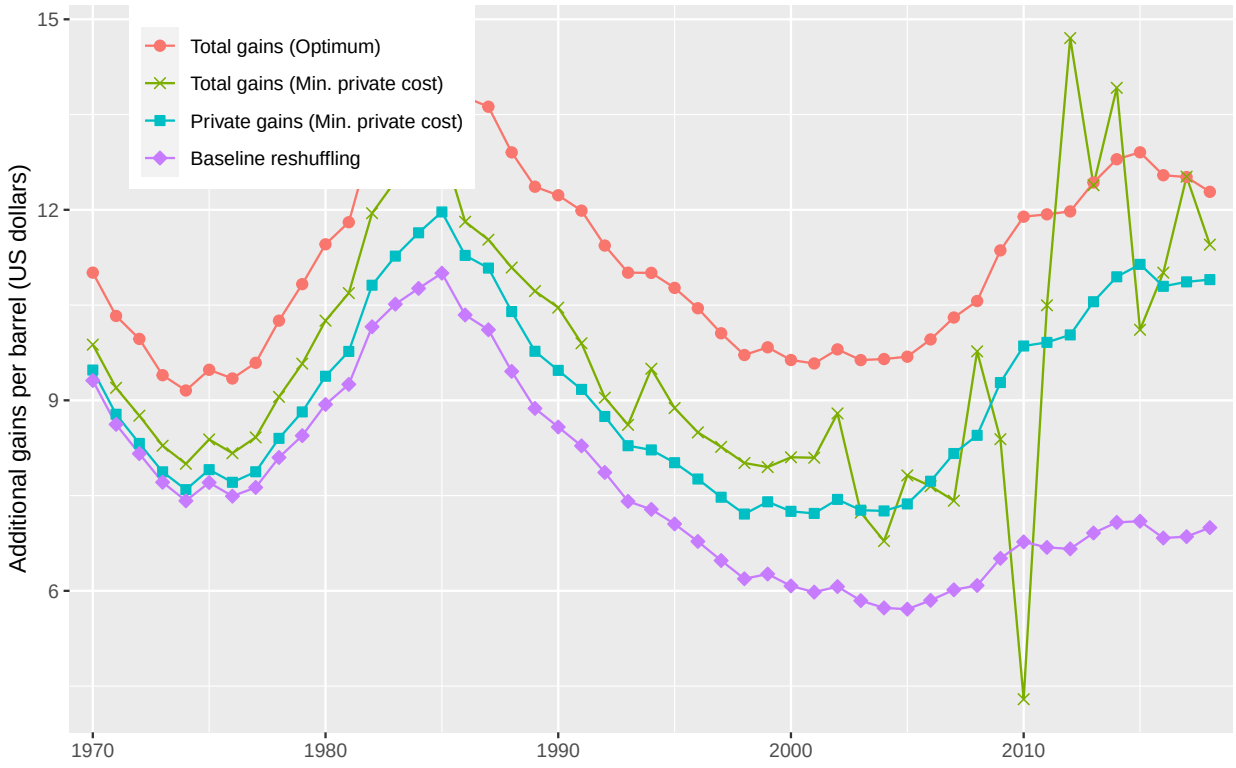

Notes: This figure displays the gains (in US Dollars per barrel) from starting different counterfactuals in year t instead of $t+1$ for t between 1970 and 2018, divided by World production in year t. See the note to Figure 4 and Sections 3 and 4 for the description of the different counterfactuals.

Table F1: Total gains and emission reductions: Limiting production changes at the country level.

	Energy-security constraint		Country annual productions fixed	
	Total gains (trillion US$)	CO_2 decrease ($GtCO_2$)	Total gains (trillion US$)	CO_2 decrease ($GtCO_2$)
Optimum	7.14	17.61	6.28	17.21
Minimal private costs	5.17	2.45	4.45	2.75
Baseline reshuffling	2.89	0	2.01	0

Notes: This table shows the results from our main exercise but with additional feasibility constraints. Each line refers to a distinct counterfactual supply. For the description of the different counterfactuals, see the note to Table 1. Columns *Total gains* (in trillions of US Dollars) and *CO_2 decrease* (in gigatons of CO_2) are calculated relative to the baseline. In the first two columns, *Energy-security constraint*, the counterfactual production each year over the 1992-2018 period in each country is assumed to be greater than (or equal to) the minimum of the country's historical consumption and production that year. In the last two columns, *Country annual productions fixed*, the counterfactual production each year over the 1992-2018 period in each country is assumed to be the country's historical production that year.

Table F2: Total gains and emission reductions: End of the Oil era, discount rate and resource-discovery constraint.

	(1) Oil era ends: 2066		(2) Oil era ends: 2080	
	Total gains (trillion US$)	CO_2 decrease ($GtCO_2$)	Total gains (trillion US$)	CO_2 decrease ($GtCO_2$)
Optimum	8.67	20.77	8.81	23.24
Clean future	1.38	10.34	1.83	12.91
Minimal private costs	5.89	0.69	5.88	1.84
Baseline reshuffling	5.12	0	5.23	0
	(3) Discount rate: 1.5%		(4) No discovery constraint	
	Total gains (trillion US$)	CO_2 decrease ($GtCO_2$)	Total gains (trillion US$)	CO_2 decrease ($GtCO_2$)
Optimum	6.85	16.90	8.81	17.66
Clean future	0.88	6.19	0.99	7.64
Minimal private costs	4.82	1.86	6.63	1.87
Baseline reshuffling	2.30	0	4.65	0

Notes: Each row refers to a distinct counterfactual supply. For the description of the different counterfactuals, see the note to Table 1. Columns *Total gains* (in trillions of US Dollars) and *CO_2 decrease* (in gigatons of CO_2) are calculated relative to the baseline. Sub-panels correspond to changes in the modeling parameters: (1)-(2), carbon neutrality is reached in 2066 or 2080, respectively, instead of 2050 (see Appendix C for the construction of post-2018 demand); (3), the discount rate used to construct the counterfactuals and value the gains is 1.5% instead of 3%; and (4), the discovery constraint is relaxed and all resources discovered post-1992 are assumed to be available in 1992.

Table F3: Total gains and emission reductions: Alternative capacity constraints.

	(1) Capacity constraint: 0.05 reserves		(2) Capacity constraint: 0.15 reserves	
	Total gains (trillion US$)	CO_2 decrease ($GtCO_2$)	Total gains (trillion US$)	CO_2 decrease ($GtCO_2$)
Optimum	8.68	17.55	8.84	17.68
Clean future	0.98	7.45	1.00	7.65
Minimal private costs	6.54	1.88	6.65	1.85
Baseline reshuffling	4.56	0	4.67	0
	(3) Capacity constraint: 10% of current reserves		(4) 25% of reserves are not exploitable	
	Total gains (trillion US$)	CO_2 decrease ($GtCO_2$)	Total gains (trillion US$)	CO_2 decrease ($GtCO_2$)
Optimum	8.49	17.17	6.67	15.40
Clean future	0.89	6.72	0.75	5.47
Minimal private costs	6.45	1.96	4.90	2.01
Baseline reshuffling	4.46	0	3.81	0

Notes: This table shows the results from our main exercise but with alternative capacity constraints. Each line refers to a distinct counterfactual supply. For the description of the different counterfactuals, see the note to Table 1. Columns *Total gains* (in trillions of US Dollars) and *CO_2 decrease* (in gigatons of CO_2) are calculated relative to the baseline. Sub-panels correspond to changes in extractive-capacity constraint: (1)-(2), the field capacity constraint is set to the maximum of observed production since 1970 and either 5% or 15% of 1970 reserves (instead of 10%); (3), the upper limit on the rate of extraction (production-to-current-reserves ratio) in the counterfactuals is $max\{y_d, 10\%\}$, where y_d is the maximal extraction rate, in any year, for that field; and (4), we set exploitable reserves equal to 75% of the initial reserves or to the cumulative production over the 1992-2018 period, if the latter is greater, for each field. For the updated exploitable reserves, the capacity constraint is as defined in the main approach, that is, the upper limit on annual production is 10% of the field initial reserves or the maximal annual production of the field over the period 1970-2018, if the latter is greater.

Table F4: Total gains and emission reductions: Alternative measures of carbon intensity.

	(1) Flaring: 10%-cut		(2) CI (CPD)	
	Total gains (trillion US$)	CO_2 decrease ($GtCO_2$)	Total gains (trillion US$)	CO_2 decrease ($GtCO_2$)
Optimum	8.65	16.61	9.06	19.23
Clean future	0.93	6.84	1.07	8.32
Min. private costs	6.64	1.92	6.63	1.84
	(3) Discarding midstream pollution		(4) Adding downstream pollution	
	Total gains (trillion US$)	CO_2 decrease ($GtCO_2$)	Total gains (trillion US$)	CO_2 decrease ($GtCO_2$)
Optimum	8.52	15.50	9.14	19.31
Clean future	0.89	6.79	0.99	7.26
Min. private costs	6.53	1.38	6.89	3.13
	(5) CI varying with depletion (medium)		(6) CI varying with depletion (high)	
	Total gains (trillion US$)	CO_2 decrease ($GtCO_2$)	Total gains (trillion US$)	CO_2 decrease ($GtCO_2$)
Optimum	8.82	19.18	8.89	20.03
Clean future	1.29	9.63	1.41	10.47
Min. private costs	6.21	-0.25	6.09	-0.86
	(7) CI varying with depletion (low)			
	Total gains (trillion US$)	CO_2 decrease ($GtCO_2$)		
Optimum	8.77	17.94		
Clean future	1.15	8.51		
Min. private costs	6.38	0.60		

Notes: This table shows the results from our main exercise but with alternative carbon-intensity estimates. Each line refers to a distinct counterfactual supply. For the description of the different counterfactuals, see the note to Table 1. Columns *Total gains* (in trillions of US Dollars) and *CO_2 decrease* (in gigatons of CO_2) are calculated relative to the baseline. Each sub-panel corresponds to a variation in deposit-level carbon-intensity estimation: (1), upstream carbon intensities (CI) are updated to account for a 10%-reduction in flaring for all deposits where this practice is used; (2), upstream field-level CI are estimated using the Co-Product Displacement (CPD) approach (see Appendix B); (3), carbon intensities only account for upstream emissions instead of both upstream and midstream emissions; (4), carbon intensities account for upstream, midstream and downstream emissions; and (5-7), carbon-intensity estimates vary by field depletion. See Appendices B.3 and B.1.1 for a description of the last two approaches.

Table F5: Total gains and emission reductions: Alternative cost constructions.

	(1) Average costs		(2) Only future costs		(3) Time-varying costs	
	Total gains (trillion US$)	CO_2 decrease ($GtCO_2$)	Total gains (trillion US$)	CO_2 decrease ($GtCO_2$)	Total gains (trillion US$)	CO_2 decrease ($GtCO_2$)
Optimum	9.11	18.12	8.99	17.63	6.97	20.48
Clean future	0.89	6.44	0.87	6.84	1.17	8.21
Min. private cost	6.84	1.83	6.73	1.04	4.82	5.65
Baseline reshuffling	4.87	0	4.24	0	2.61	0

Notes: This table shows the results from our main exercise but with alternative estimates of private extraction cost. Each line refers to a distinct counterfactual supply. For the description of the different counterfactuals, see the note to Table 1. Columns *Total gains* (in trillions of US Dollars) and *CO_2 decrease* (in gigatons of CO_2) are calculated relative to the baseline. Each sub-panel corresponds to a variation in deposit-level cost estimation: (1), extraction costs are calculated as average extraction costs; (2), extraction costs are calculated as LCOE, but removing the observed capital and operational expenditures paid strictly before the start of optimization as well as production before that date; and (3), extraction costs are the observed levels when available. See Appendix C.3.2 for a description of the alternative cost estimations.

Table F6: Total gains and emission reductions: Imperfect substitution between oils.

	High-value products' quantities cannot decrease		Fixed productions by Oil category	
	Total gains (trillion US$)	CO_2 decrease ($GtCO_2$)	Total gains (trillion US$)	CO_2 decrease ($GtCO_2$)
Optimum	8.81	17.66	8.51	16.63
Clean future	0.99	7.64	0.99	7.64
Minimal private costs	6.63	1.87	6.46	1.85
Baseline reshuffling	4.65	0	4.93	0

Notes: This table shows the results from our main exercise but with imperfect substitution between oils. Each line refers to a distinct counterfactual supply. For the description of the different counterfactuals, see the note to Table 1. Columns *Total gains* (in trillions of US Dollars) and *CO_2 decrease* (in gigatons of CO_2) are calculated relative to the baseline. In the first two columns, *High-value products' quantities cannot decrease*, the annual productions of each of three high-value petroleum products (gasoline, diesel, jet fuel) cannot be smaller than the observed productions over the 1992-2018 period while fixing product slates of each crude. To compute crudes' product slates, we first relate each crude (field) to its best refining configuration (deep/medium conversion or hydroskimming) based on its API gravity and sulfur content following PRELIM (see Appendix B.2). We then estimate the average product slate (share of gasoline, diesel, jet fuel and residuals) of each of the three refinery types. Averages were computed from 75 crudes matched with existing oil fields available in the Oil-Climate Index data. In the last two columns, *Fixed productions by Oil category*, oil productions are split into two categories: the first consists of only light and regular oil, the second of all other types of oil resources. We constrain the annual production of each of these two categories in the counterfactual to be the same as in the baseline.